ABSTRACT

Title of dissertation: Control of Piecewise Smooth Systems: Generalized Absolute Stability and Applications to Supercavitating Vehicles

Guojian Lin, Doctor of Philosophy, 2008

Dissertation directed by: Professor Eyad H. Abed
Department of Electrical and Computer Engineering

Professor Balakumar Balachandran
Department of Mechanical Engineering

Many systems in engineering applications are modeled as piecewise smooth systems. The piecewise smoothness presents great challenges for stability analysis and control synthesis for these systems. Over the years, the theory of absolute stability has been one of the few tools developed by control theory researchers to meet these challenges. For systems in which the nonlinearity is known to be bounded within certain sectors, many stability and control problems can be addressed using results from absolute stability theory.

During the last few decades, many important advances have been made in the study of the absolute stability. In these studies, it is commonly assumed that the sector bound for the system nonlinearity is *symmetric* with respect to the origin in state space. However, in many practical engineering systems, the nonlinearity does not satisfy such a symmetry assumption. To study stability and control problems for these systems, in this work the author studies generalized absolute stability problems involving *asymmetric* sector bounds. Nonlinear systems with Lure' structure

are considered. For second-order systems, conditions that are both necessary and sufficient for generalized absolute stability are obtained. These conditions can be easily tested in engineering applications. For general finite-order systems, sufficient conditions are provided for generalized absolute stability. The derived conditions may be easily tested by using numerical tools for linear programming. With the generalizations in this work, absolute stability theory becomes a more powerful tool in the sense that it applies to an extended class of piecewise smooth systems in which the nonlinearities can be asymmetric with respect to the state variables.

This work includes general theoretical questions as well as detailed investigations of an application to models of supercavitating vehicles. For these high-speed underwater vehicles, the dive-plane motion is naturally modeled as a piecewise smooth system with a dead zone. The strong nonlinear planing force plays an important role in determining the dive-plane dynamics. To design control laws that stabilize the dive-plane motion, the necessary and sufficient condition for generalized absolute stability of second-order systems is applied to a reduced-order model obtained through the backstepping control approach. The obtained sufficient conditions for generalized absolute stability of finite-order systems can also be successfully applied for stabilizing the dive-plane motion. In comparison with alternative control approaches, control designs with the aid of theoretical findings in generalized absolute stability lead to stability that is robust to the modeling errors in the nonlinearity such as the magnitude, local slope and the dead zone location.

The dissertation also includes basic results on bifurcation and bifurcation control of supercavitating vehicles. The presence of bifurcations in the dive-plane dy-

namics is demonstrated, and control techniques for modifying the bifurcation behavior to improve the vehicle dynamic performance are developed. These results complement the absolute stability results to give a more complete picture of the dynamics and control of supercavitating vehicles.

Control of Piecewise Smooth Systems:

Generalized Absolute Stability and

Applications to Supercavitating Vehicles

by

Guojian Lin

Dissertation submitted to the Faculty of the Graduate School of the
University of Maryland, College Park in partial fulfillment
of the requirements for the degree of
Doctor of Philosophy
2008

Advisory Committee:

Professor Eyad. H. Abed, Chairman/Advisor
Professor Balakumar Balachandran, Co-Advisor
Professor William S. Levine
Assistant Professor Nuno Martins
Associate Professor Ben Shapiro

DEDICATION

To my wife Pu Peng

Acknowledgments

I would like to express my deepest gratitude to my advisors, Professor Eyad H. Abed and Professor Balakumar Balachandran for their invaluable guidance, encouragement and support throughout my graduate studies at the University of Maryland. They have been a great source of inspiration throughout the years. Thanks are also due to Professors Williams S. Levine, Nuno Martins, and Ben Shapiro for serving on my Ph.D. dissertation committee.

I would like to thank Dr. Ivan N. Kirschner of Alion Science and Technology Inc. and Mr. Ben Rosenthal of Navatek, Ltd. for helpful discussions on supercavitating vehicles. I am also grateful to Mr. Vince Nguyen for many helpful discussions throughout these years at the University of Maryland.

I would like to acknowledge financial support from the Office of Naval Research (ONR) through the grant No. N000140310103. Dr. Kam Ng is the technical monitor for this work.

It is impossible to remember all, and I apologize to those I've inadvertently left out.

Table of Contents

List of Figures

Chapter 1

Introduction

1.1 Piecewise Smooth Systems

In engineering applications, many systems are modeled as a set of piecewise smooth differential equations. In other words, these systems have a nonsmooth vector field. Here a nonsmooth function refers to a function that is C^0 continuous, that is, the function is continuous, but its first-order or higher-order derivative is discontinuous. Examples of piecewise smooth systems include nonsmooth friction force models [34], suspension bridge models in structure analysis [15], nuclear reactor safety systems [67], a thermodynamical process [11], switching circuits in power electronics [8] and tunnel diodes [47].

Piecewise smooth systems can also result from nonsmooth control of a smooth system. In some control designs, nonsmoothness is introduced intentionally in order to achieve desired closed-loop system dynamics. Besides the supercavitating vehicle example in Chapter 6, relay feedback in [28], bifurcation control in [61], switching control of nonlinear systems in [18] and hybrid control in [29] are examples that apply nonsmooth control actions.

Piecewise smooth system can in some cases be used to approximate a nonlinear smooth system. For example, the authors in [58] analyzed a nonlinear system by approximating it with a piecewise smooth system.

For the three reasons above, piecewise smooth models can be found in many engineering problems. Correspondingly, it is of importance to study the stabilization and control of piecewise smooth systems. In consideration of the fact that modeling errors often occur in these piecewise smooth models, in this work a robust stability analysis tool, absolute stability, is adopted for the purpose of stability analysis and control synthesis. By designing control laws to ensure the asymptotic stability of the closed-loop system as long as the nonlinearity is bound within certain sectors, the absolute stability is achieved and the piecewise smooth system is stable with robustness to the modeling errors in the nonlinearity.

1.2 Literature on Absolute Stability

Absolute stability is one of the most well-known open problems in control theory. Since the absolute stability concept was introduced in the 1940s, there have been extensive literatures on this subject ([2] [45] [64] [43] [51] [52] [26] [30] [54] [59]). Many important results have been achieved including the well-known circle criterion and Popov criterion. Details of the circle criterion and Popov criterion can be found in nonlinear dynamics and control literatures, for example, [30].

During the last decade, switched systems received numerous attention from researchers in the control system community. Because the absolute stability problem

is closely related to the stability analysis of switched systems, this subject gained revived interest among researchers in control systems in recent years and this leads to a number of published studies ([5] [14] [13] [22] [39] [60] [25]).

In regard to solving the absolute stability problem, there are two fundamentally distinct approaches – frequency-domain based methods and time-domain based methods. Frequency-domain based results involve the transfer function of the linear part and include tools such as the circle criterion and the Popov criterion. Time-domain based methods generally involve the usage of Lyapunov functions and generalized Lyapunov functions. Time-domain based results include sufficient conditions in [51] [63], and necessary and sufficient conditions in [43], which, however, are not easily verifiable and not feasible in practice even with advanced numerical tools.

In contrast with the extensive literature on absolute stability, a trackable solution to the absolute stability problem giving conditions that are both necessary and sufficient has not been available. However, for the special case of second-order systems, very recent work ([42] by Margaliot and Langholz, and [35] by Leonov) has resulted in new necessary and sufficient conditions for absolute stability that is easily trackable.

Since the introduction of the absolute stability concept, theoretical results on absolute stability have been extensively applied in various engineering applications. For example, absolute stability results were used in the stability analysis of systems with actuation limits [44] [33] and systems involving stick-slip frictions [10]. In addition, absolute stability results were also applied in the control of chaotic motions

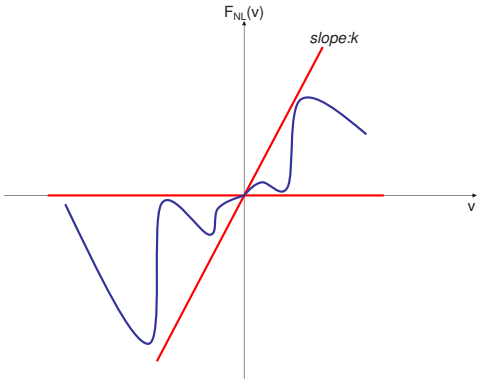

Figure 1.1: Sector conditions in classical absolute stability studies.

[9], nonlinear observer design [4], DVD storage drive controller design [24], control of material handling systems [41], recursive parameter identifications [62], dynamic analysis of musical instruments [66], control of Chua's circuits [36], a PWM system [50], a Coulomb friction system [65], gear meshing dynamics in automobile engines [20], supercavitating vehicles [37] and many more.

Recently, Hu et al. [27] extended the classical absolute stability concept to admit more general sector conditions. The sector bounds, which are *linear* functions in the setting of the classical absolute stability, are allowed to be *piecewise linear* functions that are symmetric with respect to the origin. Sufficient conditions are found for the generalized absolute stability by utilizing common quadratic Lyapunov functions.

1.3 Generalization of Classical Absolute Stability

However in all studies on the absolute stability problem so far, the sector boundaries have been assumed to be odd functions, such as the one illustrated in Figure 1.1. In other words, the sector conditions are symmetric with respect to the origin. However in engineering systems, a general nonlinearity need not satisfy this symmetry assumption. Asymmetric nonlinearities are encountered, for instance, in dynamic models of amplifier circuits [3], autonomous underwater vehicles [7], earthquake engineering [17], and hard disk drives [23].

Even if a nonlinearity is known to be symmetric, it may be desired to operate the system at an equilibrium point other than the origin. This bias from the origin would transform the symmetric nonlinearity to a nonsymmetric one. Moreover, switching control laws may lead to asymmetric nonlinearities. Therefore it is important both for theory and practice, to generalize the classical absolute stability results to allow nonsymmetric sector conditions.

Driven by the need in the stabilization and control of many piecewise smooth engineering systems with *asymmetric* nonlinearities, the author of this dissertation generalized the classical absolute stability concept to allow for *asymmetric* sector bounds and correspondingly, derived necessary and sufficient conditions for the generalized absolute stability.

The symmetry assumption in the sector boundary, illustrated in Figure 1.1, is dropped in this study. Instead, we allow the sector boundaries to be asymmetric, as depicted for instance in Figures 1.2 and 1.3. For an engineering system with

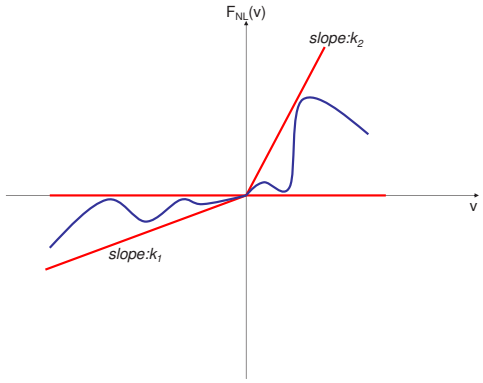

Figure 1.2: Nonlinearity bound in the asymmetric sector $(0, k_1, k_2)$

.

the nonlinearity bound by an asymmetric sector bound, one can expect to design a less conservative control law to robustly stabilize the system by applying results on generalized absolute stability in this work, compared with a control law that is designed according to the existing results on classical absolute stability.

It is interesting that the generalization of the absolute stability concept is trivial for first-order systems. Consider a first-order system

$$\dot{x} = Ax + b\phi(cx) \tag{1.1}$$

where all quantities are scalar and the nonlinearity $\phi(.)$ is bound in the asymmetric sector $(0, k_1, k_2)$ as illustrated in Figure 1.2. It is straight-forward to show that the system is absolutely stable if and only if $A < 0, A + bck_1 < 0, A + bck_2 < 0$. This condition is equivalent to $A < 0, A + bcK$ where $K = \max\{k_1, k_2\}$. On the other hand, this is necessary and sufficient condition for the system (1.1) where the nonlinearity $\phi(.)$ is bound in the symmetric sector $(0, K)$ as illustrated in Figure 1.1.

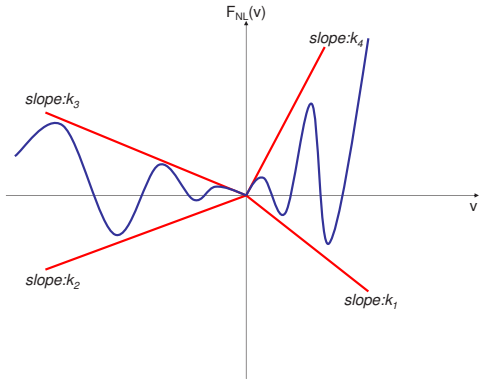

Figure 1.3: Nonlinearity bound in the more general asymmetric sector (k_1, k_2, k_3, k_4)

Therefore a system with the nonlinearity bound by the asymmetric sector bound $(0, k_1, k_2)$ is absolutely stable if and only if the system with the nonlinearity bound by the symmetric sector bound $(0, \max\{k_1, k_2\})$. Consequently the generalization that allows for asymmetric sector bounds is of trivial value for first-order systems.

However for second-order and high-order systems, the generalization is nontrivial and there is need to derive necessary and sufficient conditions for the generalized absolute stability. In Section 7.2.2, we give a third-order system example that is absolutely stable with the asymmetric sector bound $(0, 0.1, 0.5)$ but not absolutely stable with the symmetric sector bound $(0, 0.5)$.

In this dissertation, we are interested in a system of Lure's form with one single nonlinearity. By Lure's form, we mean continuous-time systems that can be formulated as a feedback interconnection between a linear system and a nonlinearity.

By relaxing the symmetric constraints on the sector bounds in the generalized absolute stability, control laws can be designed to ensure robust stability of a more general class of dynamic systems. However, the presence of nonsymmetric sector

bounds complicates the stability analysis considerably and makes inapplicable the frequency-domain analytical tools such as the circle criterion. With the aid of the geometry-related tools, necessary and sufficient conditions for the generalized absolute stability of second-order systems are derived. For a general finite-order systems, sufficient conditions are given with the help of generalized Lyapunov function methods. It is noted that for high-order systems, necessary and sufficient conditions are not available to date even for the classical absolute stability that was introduced long time ago.

1.4 Organization of Dissertation

The rest of this dissertation proceeds as follows. In the next chapter, theoretical background materials that will be employed in subsequent chapters are collected. The definition and some conditions for the classical absolute stability will be introduced. Furthermore, the linear programming and backstepping control are briefly introduced as they will be used in other chapters.

In Chapter 3, two recent works, which give necessary and sufficient conditions for the classical absolute stability of second-order systems, are introduced. Further, the relationship between these two independent results are examined. After correcting some mistakes in the original results, it is proved that these two results are in fact equivalent to each other.

In Chapter 4, the classical absolute stability concept is generalized to admit asymmetric sector boundaries. The focus in this chapter is on second-order or planar

systems. Conditions that are both necessary and sufficient, are derived for generalized absolute stability of these systems. These conditions include as a special case the conditions for the classical absolute stability, which are elaborated in Chapter 3.

In Chapter 5, the generalized absolute stability problem is considered for high-order systems. It is proved that a piecewise linear Lyapunov function exists if and only if the system is absolutely stable. Furthermore, with the aid of piecewise linear Lyapunov functions, sufficient conditions are established.

In Chapter 6, an engineering system - the supercavitating vehicle system is introduced. The dive-plane model and some dynamical behavior of this system is presented. Without robustness requirement, two simple control schemes are proposed to stabilize the dive-plane motion. Through nonlinearity analysis including the bifurcation study, the tail-slap phenomenon of supercavitating vehicles is interpreted as a limit cycle motion.

In Chapter 7, a few examples are utilized to illustrate the application of the theoretic results that are derived in the previous chapters. The necessary and sufficient conditions for generalized absolute stability of second-order systems are applied to the supercavitating vehicle model through a backstepping control approach. Following that, the sufficient conditions for a general finite-order system are applied to three examples including a second-order system, a third-order system and the fourth-order dive-plane model of supercavitating vehicle.

In Chapter 8, conclusion remarks are collected and a list of future work is provided.

Chapter 2

Preliminary Material

In this chapter, we review some background material that will be employed in the remaining chapters. The topics we discuss include: definition and some conditions for classical absolute stability; linear programming; and backstepping control.

2.1 Absolute Stability

2.1.1 Definition

First let us review the standard definition of absolute stability. This definition involves the following notion of sector boundaries. A nonlinearity $\phi(.)$ is said to be bound in the sector (k_l, k_h) if the following inequality holds for all $y \in \Re$:

$$k_l y^2 \leq y\phi(y) \leq k_h y^2 \tag{2.1}$$

A nonlinearity satisfying such a sector bound is illustrated in Figure 1.1.

A system in the so-called Lure' form (2.2) is said to be *absolutely stable* if the origin is globally uniformly asymptotically stable for *any* nonlinearity $\phi(\cdot)$ bound in

the sector (k_l, k_h).

$$\begin{aligned} \dot{x} &= Ax + Bu \\ y &= C^T x \\ u &= -\phi(y) \end{aligned} \tag{2.2}$$

Here the dimensions of the various quantities are as follows: $x \in \Re^n, u \in \Re, y \in \Re, A \in \Re^{n\times n}, B \in \Re^n, C \in \Re^n$.

It is important to point out that the absolute stability concept is closely related to a problem that has received attention from many researchers in the last two decades – stability analysis of a switched linear system with arbitrary switchings. A switched linear system can be described as

$$\dot{x} = A_\sigma x \tag{2.3}$$

where $x \in \Re^n$ and $A_i \in \Re^{n\times n}$ for $i = 1, 2, ..., M$. Here the switching signal $\sigma(t)$ is a piecewise constant function: $[0, \infty) \to P = \{1, 2, ..., M\}$. Consider such a switched linear system with an arbitrary switching signal σ. Let $M = 2$ and

$$\begin{aligned} A_1 &= A + k_l BC^T \\ A_2 &= A + k_h BC^T \end{aligned} \tag{2.4}$$

It is straightforward to show that solving the absolute stability problem (2.2) implies deriving the necessary and sufficient conditions for global asymptotic stability of the origin of the switched linear system (2.4).

2.1.2 Frequency Domain Results

Roughly speaking, the absolute stability problem has been studied with methods of two categories: frequency domain based approaches and time domain based approaches. In this section we will introduce some results from the frequency domain based approaches. Results from the time domain based approaches will be introduced in the next section.

Without loss of generality, it is assumed that $k_l = 0$ in the absolute stability problem (2.2). Otherwise, a simple trick called loop transformation [30] can be applied to transform the sector condition from (k_l, k_h) to $(0, k_h - k_l)$ and correspondingly the linear part will include an additional term $k_l B C^T x$.

Making use of Lyapunov functions and positive realness concept, one can derive the circle criterion as

Theorem 2.1 The system (2.2) with $k_l = 0$ and $k_h > 0$ is absolutely stable if (A, B, C^T) is a minimal realization of $G(s) = C^T(sI - A)^{-1}B$, $G(s)$ is Hurwitz and the Nyquist plot of $G(j\omega)$ lies to the right of the vertical line defined by $Re[s] = -1/k_h$. If these conditions are satisfied only on an interval of y, then the system is absolutely stable with a finite domain that may be estimated as an ellipsoid by using the Lyapunov function. □

When the sector condition (2.1) is satisfied only in a finite interval $a \leq y \leq b$, the region of attraction (ROA) of the equilibrium point can be estimated by using Lyapunov functions. The ROA can be estimated as

$$\Omega = \{x \in \Re^4 | V(x) = x^T P x \leq c_3\} \tag{2.5}$$

where the matrix P, a row vector L, and a scalar ϵ satisfy

$$\begin{aligned} PA + A^T P &= -L^T L - \epsilon P \\ PB &= C^T K - \sqrt{2} L^T \end{aligned} \tag{2.6}$$

and $c_3 = \min V(x)$ subject to $a \leq y \leq b$. Equation (2.6) is formulated as a Riccati equation; that is,

$$P[\frac{\epsilon I}{2} + A] + [\frac{\epsilon I}{2} + A^T]P + \frac{1}{2}(KC^T - PB)(KC - B^T P) = 0 \tag{2.7}$$

The matrix P is found by numerically solving (2.7) using tools such as MATLAB, and the Lagrange method is applied to find c_3. Here, the scalar ϵ is chosen such that $1 + k_h G(s - 0.5\epsilon$ is positive real and $\frac{\epsilon}{2} I + A$ is Hurwitz. More details can be found in the reference [30].

The circle criterion allows us to investigate the absolute stability by using the Nyquist plot of $G(j\omega)$, which can be experimentally determined. Therefore the circle criterion has been widely used in engineering applications, although the derived condition is only sufficient but not necessary.

For a system involving more than one nonlinearities, correspondingly the multivariable circle criterion gives the sufficient condition for absolute stability. However, this criterion cannot be described as conditions for the Nyquist plots. It is noted that in this dissertation, we focus on systems involving only one nonlinearity.

Besides the circle criterion, the frequency domain results also include the Popov criterion, which also gives sufficient conditions for absolute stability. This criterion will not be introduced here since it is not used in the sequel. Those who are interested in it can find related information in references such as [30] and [59].

2.1.3 Time Domain Results

In this section, we introduce results from time domain based approaches. Lyapunov functions have provided a very important tool in the analysis and synthesis of control systems for dynamic systems. In particular, quadratic Lyapunov functions are widely used in stability analysis of dynamic systems because: 1) for linear systems, it is not only sufficient but also necessary for stability that a system have a quadratic Lyapunov function; and 2) in many nonlinear systems, associated linear matrix inequalities (LMI) can be formulated for seeking a Lyapunov function, and these LMI's can then be solved numerically in an efficient manner.

Similarly, to solve the absolute stability problem, it is natural to apply the quadratic Lyapunov function and to use this function to find sufficient conditions. As stated early in this chapter, the absolute stability problem (2.2) is equivalent to the stability problem of a switched linear system (2.3) with an arbitrary switching signal σ. Therefore the origin of the system (2.2) is absolutely stable if a common quadratic Lyapunov function $V(x) = x^T P x$ exists for the linear system $\dot{x} = A_1 x$ and the system $\dot{x} = A_2 x$ where $A_i, i = 1, 2$ are defined in (2.4). It is reminded that the existence of a common quadratic Lyapunov function is sufficient but not necessary for the absolute stability. Even if a common quadratic Lyapunov function cannot be found, a system may still be absolutely stable. Therefore the derived sufficient condition may be quite conservative for achieving absolute stability.

In order to reduce the conservativeness of the sufficient condition derived by using the common quadratic Lyapunov function approach, Zelentsovsky [68] applied

the nonlinear transformation of

$$y_l = x_1^{p_{l1}} x_2^{p_{l2}} ... x_n^{p_{ln}}, \quad l = 1, ..., m \tag{2.8}$$

Here p_{li} are chosen so that $p_{li} \geq 0$ and $\sum_{i=1}^{n} p_{li} = p$, and $m = \begin{pmatrix} n+p-1 \\ p \end{pmatrix}$. For example, if the original system is a 2nd-order system and the states are x_1 and x_2, then one choice of nonlinear transformations is $y_1 = x_1^2, y_2 = x_1 x_2, y_3 = x_2^2$ with $p = 2, n = 2$. It is shown that the common quadratic Lyapunov function approach with the nonlinear transformation may generate less conservative conditions for the absolute stability of the original system.

Instead of using quadratic Lyapunov functions, in the work [63], Xie *et al.* adopted two kinds of piecewise quadratic Lyapunov functions as follows:

$$V(x) = \max \{x^T P_1 x, x^T P_2 x\}, \ P_1 > 0, P_2 > 0 \tag{2.9}$$

and

$$V(x) = \min \{x^T P_1 x, x^T P_2 x\}, \ P_1 > 0, P_2 > 0 \tag{2.10}$$

Consider a linear time-varying system

$$\dot{x} = A(t)x, \quad A(t) \in Co\{A_1, A_2\} \tag{2.11}$$

where CoA_1, A_2 denotes the convex hull of A_1 and A_2 and $x \in \Re^n$. It is proved that this system is robustly stable with the Lyapunov function (2.9) if and only if there exist $\delta_1, \delta_2 \in [0, 1]$ such that the following set of LMIs have a solution for H_1 and

H_2:

$$\begin{aligned} A_1'H_1 + H_1A_1 &< 0, \qquad A_2'H_2 + H_2A_2 < 0 \\ (1-\delta_2)(A_1'H_2 + H_2A_1) + \delta_2(H_2 - H_1) &< 0 \\ (1-\delta_1)(A_2'H_1 + H_1A_2) - \delta_1(H_2 - H_1) &< 0 \\ 0 < H_1 &< I, \qquad 0 < H_2 < I. \end{aligned} \tag{2.12}$$

Recall that this robust stabilization problem is equivalent to the absolute stability problem with the choice of (2.4). With a second-order system example, the authors of this paper showed that the usage of the two-term piecewise quadratic Lyapunov functions further reduces the conservativeness of the sufficient conditions for the absolute stability, although computation time is increased.

Recently, Hu *et al.* [27] extended the classical absolute stability concept to admit more general sector conditions. The sector conditions are allowed to be piecewise linear functions that is either convex or concave. Common quadratic Lyapunov functions are utilized to generate sufficient conditions for the absolute stability and compute the region of attraction if the absolute stability does not hold globally.

2.2 Linear Programming

Linear programming is a special category of convex optimization problems in which the objective function and the constraints are linear [19]. Since its development in late 1940s, linear programming has found applications in many optimization problems in various disciplines such as microeconomics, business management and engineering.

A linear programming problem can be described in the standard form:

$$\begin{aligned} &maximize && c^T x \\ &subject\ to && Ax \leq b \end{aligned} \tag{2.13}$$

where $c \in \Re^n, x \in \Re^n, A \in \Re^{mxn}, b \in \Re^m$. It is straightforward to show that all linear programming problems, for example, one that minimizes a linear objective function with equality constraints, may be written in the standard form. It is noted that each linear programming problem corresponds to a dual problem. For example, the dual problem for the standard form (2.13) is

$$\begin{aligned} &minimize && b^T x \\ &subject\ to && A^T x \geq c \end{aligned} \tag{2.14}$$

It is reminded that not all linear programming problems are feasible. For a feasible linear programming problem, however, the optimal solution can be found in a very efficient manner because the local optima are also global optima and the optimum is always attained at a vertex of the convex polyhedron corresponding to the inequality constraints. Linear programming problems are often solved by simplex-based methods and interior point methods.

The command *linprog* from the optimization toolbox of $Matlab^{TM}$ implements the simplex algorithm to solve a linear programming problem. There is almost no practical limit on the number of variables and constraints that the Matlab solver can handle. Nonetheless, for a large-scale linear programming problem, one might want to choose other solvers, such as the GNU Linear Programming Kit (GLPK) [21], to achieve improved efficiency.

2.3 Backstepping Control

Consider the system

$$\begin{aligned} \dot{\eta} &= f(\eta) + g(\eta)\xi \\ \dot{\xi} &= u \end{aligned} \tag{2.15}$$

where $\eta \in \Re^n, \xi \in \Re, u \in \Re, f \in \Re^n, g \in \Re^n$ and $f(0) = 0$.

We want to design a state feedback control law to stabilize the origin of this system. Suppose a control law $\xi = \phi(\eta)$ with $\phi(0) = 0$ asymptotically stabilizes the state η. In other words, the origin of the system $\dot{\eta} = f(\eta)+g(\eta)\phi(\eta)$ is asymptotically stable. Consequently for this system one can find a Lyapunov function $V(\eta)$ with the following inequality satisfied for all η. Here $W(\eta)$ is positive definite.

$$\frac{\partial V}{\partial \eta}[f + g\phi] \leq -W(\eta) \tag{2.16}$$

After the change of variables $z = \xi - \phi(\eta)$, the system (2.15) becomes

$$\begin{aligned} \dot{\eta} &= [f(\eta) + g(\eta)\phi(\eta)] + g(\eta)z \\ \dot{z} &= u - \dot{\phi} \end{aligned} \tag{2.17}$$

With the notation of $v = u - \dot{\phi}$ and the choice of control effort $v = -\frac{\partial V}{\partial \eta}g(\eta) - kz, k > 0$, one can easily prove the asymptotical stability of the origin of the system (2.17) by using the Lyapunov function $V_a(\eta, \xi) = V(\eta) + 0.5z^2$. The associated state feedback control law is thus obtained as

$$u = \frac{\partial \phi}{\partial \eta}[f(\eta) + g(\eta)\xi] - \frac{\partial V}{\partial \eta}g(\eta) - k[\xi - \phi(\eta)] \tag{2.18}$$

In summary, the backstepping control is stated in the following lemma.

Lemma 2.1 Consider the system (2.15). Let $\phi(\eta)$ be a stabilizing state feedback control for the state η with $\phi(0) = 0$, and $V(\eta)$ be a Lyapunov function that satisfies (2.16) with some positive definite function $W(\eta)$. Then, the state feedback control (2.18) stabilizes the origin of (2.15), with $V(\eta) + 0.5[\xi - \phi(\eta)]^2$ as a Lyapunov function. Moreover, if all the assumptions hold globally and $V(\eta)$ is radially unbounded, the origin is globally asymptotically stable. $\square$

Next a more general system is considered:

$$\begin{aligned} \dot{\eta} &= f(\eta) + g(\eta)\xi \\ \dot{\xi} &= f_a(\eta, \xi) + g_a(\eta, \xi)u \end{aligned} \tag{2.19}$$

where $\eta \in \Re^n, \xi \in \Re^m, u \in \Re^m, f \in \Re^n, g \in \Re^{n\times m}, f_a \in \Re^m, g_a \in \Re^{m\times m}$ and $f(0) = 0$. This system can be transformed to the form (2.15) by using the control input

$$u = g_a(\eta, \xi)^{-1}[v - f_a(\eta, \xi)] \tag{2.20}$$

so that $\dot{\xi} = v$.

In the above, the stabilization of the state ξ is achieved by feedback linearization that requires a fairly accurate knowledge of the nonlinearity $f_a(\eta, \xi)$. However, in practical engineering systems, this exact knowledge is in general not attainable. As an alternative, the state ξ may be stabilized by using other control schemes, for example, the one that will be illustrated in Chapter 6 in stabilization of the dive-plane motion of supercavitating vehicles.

Chapter 3

Classical Absolute Stability for Second-Order Systems

In this chapter, we will focus on classical absolute stability of second-order systems, that is, absolute stability of second-order systems with symmetric sector bounds. Absolute stability of second-order systems with nonsymmetric sector bounds will be discussed in the next chapter.

Despite the extensive literature on absolute stability of nonlinear systems, even for the particular cases of second-order systems, a complete solution for the absolute stability problem has not been found until very recently in two independent papers [42] and [35]. In [42], Margaliot and Langholz discovered a necessary and sufficient condition for absolute stability of second-order systems by identifying the most destabilizing nonlinearity within the sector bounds. In [35], Leonov derived a necessary and sufficient condition for absolute stability of second-order systems by comparing the vector field of the nonlinear system with that of various piecewise linear systems.

Although the above-mentioned two papers addressed the same problem, the two results appear quite different. In this chapter, the existing results are refined to correct some mistakes in the original work and to make them easier to apply in practice. Furthermore, the refined two results are proved to be equivalent to each other. The rest of this chapter is organized as follows. In Section 3.1, Leonov's

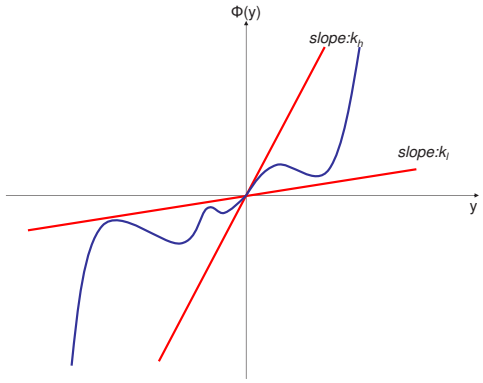

Figure 3.1: A nonlinearity bound in the sector (k_l, k_h)

result on absolute stability is introduced and refined. In Section 3.2, Margaliot and Langholz's result is presented and revised. In Section 3.3, the connection between these two results is established. To illustrate the application of these results, an example is given in Section 3.4.

3.1 Orginal Theory and Refinement: Leonov's Result

First let us review briefly the standard definition of sector boundaries and absolute stability. A nonlinearity $\phi(.)$ is said to be bound in the sector (k_l, k_h) if the following inequality holds for all y values

$$k_l y^2 \leq y\phi(y) \leq k_h y^2 \tag{3.1}$$

Such a nonlinearity is illustrated in Figure 3.1.

A system of the so-called Lure's form (3.2) is said to be *absolutely stable* if the origin is globally uniformly asymptotically stable for *any* nonlinearity $\phi(.)$ bound in

the sector (k_l, k_h).

$$\begin{aligned} \dot{x} &= Ax + Bu \\ y &= C^T x \\ u &= -\phi(y) \end{aligned} \tag{3.2}$$

Here we focus on second-order systems with a single nonlinearity where $x = (x_1\ x_2)^T \in \Re^2, u \in \Re^1, A \in \Re^{2\times 2}, B \in \Re^2$ and $C \in \Re^2$. In Leonov's work, the two-dimensional state space (x_1, x_2) is divided into the following four regions.

$$\begin{aligned} \Omega_1 &= \{(x_1, x_2) : x_2 \geq 0, ax_2 + bx_1 \geq 0\} \\ \Omega_2 &= \{(x_1, x_2) : x_2 \geq 0, ax_2 + bx_1 \leq 0\} \\ \Omega_3 &= \{(x_1, x_2) : x_2 \leq 0, ax_2 + bx_1 \leq 0\} \\ \Omega_4 &= \{(x_1, x_2) : x_2 \leq 0, ax_2 + bx_1 \geq 0\} \end{aligned}$$

Suppose there is a second-order linear system

$$\begin{aligned} \dot{x}_1 &= x_2 \\ \dot{x}_2 &= -\hat{\lambda}x_2 - \hat{\mu}x_1 \end{aligned} \tag{3.3}$$

By specifying different values in each of the four regions for the linear coefficients $\hat{\lambda}$ and $\hat{\mu}$, we define a system *PLS* as a system of the form (3.3) with

$$\hat{\lambda} = \begin{cases} \lambda + k_l a & \text{if } (x_1, x_2) \in \Omega_1 \text{ or } \Omega_3 \\ \lambda + k_h a & \text{if } (x_1, x_2) \in \Omega_2 \text{ or } \Omega_4 \end{cases} \tag{3.4}$$

and

$$\hat{\mu} = \begin{cases} \mu + k_l b & \text{if } (x_1, x_2) \in \Omega_1 \text{ or } \Omega_3 \\ \mu + k_h b & \text{if } (x_1, x_2) \in \Omega_2 \text{ or } \Omega_4 \end{cases} \tag{3.5}$$

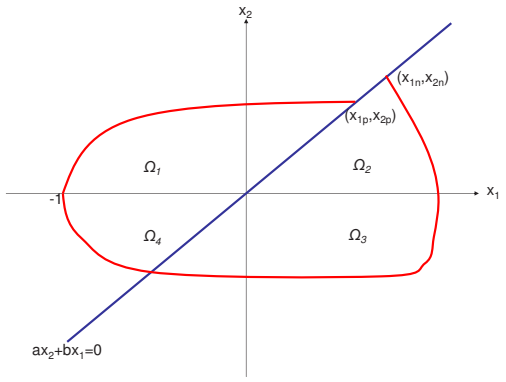

Figure 3.2: Definition of x_{1n} and x_{1p} when $a > 0$ and $b > 0$.

where λ, μ, a, b are constants.

Suppose one trajectory of the system PLS starts from the point $(-1, 0)$ and intersects with the line $ax_2 + bx_1 = 0$ at a point (x_{1p}, x_{2p}) with $x_{1p} > 0$; another trajectory of this system starts from the point $(-1, 0)$, and, in a negative time, intersects with the line $ax_2 + bx_1 = 0$ at a point (x_{1n}, x_{2n}) with $x_{1n} > 0$. Figure 3.2 illustrates the regions Ω_i $(i = 1, 2, 3, 4)$ and these special trajectories for the case when $a > 0$ and $b < 0$. These regions and trajectories can be constructed in a similar manner for the case when $a > 0$ and $b > 0$.

With the above-mentioned definitions, we are ready to state Leonov's result in Theorem 3.1.

$$\begin{aligned} \dot{x}_1 &= x_2 \\ \dot{x}_2 &= -\lambda x_2 - \mu x_1 - F_{NL}(t, ax_2 + bx_1) \end{aligned} \tag{3.6}$$

Theorem 3.1 [35]: For a second-order system of the form (3.6) where F_{NL} is any nonlinearity bound in the sector $(0, k)$, when $a > 0$, the system is absolutely

stable if and only if $\lambda > 0, \mu > 0, \lambda + ak > 0, \mu + bk > 0$ and one of the following five conditions is satisfied. When $a < 0$, the system is absolutely stable if and only if the same conditions hold where a, b, μ, λ are replaced with $-a, -b, \mu + ka, \lambda + kb$ respectively. If $a = 0$, the system is absolutely stable if and only if these conditions hold with $a \to 0$. Furthermore, the nonlinear system is absolutely stable for $k = \infty$ if one of the first three conditions hold.

1. $b = 0$
2. $b < 0$ and $\lambda^2 \geq 4\mu$
3. $b > 0, \lambda^2 \geq 4\mu$ and $\frac{\lambda}{2} + \sqrt{\frac{\lambda^2}{4} - \mu} \geq \frac{b}{a}$
4. $b > 0$; Condition 3 does not hold; and $(\lambda + ak)^2 \geq 4(\mu + bk)$, $\frac{\lambda+ak}{2} - \sqrt{\frac{(\lambda+ak)^2}{4} - (\mu + bk)} \leq \frac{b}{a}$
5. Conditions 1-4 do not hold and $x_{1n} - x_{1p} > 0$ where the quantities x_{1n}, x_{1p} are associated with $k_l = 0, k_h = k$.

Proof Compare the vector field of the nonlinear system with that of the system *PLS* and construct closed curves in the planar state space. Details can be found in the reference [35]. □

It is important to point out that if the second condition holds, the system is not absolutely stable for $k = \infty$ because the condition $\mu + bk > 0$ breaks down when $b < 0$. This mistake will be corrected in Theorem 3.2.

Below we will refine Theorem 3.1 to make it easier to apply in practice. With respect to the same problem as that in Theorem 3.1, we have the following result.

Theorem 3.2: For a second-order system of the form (3.6) where F_{NL} is any nonlinearity bound in the sector $(0, k)$, when $a > 0$, the system is absolutely stable if and only if $\lambda > 0, \mu > 0, \lambda + ak > 0, \mu + bk > 0$ and one of the following four conditions is satisfied. When $a < 0$, the system is absolutely stable if and only if the same conditions hold where a, b, μ, λ are replaced with $-a, -b, \mu + ka, \lambda + kb$ respectively. If $a = 0$, the system is absolutely stable if and only if these conditions hold with $a \to 0$. Furthermore, the nonlinear system is absolutely stable for $k = \infty$ if the first or the third condition holds.

1. $b = 0$
2. $b < 0$ and $\lambda^2 \geq 4\mu$
3. $b > 0, \lambda^2 \geq 4\mu$ and $\frac{\lambda}{2} + \sqrt{\frac{\lambda^2}{4} - \mu} \geq \frac{b}{a}$
4. $b > 0$; Condition 3 does not hold; $(\lambda + ak)^2 \geq 4(\mu + bk)$, and $\frac{\lambda + ak}{2} \leq \frac{b}{a}$
5. Conditions 1-4 do not hold and $x_{1n} - x_{1p} > 0$ where the quantities x_{1n}, x_{1p} are associated with $k_l = 0, k_h = k$.

Proof It is clear that the difference between this theorem and Theorem 3.1 exists in Condition 4. When Condition 3 does not hold and $\lambda^2 < 4\mu$, we have $b^2 - ab\lambda + a^2\mu > b^2 - ab\lambda + a^2\lambda^2/4 \geq 0$. When the last part of Condition 3 does not hold, that is, $\frac{\lambda}{2} + \sqrt{\frac{\lambda^2}{4} - \mu} < \frac{b}{a}$, it is clear that $b^2 - ab\lambda + a^2\mu > 0$. When $\frac{\lambda + ak}{2} \leq \frac{b}{a}$, the inequality $\frac{\lambda + ak}{2} + \sqrt{\frac{(\lambda + ak)^2}{4} - (\mu + bk)} \geq \frac{b}{a}$ can be proved to be equal to the inequality $b^2 - ab\lambda + a^2\mu > 0$. Therefore Condition 4 of Theorem 3.1 is simplified as Condition 4 in this theorem. □

3.2 Original Theory and Refinement: Margaliot and Langholz's Result

First integrals are widely used in the study of Hamiltonian systems [6]. For a general system that is not Hamiltonian, Margaliot and Langholz [42] generalized the concept of first integrals. The generalized first integrals are then utilized to identify the worst case switching law (WCSL) that results in a least-stable nonlinear system among the admissible set of nonlinear systems. By applying the WCSL, the maximal sector boundary $(0, k^*)$ for absolute stability is determined by solving a nonlinear equation numerically. The system is then absolute stable with any sector $(0, k)$ where $0 < k < k^*$, and not absolute stable with any sector $(0, k)$ where $k \geq k^*$.

A linear Hamiltonian system

$$\dot{x} = Ax \tag{3.7}$$

admits a classical first integral, that is, a function $H(x)$ which satisfies $H(x(t)) \equiv H(x(0))$ along any trajectory. However, for a general linear system that is not Hamiltonian, the concept of first integrals does not apply. Instead, a function $H^A(x(t))$, called a generalized first integral, can be constructed to be piecewise constant along any trajectory. The generalized first integral for a second-order linear system (3.7) can be constructed by considering two cases: in one case, the matrix A has a pair of complex eigenvalues and in the other case, the matrix A has real eigenvalues. It is noted that the generalized first integral is introduced to study absolute stability. Therefore the system (3.7) is assumed to be stable because otherwise the system is not absolutely stable and there is no need to introduce the generalized first integral.

In the first case, the system has a pair of complex eigenvalues. We denote one eigenvalue as $\lambda_1 = \alpha + j\beta$ with $\alpha < 0$ and $\beta < 0$ and the eigenvector of A^T corresponding to this eigenvalue as $z_1 = w - jv$. With $P = ww^T + vv^T$, the generalized first integral is constructed as

$$H^A(x) = x^T P x e^{\frac{2\alpha}{\beta} \arctan \frac{v^T x}{w^T x}} \tag{3.8}$$

This generalized first integral assumes a constant value almost everywhere. At times when $w^T x(t) = 0$, the function value jumps from one constant to another.

In the second case, the matrix A has two negative real eigenvalues. We denote the two eigenvalues as $0 > \lambda_1 > \lambda_2$, and the eigenvectors of A^T corresponding to these eigenvalues as w_1 and w_2. The generalized first integral is then constructed to be

$$H^A(x) = \frac{(w_1^T x)^{\frac{\lambda_2}{\lambda_1}}}{w_2^T x} \tag{3.9}$$

The system studied by Margaliot and Langholz [42] is a second-order nonlinear system of the form

$$\begin{aligned} \dot{x} &= Ax + B\phi(t, y) \\ y &= C^T x \end{aligned} \tag{3.10}$$

where $x \in \Re^2, y \in \Re^1, A \in \Re^{2\times 2}, B \in \Re^2, C \in \Re^2$ and the scalar function $\phi(t, y)$ represents any nonlinearity bound by the sector $(0, k)$. It is straightforward to see that this nonlinear system is equivalent to the system (3.11) where $0 \leq \delta(t, x) \leq 1$ and $B_k = A + kBC^T$.

$$\dot{x} = \delta(t, x)Ax + (1 - \delta(t, x))B_k x \tag{3.11}$$

Now we are ready to state Margaliot and Langholz's main result.

Theorem 3.3 [42]: For the second-order system (3.11), the worst case switching law (WCSL) $\delta(t,x)$ is given as

$$\delta(t,x) = \begin{cases} 1 & \text{if } x \in P^A \\ 0 & \text{otherwise} \end{cases} \tag{3.12}$$

where $P^A = \{x : \dot{H}^A_{B_k} = \nabla H^A(x) B_k x < 0\}$. The nonlinear system is absolutely stable for $k < k^*$. When $k = k^*$, any trajectory $\tilde{x}(t)$ of the system with the WCSL, starting from a non-origin point is closed. The constant k^* can be found by solving a transcendental equation numerically.

Proof By specifying a Lyapunov function, the WCSL can be identified and the absolute stability is proved. Details can be found in the reference [42]. □

In Theorem 3.3, the quantity k^* plays a key role in determining absolute stability. However, in some cases, such a k^* does not exist and accordingly we refine Theorem 3.3 as follows.

Theorem 3.4: For the second-order system (3.11), the worst case switching law (WCSL) $\delta(t,x)$ is given as

$$\delta(t,x) = \begin{cases} 1 & \text{if } x \in P^A \\ 0 & \text{otherwise} \end{cases} \tag{3.13}$$

where $P^A = \{x : \dot{H}^A_{B_k} = \nabla H^A(x) B_k x < 0\}$. Starting from a non-origin point, any trajectory $\tilde{x}(t)$ of the nonlinear system with the WCSL is either 1) not closed for

any $k \geq 0$, or 2) closed if and only if $k = k^*$ where k^* can be found by solving a transcendental equation numerically.

Proof If k^* exists, the proof can be found in the reference [42]. The proof of this theorem becomes complete if an example can be shown where the quantity k^* does not exist.

For a system (3.6) with $a = 1, b = -1, \mu = 1, \lambda = 3$, a special system of the general form 3.11, it is straightforward to find the WCSL to be:

$$\delta(t, x) = \begin{cases} 1 & \text{if } x_2(ax_2 + bx_1) \geq 0 \\ 0 & \text{otherwise} \end{cases} \tag{3.14}$$

According to the definitions in Section 3.1, the regions (x_1, x_2) where $x_2(ax_2+bx_1) \geq 0$ are Ω_1 and Ω_3. Within Ω_1 and Ω_3, the stable manifolds are located in the first and third quadrants, as is shown Figure 3.3. Therefore starting from a point $(c_i, 0)$, where $c_i < 0$, the system trajectory is attracted to the origin and will never enter the region Ω_2. Based on the index theory [30], any closed orbit of this system must encircle the origin. As a result, this system has no closed trajectory. It is noted that this fact holds regardless of the k value because the vector field of the system with the WCSL in the regions Ω_1 and Ω_3 does not contain k. □

3.3 Equivalence of the Two Results

Leonov's result is based on systems of the particular form (3.6). In contrast, Margaliot and Langholz's result is based on systems of the general form (3.10). This difference is not critical though, because the general form can be transformed

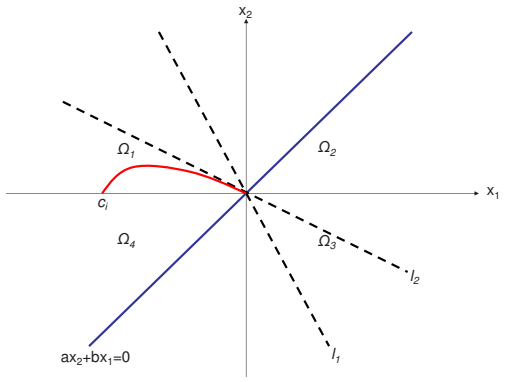

Figure 3.3: A system example in which there exists no k^* and none of system trajectories is closed. Dotted straight lines are stable manifolds.

to the special form through the state transformations in the Appendix A.1 when the system is controllable. For simplicity and without loss of generality we will focus on systems of the special form (3.6) for the purpose of comparison between these two results.

The following theorem establishes a connection between the WCSL in Margaliot and Langholz's result and the nonlinear system *PLS* in Leonov's result.

Theorem 3.5: The system (3.11) with $\delta(t, x)$ being the WCSL is the nonlinear system *PLS* that is used to prove Theorem 3.1 and Theorem 3.2.

Proof To find the WCSL, we first identify the matrices A and B_k in (3.11)

for the system (3.6)

$$A = \begin{pmatrix} 0 & 1 \\ -\mu & -\lambda \end{pmatrix} \tag{3.15}$$

$$B_k = \begin{pmatrix} 0 & 1 \\ -(\mu + kb) & -(\lambda + ka) \end{pmatrix} \tag{3.16}$$

Here two cases are considered where the matrix A has different types of eigenvalues. In the first case, $\Delta = \lambda^2 - 4\mu < 0$ and the matrix A has a pair of complex conjugate eigenvalues. According to the discussions in Section 3.2, the generalized first integral and the boundary function of P^A are determined as

$$H^A = [\mu x_1^2 + \lambda x_1 x_2 + x_2^2] e^{\frac{2\lambda}{\sqrt{4\mu-\lambda^2}} \arctan \frac{\sqrt{4\mu-\lambda^2} x_1}{\lambda x_1 + 2x_2}} \tag{3.17}$$

$$\nabla H_A(x) B_k x = -2kx_2(bx_1 + ax_2) e^{\frac{2\lambda}{\sqrt{4\mu-\lambda^2}} \arctan \frac{\sqrt{4\mu-\lambda^2} x_1}{\lambda x_1 + 2x_2}} \tag{3.18}$$

In the second case, $\Delta = \lambda^2 - 4\mu > 0$ and the matrix A has real eigenvalues. The generalized first integral and the boundary function of P^A are accordingly determined as

$$H^A = \frac{(\frac{\lambda+\sqrt{\Delta}}{2} x_1 + x_2)^{\frac{-\lambda-\sqrt{\Delta}}{-\lambda+\sqrt{\Delta}}}}{\frac{\lambda-\sqrt{\Delta}}{2} x_1 + x_2} \tag{3.19}$$

$$\nabla H_A(x) B_k x = -2kx_2(bx_1 + ax_2) \frac{\sqrt{\Delta}(\frac{\lambda+\sqrt{\Delta}}{2} x_1 + x_2)^{\frac{-2\sqrt{\Delta}}{-\lambda+\sqrt{\Delta}}}}{(\frac{\lambda-\sqrt{\Delta}}{2} x_1 + x_2)^2 (\lambda - \sqrt{\Delta})} \tag{3.20}$$

In both cases, we have $P^A = \Omega_1 \cup \Omega_3$ and therefore this theorem is proved. □

Furthermore, it is discovered that Leonov's result is equivalent to Margaliot and Langholz's result although different approaches are applied.

Theorem 3.6: Refined Leonov's result is equivalent to refined Margaliot and Langholz's result. That is, Theorem 3.2 is equivalent to Theorem 3.4.

Proof This theorem is proved by verifying the equivalence between Conditions 1-4 in Theorem 3.2 and cases 1)-2) in Theorem 3.4.

If Condition 1 or Condition 2 holds, then we have a similar situation as that in the proof of Theorem 3.4 (Figure 3.3). It is clear that closed trajectories are impossible and k^* does not exist. If Condition 3 holds, the system is absolutely stable according to Theorem 3.2. The absolute stability implies global asymptotic stability of the origin in the nonlinear system *PLS*. Thus this system has no closed trajectories and k^* does not exist.

If Condition 4 is satisfied, the system is absolutely stable and a closed trajectory does not exist in the system (3.11) with the WCSL. If the value of k is increased and Condition 4 breaks down, one need to check Condition 5 in order to determine whether the system is absolutely stable.

In the following Condition 5 is examined. In this case, the condition $x_{1n} - x_{1p} > 0$ (Figure 3.2) is equivalent to the condition $x_{1l} > -1$ (Figure 3.4). From the symmetry of the vector field of the nonlinear system *PLS*, these conditions are also equivalent to the condition $x_{1r} < 1$.

In order to check the condition $x_{1r} < 1$, here two cases are considered to find $\frac{dx_{1r}}{dk}$ depending upon the type of eigenvalues of the system *PLS* in the region Ω_2 and Ω_4.

1. The Jacobian matrix in the region Ω_2 and Ω_4 has two negative real eigen-

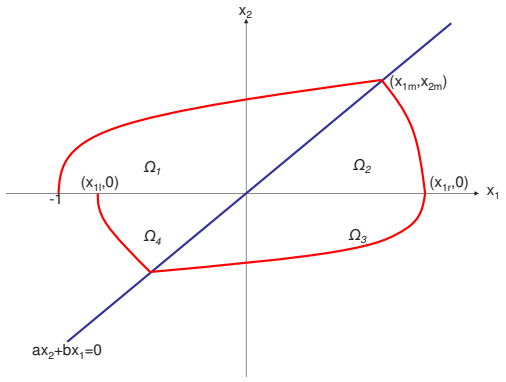

Figure 3.4: Illustration for the proof of Theorem 3.6.

values. After cumbersome algebraic manipulations, we have

$$\frac{dx_{1r}}{dk} = \frac{2x_{1m}e^{-\frac{\lambda_2 t_2}{2}}}{a\Delta_2\sqrt{(2\mu_2 a-\lambda_2 b)^2-b^2\Delta_2}}[-2b+(\lambda_2 b-2\mu_2 a)t_2](b^2+\mu_2 a^2-\lambda_2 ab)>0 \tag{3.21}$$

where $t_2 = \frac{1}{\sqrt{\Delta_2}}\ln\frac{2\mu_2 a+b(-\lambda_2-\sqrt{\Delta_2})}{2\mu_2 a+b(-\lambda_2+\sqrt{\Delta_2})} > 0$, $\Delta_2 = \lambda_2^2-4\mu_2 > 0$, $\lambda_2 = \lambda+ka$, $\mu_2 = \mu+kb$.

2. The Jacobian matrix in the region Ω_2 and Ω_4 has a pair of complex eigenvalues with negative real parts. After cumbersome algebraic manipulations, we have

$$\frac{dx_{1r}}{dk} = 2e^{\alpha_2 t_2}x_{1m}\cos\beta_2 t_2\frac{\mu_2 a^2+b^2-\lambda_2 ab}{a\Delta_2}\left(\frac{2b}{2\mu_2 a-\lambda_2 b}+t_2\right)>0 \tag{3.22}$$

where $t_2 = \frac{1}{\beta_2}\arctan\frac{b\sqrt{-\Delta_2}}{2\mu_2 a-\lambda_2 b} > 0$, $\alpha_2 = -\frac{\lambda}{2}$, $\beta_2 = -\frac{\sqrt{-\Delta_2}}{2}$

Suppose Condition 5 holds for some k. As k is increased, x_{1r} increases. For any $k > 0$, $x_{1r} < 1$; or at some value $k = k^*$, $x_{1r} = 1$. These correspond to case 1) and 2) in Theorem 3.4 respectively. □

3.4 Example

Refinement of the absolute stability conditions in previous sections corrects some mistakes in the original works and makes them easier to apply in applications. In this section, a system example is given to illustrate application of the refined results and also the connection between the refined version of the work [35] and [42].

Suppose there is a system

$$\begin{pmatrix} \dot{\hat{x_1}} \\ \dot{\hat{x_2}} \end{pmatrix} = \begin{pmatrix} -1 & -5/8 \\ -25/8 & -3 \end{pmatrix} \begin{pmatrix} \hat{x_1} \\ \hat{x_2} \end{pmatrix} + \begin{pmatrix} -1 \\ -1 \end{pmatrix} F_{NL}(t, \hat{x_1} + \hat{x_2}) \tag{3.23}$$

with the nonlinearity F_{NL} bound in the sector $(0, 1)$.

After the state transformation

$$\begin{pmatrix} x_1 \\ x_2 \end{pmatrix} = \begin{pmatrix} -2 & 2 \\ 0.75 & 0.25 \end{pmatrix} \begin{pmatrix} \hat{x_1} \\ \hat{x_2} \end{pmatrix} \tag{3.24}$$

the system becomes one in the form (3.6) with $a = 0.25, b = 2, \lambda = 4, \mu = 1, k = 1$. It is straightforward to show that Condition 4 of Theorem 3.2 is satisfied and therefore this system is absolutely stable. The determination of absolute stability here only involves some simple algebraic calculations.

To illustrate the result of Theorem 3.6, we identify the nonlinear system *PLS* in Leonov's approach and also the WCSL $\delta(t, x)$ that are associated with this system.

According to (3.4) and (3.5), the system *PLS* is:

$$\begin{pmatrix} \dot{x_1} \\ \dot{x_2} \end{pmatrix} = \begin{cases} \begin{pmatrix} x_2 \\ -4x_2 - x_1 \end{pmatrix} & \text{if } x_2(0.25x_2 + 2x_1) \geq 0 \\ \begin{pmatrix} x_2 \\ -4.25x_2 - 3x_1 \end{pmatrix} & \text{if } x_2(0.25x_2 + 2x_1) \leq 0 \end{cases} \tag{3.25}$$

Following the definition of the WCSL in Theorem 3.3, we find

$$P^A = \{x : \nabla H^A(x) B_k x < 0\} = \{(x_1, x_2) : x_2(0.25x_2 + 2x_1) \geq 0\} \tag{3.26}$$

and the WCSL:

$$\delta(t, x) = \begin{cases} 1 & \text{if } x_2(0.25x_2 + 2x_1) \geq 0 \\ 0 & \text{if } x_2(0.25x_2 + 2x_1) \geq 0 \end{cases} \tag{3.27}$$

Therefore the system (3.11) with the WCSL is exactly the nonlinear system *PLS* and Theorem 3.5 is confirmed.

To compute the quantity k^*, we first find that Condition 4 of Theorem 3.2 is violated if k is increased to be greater than 2.04. By increasing k further, we need to check Condition 5 of Theorem 3.2. It can be numerically found that $k^* = \infty$ for this system. In other words, this system is absolutely stable for any nonlinearity living in the first and third quadrants.

Chapter 4

Generalized Absolute Stability for Second-Order Systems

In the previous chapter, necessary and sufficient conditions for absolute stability of second-order systems are studied. The absolute stability in that setting is associated with nonlinearities that are within a *symmetric* sector bound. In the current chapter, this classical absolute stability concept is generalized to allow *nonsymmetric* sector bounds.

In Section 4.1, motivation for this generalization is given. In Section 4.2, the problem to be solved in the remaining parts of this chapter is formulated. In Section 4.3, duality in the generalized absolute stability is introduced. In Section 4.4, necessary and sufficient condition is elaborated. Finally in Section 4.5, the nonsymmetric sector bound is further generalized and associated necessary and sufficient condition is given.

4.1 Motivation for the Generalization

Since the introduction of the absolute stability concept in the 1940s, the sector bound of nonlinearities has been symmetric with respect to the origin (illustrated in Figure 4.1). However in practical engineering systems, a general nonlinearity and associated sector bound does not satisfy this symmetry assumption. For instance, nonsymmetric nonlinearities are encountered in dynamic models of amplifier circuits

[3], engineering control systems [32], autonomous underwater vehicles [7], earthquake engineering [17], and hard disk drives [23].

Nonlinearities in some other engineering systems have the symmetric property. For some reasons such as navigation and guidance, one may desire to operate these systems at an equilibrium point other than the origin. This bias from the origin would then transform the symmetric nonlinearity to a nonsymmetric one with respect to the equilibrium point.

Therefore it is of important value, in both theoretic development and engineering practice, to generalize the classical concept of absolute stability to allow nonsymmetric sector bounds, both in theory and in practice. One may argue that a nonsymmetric sector bound can always be relaxed to a larger symmetric one. However, by doing this, conservativeness is introduced in stability analysis and controller design of the system. In some cases, the relaxation of sector bounds may even leads to infeasibility in stabilization effort.

4.2 Problem Statement

For the purpose of comparison, the classical symmetric sector bound is illustrated again here in Figure 4.1.

The nonsymmetric sector bounds are defined by using the following piecewise linear functions where $k_i, i = 1, 2$ are positive real numbers:

$$\rho_{k_1,k_2}(v) = \begin{cases} k_1 v & \text{if } v \leq 0 \\ k_2 v & \text{if } v > 0 \end{cases} \tag{4.1}$$

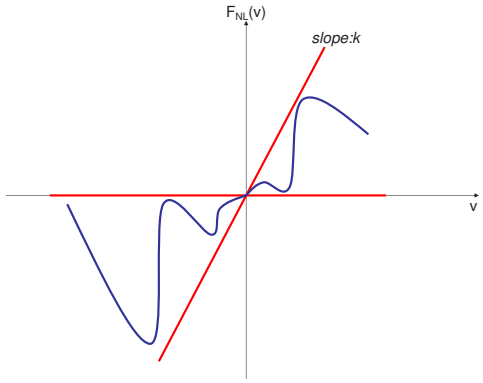

Figure 4.1: Sector conditions in classical absolute stability studies.

A nonsymmetric sector bound is then defined as follows. One such sector bound is illustrated in Figure 4.2.

Definition 4.1: A nonlinearity $F_{NL}(t, v)$ lies in the sector $(0, k_1, k_2)$ if

$$0 \leq vF_{NL}(t, v) \leq v\rho_{k_1,k_2}(v). \tag{4.2}$$

If $k_1 \neq k_2$, the nonlinearity is said to be bound by a *nonsymmetric* sector with respect to the variable v. Otherwise ($k_1 = k_2 = k$), the nonlinearity is bound in a symmetric sector, which is associated with the classical absolute stability concept.

As a further generalization, the following definition is introduced and corresponding illustration is presented in Figure 4.3.

Definition 4.2: A nonlinearity $F_{NL}(t, v)$ is said to be bound in sector (k_1, k_2, k_3, k_4) if

$$\begin{aligned} k_2 v \leq F_{NL}(t, v) \leq k_3 v \qquad & \text{if } v \leq 0 \\ k_1 v \leq F_{NL}(t, v) \leq k_4 v \qquad & \text{if } v > 0 \end{aligned} \tag{4.3}$$

It is noted that in Definition 4.1, $k_1 > 0, k_2 > 0$ whereas in Definition 4.2,

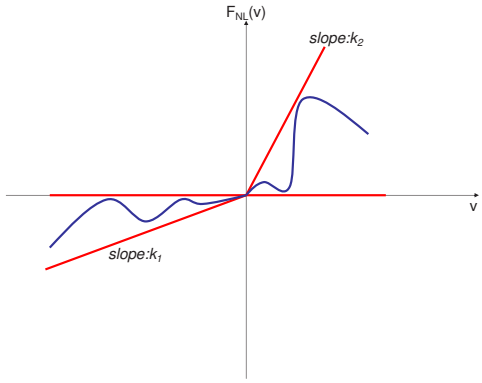

Figure 4.2: Nonlinearity bound in the nonsymmetric sector $(0, k_1, k_2)$

.

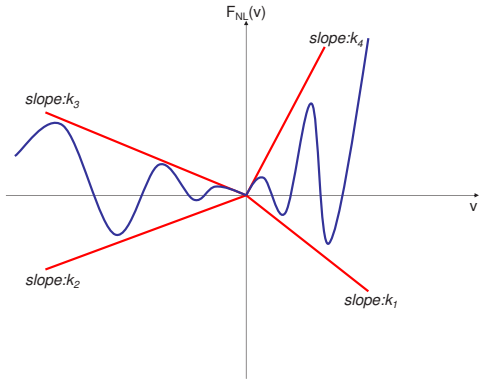

Figure 4.3: Nonlinearity bound in the more general asymmetric sector (k_1, k_2, k_3, k_4)

$k_i, i = 1, 2, 3, 4$ can be positive or negative if only they satisfy the inequalities $k_1 < k_4, k_2 > k_3$. Apparently, the sector $(0, k_1, k_2)$ is equivalent to the sector $(0, k_1, 0, k_2)$.

Based on the generalizations of sector bounds, two main problems of this chapter are formulated as follows.

Problem 4.1: Determine necessary and sufficient conditions for global asymptotic stability at the origin for the second-order nonlinear system

$$\begin{aligned} \dot{x} &= y \\ \dot{y} &= -\alpha y - \beta x - F_{NL}(t, ay + bx) \end{aligned} \tag{4.4}$$

where the nonlinearity $F_{NL}(t, \cdot)$ is bound in the nonsymmetric sector $(0, k_1, k_2)$. □

Problem 4.2: Determine necessary and sufficient conditions for global asymptotic stability at the origin for the second-order nonlinear system (4.4) where the nonlinearity $F_{NL}(t, \cdot)$ is bound in the nonsymmetric sector (k_1, k_2, k_3, k_4). □

It is important to point out that the particular form (4.4) is chosen without loss of generality because any controllable second-order Lur'e system can be put into this form by using some appropriate state transformation, as shown in the Appendix A.1.

4.3 Duality

Regarding the absolute stability of systems with nonsymmetric sector bounds, here a duality principle is established.

Theorem 4.1: The nonlinear system (4.4) with the sector bound $(0, k_1, k_2)$ is absolutely stable if and only if the system (4.4) with the sector bound $(0, k_2, k_1)$ is

absolutely stable.

Proof For the nonlinear system (4.4) with the sector bound $(0, k_1, k_2)$, we carry out the state transformation $\hat{x} = -x, \hat{y} = -y$. The system equation in the new states reads as:

$$\begin{aligned} \dot{\hat{x}} &= \hat{y} \\ \dot{\hat{y}} &= -\alpha\hat{y} - \beta\hat{x} - \hat{F}_{NL}(t, a\hat{y} + b\hat{x}) \end{aligned} \tag{4.5}$$

Here $\hat{F}_{NL}(t, a\hat{y} + b\hat{x}) = -F_{NL}(t, ay + bx)$. Making use of the fact that $F_{NL}(t, \cdot)$ is bound by the sector $(0, k_1, k_2)$, it is straightforward to show that the nonlinearity $\hat{F}_{NL}(t, \cdot)$ is bound by the sector $(0, k_2, k_1)$. Therefore the absolute stability of the system (4.4) with the sector bound $(0, k_1, k_2)$ is equivalent to that of the system (4.5) with the sector bound $(0, k_2, k_1)$. □

For nonlinear systems with a more general nonsymmetric sector bound, the following theorem holds.

Theorem 4.2: The nonlinear system (4.4) with the sector bound (k_1, k_2, k_3, k_4) is absolutely stable if and only if the system (4.4) with the sector bound (k_3, k_4, k_1, k_2) is absolutely stable.

Proof The proof of this theorem is similar as that of Theorem 4.1, in which the key step is the state transformation $\hat{x} = x, \hat{y} = -y$. □

4.4 Solution to Problem 4.1: Generalization of Sector Bounds

In this section, necessary and sufficient condition is derived for Problem 4.1, through application of Leonov's approach of vector field comparison. As a first step,

a few definitions are given including the following regions

$$\begin{aligned} \Omega_1 &= \{y \geq 0, ay + bx \geq 0\} \\ \Omega_2 &= \{y \geq 0, ay + bx \leq 0\} \\ \Omega_3 &= \{y \leq 0, ay + bx \leq 0\} \\ \Omega_4 &= \{y \leq 0, ay + bx \geq 0\} \end{aligned} \tag{4.6}$$

a linear system

$$\begin{aligned} \dot{x} &= y \\ \dot{y} &= -\mu x - \lambda y \end{aligned} \tag{4.7}$$

and various linear systems

1. LS_{13}: system (4.7) with $\mu = \beta, \lambda = \alpha$.

2. LS_2: (4.7) with $\mu = \beta + k_1 b, \lambda = \alpha + k_1 a$.

3. LS_4: (4.7) with $\mu = \beta + k_2 b, \lambda = \alpha + k_2 a$.

In the following, we denote the quantity p associated with the system q as $p|_q$. For convenience, we name the nonlinear system in Problem 4.1 as NLS_1. Then in the regions Ω_1 and Ω_3, it can be shown that

$$\frac{\dot{y}}{\dot{x}}|_{NLS_1} = \frac{-\alpha y - \beta x - F_{NL}}{y} \leq \frac{-\alpha y - \beta x}{y} = \frac{\dot{y}}{\dot{x}}|_{LS_{13}} \tag{4.8}$$

Similarly in the region Ω_2, we have

$$\frac{\dot{y}}{\dot{x}}|_{NLS_1} \leq \frac{\dot{y}}{\dot{x}}|_{LS_2} \tag{4.9}$$

In the region Ω_4, we have

$$\frac{\dot{y}}{\dot{x}}|_{NLS_1} \leq \frac{\dot{y}}{\dot{x}}|_{LS_4} \tag{4.10}$$

Here we first look at the case when $a > 0$. For different values of the system parameters $a, b, \alpha, \beta, k_1, k_2$, the following propositions are given. These propositions are then summarized in Theorem 4.3 giving necessary and sufficient condition for Problem 1 when $a > 0$. The cases when $a < 0$ and $a = 0$ will be addressed in Theorem 4.4 and Theorem 4.5 respectively.

Proposition 4.1: If $a > 0$, then the uncertain system in Problem 4.1 is not absolutely stable if one or more of the following conditions does not hold.

1. $\alpha > 0$
2. $\beta > 0$
3. $\beta + bk_1 > 0$
4. $\beta + bk_2 > 0$

Proof: If $\alpha \leq 0$ or $\beta \leq 0$, the system in Problem 4.1 is unstable with a trivial nonlinearity $F_{NL}(t, u) = 0$. Regarding the last two conditions, we consider a system PLS that has the same vector field as that of the linear system LS_i in the region Ω_i, where $i = 13, 2, 4$. If $\beta + bk_1 \leq 0$, the system PLS is unstable because the system LS_2 has a saddle point and the unstable manifold is located in the region Ω_2. Similarly, if $\beta + bk_2 \leq 0$, the system PLS is unstable. Therefore the last two conditions are needed to ensure absolute stability of the uncertain system in Problem 4.1. □

Proposition 4.2: If $a > 0, b = 0$ and $\alpha > 0, \beta > 0$, the uncertain system in Problem 4.1 is absolutely stable for any $k_1 > 0, k_2 > 0$.

Proof: With $a > 0$ and $b = 0$, the state space (x, y) is divided into the region Ω_1 (the half plane $y \geq 0$) and the region Ω_3 (the half plane $y \leq 0$). For the linear system LS_{13}, we have $\lambda > 0$ and $\mu > 0$ due to the assumption of $\alpha > 0$ and $\beta > 0$. If $\lambda^2 \geq 4\mu$, the origin of this linear system is a stable node and both stable manifolds lie in the second and fourth quadrants. Therefore two trajectories can be constructed ending at the points $(c, 0)$ and $(-c, 0)$ with $c > 0$, as illustrated in Figure 4.4. It is noted that the particular vector field form of the system (4.4) forces the trajectory to travel to the right in the upper half plane ($y > 0$) and to the left in the lower half plane ($y < 0$). A closed curve (not a trajectory) is then formed by joining these two trajectories with the vertical lines $x = \pm c$.

The inequality in (4.8) implies that the vector field of the uncertain system NLS_1 on the two trajectories ending at the points $(c, 0$ and $(-c, 0)$ points towards the inner side of the closed curve that is constructed. On the vertical lines $x = \pm c$, the vector field also points towards the inner side of the closed curve, as determined by the first equation in (4.4). Therefore the region enveloped by the closed curve is an invariant subspace. Clearly this invariant property remains unchanged for other positive values of c. In other words, all trajectories will ultimately be attracted to the origin and the absolute stability is proven.

If $\lambda^2 \leq 4\mu$, the origin of LS_{13} is a stable focus. A closed curve as illustrated in Figure 4.5 can be constructed. This curve is composed of the trajectory starting from the point $(c, 0)$ in a positive time, the trajectory starting from the same point in

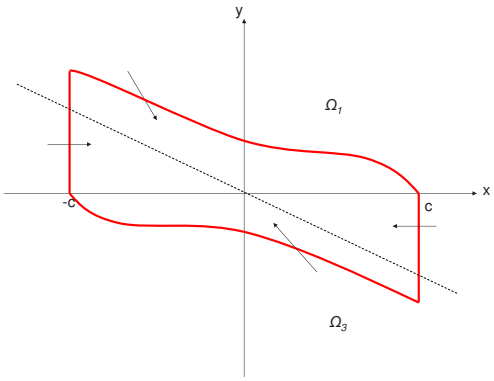

Figure 4.4: Illustration for the proof of Proposition 4.2. The origin of the system LS_{13} is a stable node.

a negative time, and a vertical line in the second quadrant. The region enveloped by this closed curve is an invariant subspace for any positive value of c. THe absolute stability in this case is thus proved. □

Proposition 4.3: If $a > 0, b < 0$, $\alpha > 0, \beta + bk_1 > 0, \beta + bk_2 > 0$ and $\alpha^2 \geq 4\beta$, the uncertain system in Problem 4.1 is absolutely stable.

Proof: With $a > 0$ and $b < 0$, the state space is divided into four regions $\Omega_i, i = 1, 2, 3, 4$ as defined in (4.6). With regards to the regions Ω_1 and Ω_3, the origin of the system LS_{13} is a stable node and both stable manifolds are in the second and fourth quadrants.

Due to the assumption $\beta + bk_1 > 0, \beta + bk_2 > 0$, the origin of the systems LS_2 and LS_4 must be either a stable focus, or a stable node. If it is a stable node, a straightforward calculation shows that the stable manifolds are in the second and fourth quadrants. In both cases (focus or node), the trajectories of the systems LS_2 and LS_4 starting from the point $(c, 0)$ and $(-c, 0)$ respectively intersect with the line

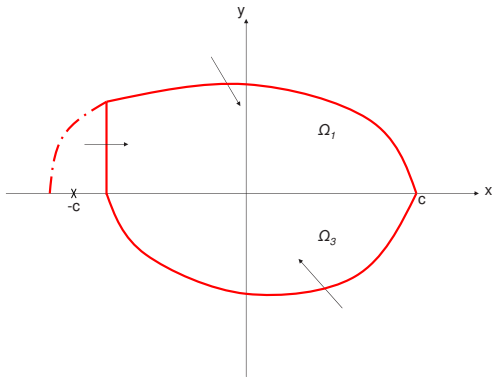

Figure 4.5: Illustration for the proof of Proposition 4.2. The origin of the system LS_{13} is a stable focus.

$ay + bx = 0$ in a negative time. Therefore we can construct a closed curve as shown in Figure 4.6. Following the same argument as that in the proof of Proposition 4.2, we can prove the absolute stability of the uncertain system in Problem 4.1 by verifying the invariant property of the region enveloped by the closed curve. □

Proposition 4.4: If $a > 0, b > 0, \alpha > 0, \beta > 0, \alpha^2 \geq 4\beta$ and $\frac{\alpha}{2} + \sqrt{\frac{\alpha^2}{4} - \beta} \geq \frac{b}{a}$, the uncertain system in Problem 4.1 is absolutely stable for any $k_1 > 0, k_2 > 0$.

Proof: In this case, the origin of the system LS_{13} is a stable node. Furthermore, at least one of the stable manifolds is located between the y axis and the line $ay + bx = 0$. Consequently a closed curve as illustrated in Figure 4.7 can be constructed. Absolute stability is then proved by using the invariant subspace argument that is used in the proof of Propositions 4.2 and 4.3. □

Proposition 4.5: If $a > 0, b > 0$, $\alpha > 0, \beta > 0$, conditions in Proposition 4.4 do not hold, and $(\alpha + ak_1)^2 \geq 4(\beta + bk_1)$, $\frac{\alpha + ak_1}{2} - \sqrt{\frac{(\alpha + ak_1)^2}{4} - (\beta + bk_1)} \leq \frac{b}{a}$, the uncertain system in Problem 4.1 is absolutely stable.

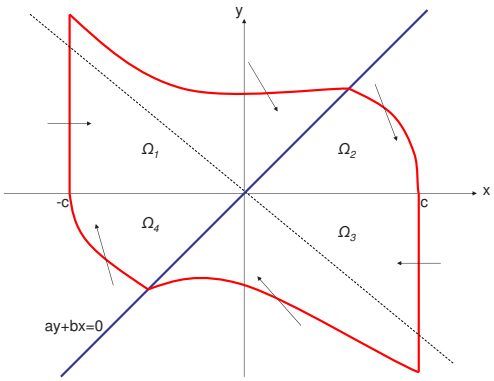

Figure 4.6: Illustration for the proof of Proposition 4.3.

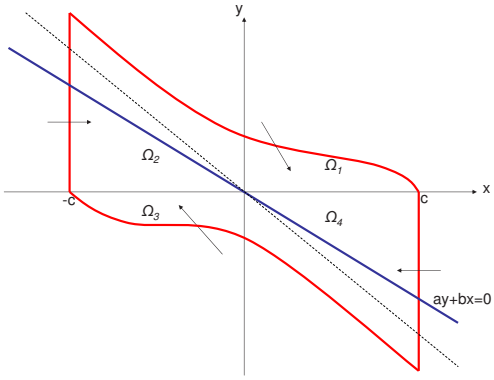

Figure 4.7: Illustration for the proof of Proposition 4.4.

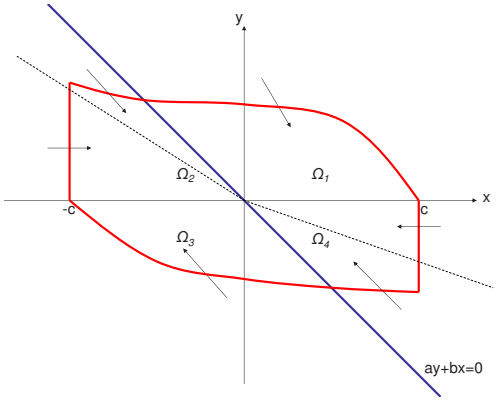

Figure 4.8: Illustration for the proof of Proposition 4.5. The origin of the system LS_4 is a node.

Proof: Because the conditions in Proposition 4.4 do not hold, the system LS_{13} has a stable focus or a stable node of which both stable manifolds are located in the regions Ω_2 and Ω_4. Therefore the trajectory of LS_{13} starting from the point $(c, 0)$ will intersect with the line $ay + bx = 0$ in a negative time. With the conditions related to k_1 in this proposition, the system LS_2 has a stable node, of which at least one of the stable manifolds is located in the region Ω_2 and Ω_4.

Regarding the system LS_4, here two cases are considered. In the first case, the origin of the system is a node. Since $\alpha + k_1 a > 0$ and $\beta + k_2 b > 0$, both stable manifolds of LS_4 is located in the second and fourth quadrants. Depending on the relative location of the stable manifolds with respect to the line $ay + bx = 0$, a closed curve as illustrated in Figures 4.8-4.10 can be constructed. Correspondingly the absolute stability is then proved by comparing the vector field on this closed curve with that of the uncertain system in Problem 4.1.

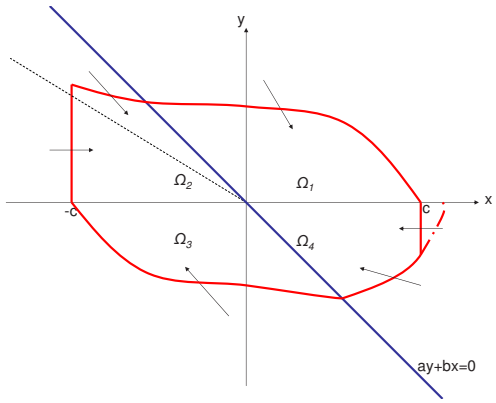

Figure 4.9: Illustration for the proof of Proposition 4.5. The origin of the system LS_4 is a focus.

In the second case, the system LS_4 has a stable focus. Depending on the relative location of the intersection point Q with respect to the point $(c, 0)$, a closed curve, as illustrated in Figure 4.9 and in Figure 4.10 respectively, can be constructed to prove the absolute stability of the uncertain system in Problem 4.1. □

Proposition 4.6: If $a > 0, b > 0$, $\alpha > 0, \beta > 0$, conditions in Proposition 4.4 do not hold, and $(\alpha + ak_2)^2 \geq 4(\beta + bk_2)$, $\frac{\alpha+ak_2}{2} - \sqrt{\frac{(\alpha+ak_2)^2}{4} - (\beta + bk_2)} \leq \frac{b}{a}$, the uncertain system in Problem 4.1 is absolutely stable.

Proof: By the duality principle in Theorem 4.1, the absolute stability in this case is equivalent to that in Proposition 4.5. □

Recall that the system PLS has the same vector field as that of the linear system LS_i in the region Ω_i, where $i = 13, 2, 4$. In Propositions 4.2-4.6, none of the trajectories of the system PLS travels through all four regions Ω_i. Next we

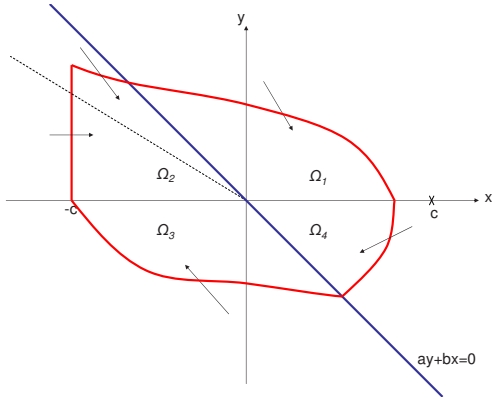

Figure 4.10: Illustration for the proof of Proposition 4.5. The origin of the system LS_4 is a focus.

consider the cases where these propositions are not applicable. That is, in these cases, each of the trajectories of the system PLS travel through all four regions. As illustrated in Figure 4.11, the trajectory of the system PLS starts from the point $(-c, 0)$, intersects with the line $ay + bx = 0$ at a point (x_1, y_1) and with the line $y = 0$ at a point $(x_2, 0)$, and finally intersects again with the line $ay + bx = 0$ at a point (x_{pc}, y_{pc}). In a negative time, the trajectory of the system PLS starting from the point $(-c, 0)$ intersects with the line $ay + bx = 0$ at a point (x_{nc}, y_{nc}). When $c = 1$, we let $x_p = x_{pc}, y_p = y_{pc}, x_n = x_{nc}, y_n = y_{nc}$. With these notations, the following two propositions give conditions for determining absolute stability of the uncertain system in Problem 1.

Proposition 4.7: When the absolute stability of the uncertain system in Problem 4.1 cannot be judged according to Propositions 4.1-4.6, the uncertain system is absolutely stable if and only if $y_n < y_p$.

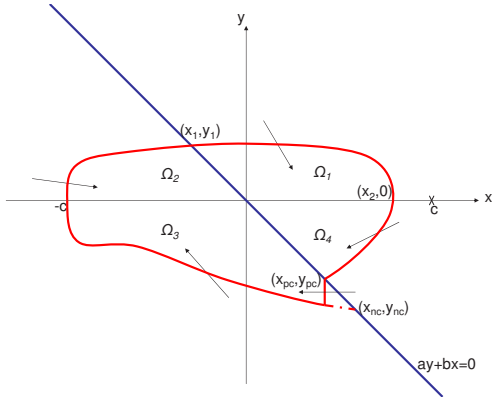

Figure 4.11: Illustration for the proof of Proposition 4.7.

Proof: Given the fact that each of the systems LS_{13}, LS_2 and LS_4 has a linear vector field, it is easily shown that $y_n < y_p \Leftrightarrow y_{nc} < y_{pc}$ for any positive number c. If $a > 0, b > 0$, a closed curve, as illustrated in Figure 4.11, can be constructed because conditions in Propositions 4.1-4.6 are not satisfied. Here the vertical line in the region Ω_3 connects the linear system trajectories. Absolute stability is then proved by applying the invariant subspace argument to the region enveloped by the closed curve. In a similar manner, absolute stability is established in the case where $a > 0, b < 0$.

If $y_n < y_p$ does not hold, an unstable trajectory can be identified for the uncertain system in Problem 4.1 with a particular choice of the following nonlinearity

$$F_{NL}(t,u) = \begin{cases} 0 & \text{if } t_0 \le t < t_1 \\ k_1 u & \text{if } t_1 \le t < t_2 \\ 0 & \text{if } t_2 \le t < t_3 \\ k_2 u & \text{if if } t_3 \le t < t_4 \\ \ldots\ldots & \end{cases} \tag{4.11}$$

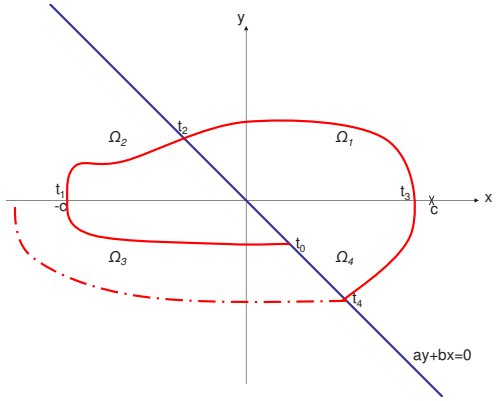

Figure 4.12: Illustration for the proof of Proposition 4.7.

where $t_j, j = 0, 1, 2, ...$ are times as shown in Figure 4.12. This nonlinearity is bound in the sector $(0, k_1, k_2)$ and the trajectory starting at t_0 goes to ∞. Therefore the uncertain system in Problem 4.1 is not absolutely stable. □

To summarize, these seven propositions combined give the following necessary and sufficient condition for absolute stability of an uncertain system in Problem 4.1.

Theorem 4.3: If $a > 0$, the uncertain system in Problem 4.1 is absolutely stable if and only if $\alpha > 0, \beta > 0$ and one of the following conditions is satisfied.

1. $b = 0$

2. $b > 0$, $\alpha^2 \geq 4\beta$ and one set of the following inequalities hold.

   - $\frac{\alpha}{2} + \sqrt{\frac{\alpha^2}{4} - \beta} \geq \frac{b}{a}$
   - $\frac{\alpha}{2} + \sqrt{\frac{\alpha^2}{4} - \beta} < \frac{b}{a}, (\alpha + ak_1)^2 \geq 4(\beta + bk_1), \frac{\alpha + ak_1}{2} \leq \frac{b}{a}$
   - $\frac{\alpha}{2} + \sqrt{\frac{\alpha^2}{4} - \beta} < \frac{b}{a}, (\alpha + ak_2)^2 \geq 4(\beta + bk_2), \frac{\alpha + ak_2}{2} \leq \frac{b}{a}$

3. $b > 0$, $\alpha^2 < 4\beta$ and one set of the following inequalities hold.

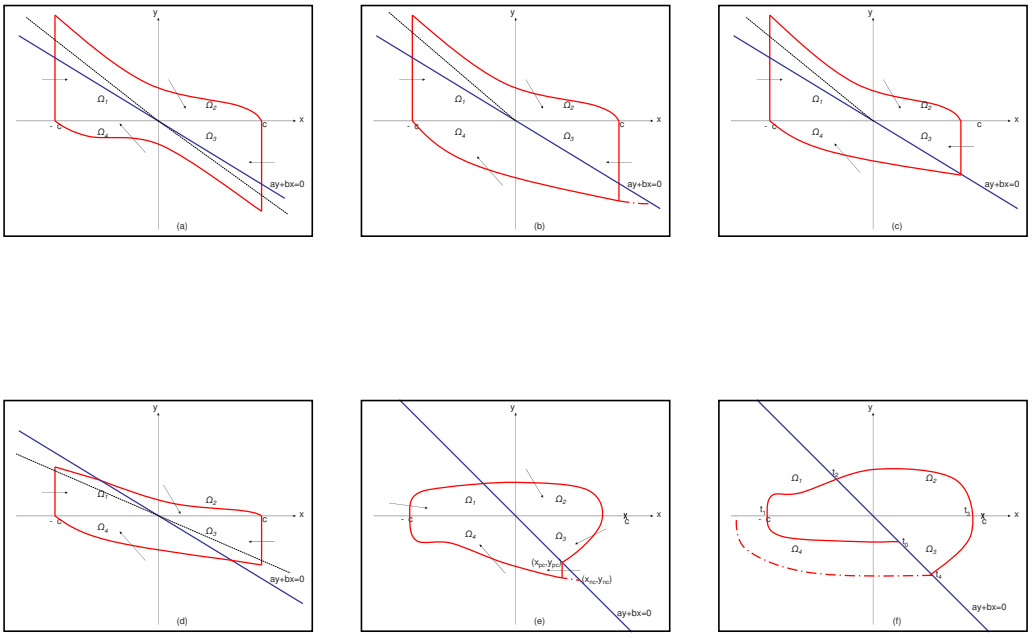

1

Figure 4.13: Illustration for the proof of last three conditions in Theorem 4.4.

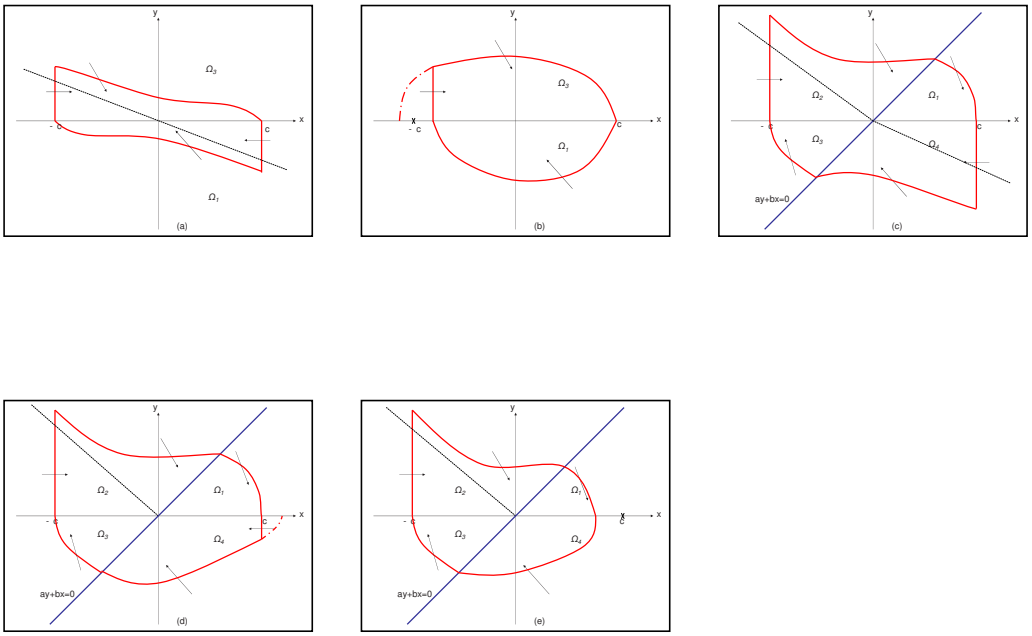

1

Figure 4.14: Illustration for the proof of the first two conditions in Theorem 4.4.

- $(\alpha + ak_1)^2 \geq 4(\beta + bk_1)$, $\frac{\alpha+ak_1}{2} \leq \frac{b}{a}$
- $(\alpha + ak_2)^2 \geq 4(\beta + bk_2)$, $\frac{\alpha+ak_2}{2} \leq \frac{b}{a}$

4. $b > 0$, Condition 2) or 3) does not hold, and $y_n < y_p$
5. $b < 0$, $\beta + k_1 b > 0, \beta + k_2 b > 0$ and $\alpha^2 \geq 4\beta$
6. $b < 0$, $\beta + k_1 b > 0, \beta + k_2 b > 0$, $\alpha^2 < 4\beta$, and $y_n < y_p$

Proof: According to Proposition 4.1, $\alpha > 0$ and $\beta > 0$ must be satisfied to ensure absolute stability. Condition 1) in this theorem comes directly from Proposition 4.2. Condition 1) is independent of k_1 and k_2 and thus the absolute stability holds for any $k_1 > 0, k_2 > 0$.

In Condition 2), the first set of inequalities comes from Proposition 4.4. The second set of inequalities in Condition 2) and the first set of inequalities in Condition 3) combined is equivalent to the conditions in Proposition 4.5. The equivalence becomes clear with some algebraic calculations. Other sets of inequalities in Condition 2) and 3) are established through the duality principle or from Proposition 4.6.

Condition 5) is directly from Proposition 4.3. Condition 4) and 6) come from Proposition 4.7. □

So far in all discussions, the assumption $a > 0$ is made. Next, the result with $a < 0$ and $a = 0$ is presented.

Theorem 4.4: If $a < 0$, the uncertain system in Problem 4.1 is absolutely stable if and only if $\alpha > 0, \beta > 0$ and one of the following conditions is satisfied.

1. $b = 0$

2. $b < 0,\ \beta + bk_1 > 0, \beta + bk_2 > 0,\ max\{\alpha + ak_1, 4(\beta + bk_1) - (\alpha + ak_1)^2\} > 0,\ max\{\alpha + ak_2, 4(\beta + bk_2) - (\alpha + ak_2)^2\} > 0$ and one set of the following inequalities hold

   - $\alpha^2 \geq 4\beta, \frac{\alpha}{2} - \sqrt{\frac{\alpha^2}{4} - \beta} \leq \frac{b}{a}$
   - $\alpha + ak_1 > 0, \frac{(\alpha+ak_1)}{2} + \sqrt{\frac{(\alpha+ak_1)^2}{4} - (\beta + bk_1)} \geq \frac{b}{a}$
   - $\alpha + ak_2 > 0, \frac{(\alpha+ak_2)}{2} + \sqrt{\frac{(\alpha+ak_2)^2}{4} - (\beta + bk_2)} \geq \frac{b}{a}$

3. $b < 0, \beta+bk_1 > 0, \beta+bk_2 > 0, \alpha^2 < 4\beta, max\{\alpha+ak_1, 4(\beta+bk_1)-(\alpha+ak_1)^2\} > 0,\ max\{\alpha + ak_2, 4(\beta + bk_2) - (\alpha + ak_2)^2\} > 0$ and $y_n < y_p$

4. $b > 0,\ max\{\alpha + ak_1, 4(\beta + bk_1) - (\alpha + ak_1)^2\} > 0,\ max\{\alpha + ak_2, 4(\beta + bk_2) - (\alpha + ak_2)^2\} > 0$ and one set of the following inequalities hold

   - $\alpha + ak_1 > 0, (\alpha + ak_1)^2 \geq 4(\beta + bk_1)$
   - $\alpha + ak_2 > 0, (\alpha + ak_2)^2 \geq 4(\beta + bk_2)$

5. $b > 0,\ (\alpha + ak_1)^2 < 4(\beta + bk_1), (\alpha + ak_2)^2 < 4(\beta + bk_2)$, and $y_n < y_p$

Proof: If the first condition is satisfied, a closed curve as illustrated in Figure 4.14 (a)(b) can be constructed ((a) if $\alpha^2 - 4\beta \geq 0$ and (b) if $\alpha^2 - 4\beta < 0$) and the absolute stability becomes clear.

When $b < 0,\ \beta + bk_1 > 0, \beta + bk_2 > 0$ must hold to ensure absolute stability. If $\beta + bk_1 \leq 0$, the system LS_2 has an unstable manifold in the region Ω_2 and thus the system PLS becomes unstable. Similarly, if $\beta + bk_2 \leq 0$, the system PLS becomes unstable. If the first set of inequalities in Condition 2) includes two that

do not involve k_1 or k_2. When these two inequalities are satisfied, at least one of the stable manifolds of the system LS_{13} is located inside the regions Ω_1 and Ω_3. The last two inequalities in the first set involve the *max* function and exclude the possibility where the system LS_2 has an unstable manifold in the region Ω_2 and the possibility where the system LS_4 has an unstable manifold in the region Ω_4. Combined together, the first set of inequalities enables one to construct a closed curve as illustrated in Figure 4.13 (d) and prove the absolute stability. In a similar manner, if the second set of inequalities holds, one can construct closed curves as illustrated in Figure 4.13 (a) (b) (c) and prove the absolute stability. The third set of inequalities is the dual version of the second one. Based on the arguments above, it is clear to find Condition 3) from Proposition 4.7.

If $b > 0$, the trajectory of the system LS_{13}, starting from the point $(c, 0)$, intersects with the line $ay + bx = 0$ in a negative time. In the fourth condition, if the first set of inequalities holds, the system LS_2 has a stable node of which both stable manifolds are located in the second and fourth quadrants. The inequality involving the *max* function excludes the possibility where the system LS_4 has an unstable manifold in the region Ω_4. Therefore one can construct the closed curves as illustrated in Figure 4.14 (c) (d) (e) to prove the absolute stability. Here, the system LS_4 has a stable node in Figure 4.14 (c) and has a focus in Figure 4.14 (d) (e). The second set of inequalities is a result of the duality principle in Theorem 4.1. Based on the arguments above, it is clear to find Condition 5) from Proposition 4.7. □

In the special case of $a = 0$, we have the following result.

Theorem 4.5: If $a = 0$, the uncertain system in Problem 4.1 is absolutely stable if and only if $\alpha > 0, \beta > 0$ and one of the following conditions is satisfied.

1. $b = 0$
2. $b > 0$ and for at least one of the indices $i = 1, 2$, $\alpha^2 \geq 4(\beta + bk_i)$
3. $b > 0$, $\alpha^2 < 4(\beta + bk_1), \alpha^2 < 4(\beta + bk_2)$ and $y_n < y_p$
4. $b < 0$, $\beta + bk_1 > 0, \beta + bk_2 > 0$ and $\alpha^2 \geq 4\beta$
5. $b < 0$, $\beta + bk_1 > 0, \beta + bk_2 > 0$, $\alpha^2 < 4\beta$ and $y_n < y_p$

Proof: If $b = 0$, the uncertain system in Problem 4.1 is degenerated to a simple linear system. This linear system is stable when $\alpha > 0, \beta > 0$.

Since $\alpha > 0, \beta > 0$, the system LS_{13} has a stable focus or a stable node of which both stable manifolds are located in the second and fourth quadrants. When $b > 0$, each of the systems LS_2 and LS_4 has a stable node or a stable focus. With $\alpha^2 \geq 4(\beta + bk_1)$, the system LS_2 has a stable node. One can construct a closed curve that is the same as that in Figure 4.14 (c)-(e) except that the line $ay + bx = 0$ here coincides with the y axis. The absolute stability is then proved by applying the invariant subspace argument. By using the duality principle in Theorem 4.1, absolute stability is proved when $b > 0$ and $\alpha^2 \geq 4(\beta + bk_2)$. Condition 3) is a direct result of Proposition 4.7.

When $b < 0$, if Condition 4) is satisfied, one can construct a closed curve, similar as the one in Figure 4.14 (d), to prove the absolute stability. Condition 5) comes from Proposition 4.7. □

Combined together, Theorem 4.3-4.5 give a complete solution to Problem 4.1. Here two comments are made regarding these results.

Comments:

1. Conditions in Theorem 4.3 and Theorem 4.4 are equivalent to that in Theorem 4.5 by taking the right limit and left limit $a \to 0$ respectively.

2. With the constraint $k_1 = k_2$, Problem 4.1 is simplified to the classical absolute stability problem with symmetric sector bounds. Therefore, with $k_1 = k_2$, these three theorems are degenerated to Leonov's results in Theorem 3.2.

4.5 Solution to Problem 4.2: Further Generalization of Sector Bounds

The results in the previous section are derived by comparing the vector field of the system *NLS* with a sequence of linear systems LS_{13}, LS_2, LS_4. In the derivation, the nonlinearity is assumed to be bound in the asymmetric sector $(0, k_1, k_2)$. Here we apply the same method and give results for more general asymmetric sector conditions.

For some other nonlinearity within such asymmetric sector bounds, the classical absolute stability results can be applied by expanding the sector bounds to symmetric ones. By doing this, the derived absolute stability conditions are conservative.

Let us call the system (4.4) with the nonlinearity bound in the asymmetric sector (k_1, k_2, k_3, k_4) *NLS_GL*. Here in this section, a generalized version of Problem 4.2 is formulated below and followed by solutions.

Theorem 4.6: If $a > 0$, the uncertain system in Problem 4.2 is absolutely stable if and only if one of the following conditions is satisfied. If $a < 0$, conditions for the absolute stability are found by the conditions in the case $a > 0$ after replacing the parameter set $(k_1, k_2, k_3, k_4, a, b)$ in Problem 4.2 with $(-k_2, -k_1, -k_4, -k_3, -a, -b)$. If $a = 0$, absolute stability conditions correspond to those in the case $a > 0$ with $a \to 0$.

1. $b = 0, \beta + bk_1 > 0, \beta + bk_3 > 0$ and one set of the following inequalities holds

   - $\alpha+ak_1 > 0, (\alpha+ak_1)^2 \geq 4(\beta+bk_1), max\{\alpha+ak_3, 4(\beta+bk_3)-(\alpha+ak_3)^2\} > 0$
   - $\alpha+ak_3 > 0, (\alpha+ak_3)^2 \geq 4(\beta+bk_3), max\{\alpha+ak_1, 4(\beta+bk_1)-(\alpha+ak_1)^2\} > 0$
   - $(\alpha + ak_1)^2 < 4(\beta + bk_1), (\alpha + ak_3)^2 < 4(\beta + bk_3)$ and $\frac{\alpha+ak_1}{\sqrt{4(\beta+bk_1)-(\alpha+ak_1)^2}} + \frac{\alpha+ak_3}{\sqrt{4(\beta+bk_3)-(\alpha+ak_3)^2}} < 0$

2. $b > 0, \beta + bk_1 > 0, \beta + bk_3 > 0,\ max\{\alpha + ak_1, 4(\beta + bk_1) - (\alpha + ak_1)^2\} > 0,\ max\{\alpha + ak_3, 4(\beta + bk_3) - (\alpha + ak_3)^2\} > 0$ and one set of the following inequalities holds

   - $\alpha + ak_1 > 0, (\alpha + ak_1)^2 \geq 4(\beta + bk_1), \frac{\alpha+ak_1}{2} + \sqrt{\frac{(\alpha+ak_1)^2}{4} - (\beta + bk_1)} \geq \frac{b}{a}$
   - $\alpha + ak_3 > 0, (\alpha + ak_3)^2 \geq 4(\beta + bk_3), \frac{\alpha+ak_3}{2} + \sqrt{\frac{(\alpha+ak_3)^2}{4} - (\beta + bk_3)} \geq \frac{b}{a}$
   - $\alpha + ak_2 > 0, (\alpha + ak_2)^2 \geq 4(\beta + bk_2), \frac{\alpha+ak_2}{2} - \sqrt{\frac{(\alpha+ak_2)^2}{4} - (\beta + bk_2)} \leq \frac{b}{a}$
   - $\alpha + ak_4 > 0, (\alpha + ak_4)^2 \geq 4(\beta + bk_4), \frac{\alpha+ak_4}{2} - \sqrt{\frac{(\alpha+ak_4)^2}{4} - (\beta + bk_4)} \leq \frac{b}{a}$
   - none of the above sets of inequalities holds and $y_n < y_p$

3. $b < 0$, $min\{max\{\beta+bk_i, -\frac{\alpha+ak_i}{2}+\sqrt{\frac{(\alpha+ak_i^2}{4}-(\beta+bk_i)}+\frac{b}{a}\}, max\{\alpha+ak_i, -\beta-bk_i, 4(\beta+bk_i)-(\alpha+ak_i)^2, -\frac{\alpha+ak_i}{2}-\sqrt{\frac{(\alpha+ak_i^2}{4}-(\beta+bk_i)}+\frac{b}{a}\}\} > 0$ with $k = 2, 4$, $min\{max\{\beta+bk_i, \frac{\alpha+ak_i}{2}-\sqrt{\frac{(\alpha+ak_i^2}{4}-(\beta+bk_i)}-\frac{b}{a}\}, max\{\alpha+ak_i, -\beta-bk_i, 4(\beta+bk_i)-(\alpha+ak_i)^2, \frac{\alpha+ak_i}{2}-\sqrt{\frac{(\alpha+ak_i^2}{4}-(\beta+bk_i)}-\frac{b}{a}\}\} > 0$ with $k = 1, 3$, and one set of the following inequalities holds

   - $\alpha + ak_1 > 0, (\alpha + ak_1)^2 \geq 4(\beta + bk_1)$
   - $\alpha + ak_3 > 0, (\alpha + ak_3)^2 \geq 4(\beta + bk_3)$
   - neither of the above sets of inequalities holds and $y_n < y_p$

Proof: When $b = 0$, the state space (x, y) is divided into the regions Ω_1 and Ω_3. If $\beta + bk_1 \leq 0$, the system LS_1 has a saddle point and the unstable manifold is located in the region Ω_1. Therefore the system NLS is unstable and the uncertain system in Problem 4.2 is not absolutely stable. Similarly $\beta + bk_3 > 0$ must hold to ensure absolute stability. The first set of inequalities includes constraints involving k_1 and k_3. With the constraints involving k_1, the system LS_1 has a stable node and both stable manifolds are located in the second and fourth quadrants. With the constraints involving k_3, the system LS_3 either has a focus or has a stable node of which both stable manifolds are located in the second and fourth quadrants. Therefore one can construct closed curves as illustrated in Figure 4.15 (a)-(c) to prove the absolute stability. The second set of inequalities is proved by applying the duality principle in Theorem 4.2. If the third set of inequalities holds, we have $x_n > x_p$ where the two quantities are illustrated in Figure 4.15 (d). The absolute stability is then proved by applying Proposition 4.6.

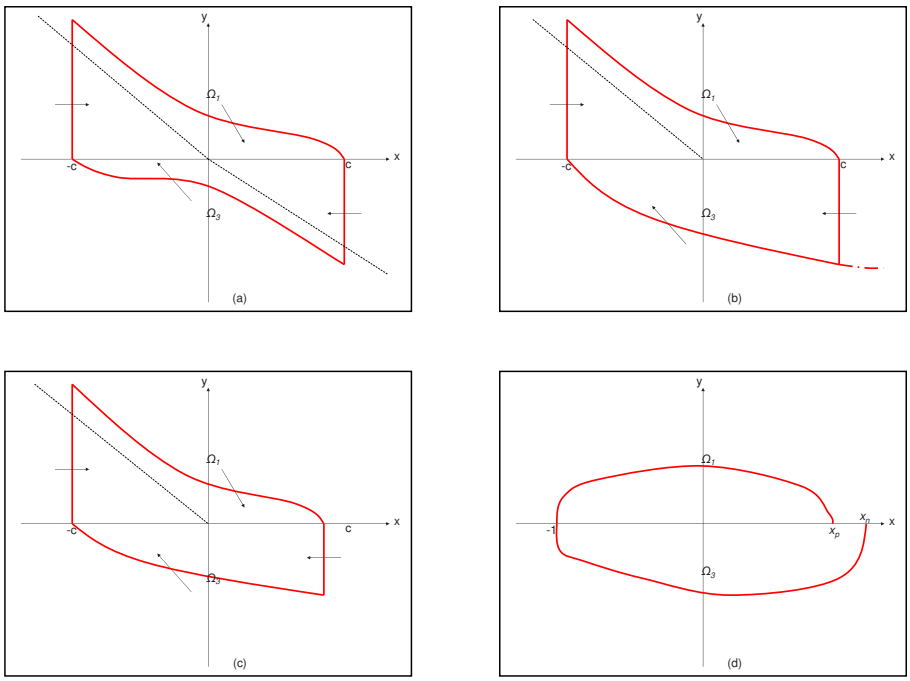

1

Figure 4.15: Illustration for the proof of Theorem 4.6 when $b = 0$.

When $b > 0$, if $\beta + bk_1 > 0$, the system LS_1 has a saddle point and thus the system PLS is unstable. Therefore the uncertain system in Problem 4.2 is not absolutely stable. The same argument leads to the condition $\beta+bk_3 > 0$. If $max\{\alpha+ ak_1, 4(\beta+bk_1)-(\alpha+ak_1)^2\} \leq 0$, the system LS_1 has an unstable node of which both unstable manifolds are located in the first and third quadrants. Therefore the system PLS is not stable and the uncertain system in Problem 4.2 is not absolutely stable. The same argument leads to the condition $max\{\alpha+ak_3, 4(\beta+bk_3)-(\alpha+ak_3)^2\} > 0$. If the first set of inequalities holds, the system LS_1 has a stable node of which at least one stable manifold is located between the y axis and the line $ay + bx = 0$. One can then construct closed curves as illustrated in Figure 4.16 (a)-(c) to prove the absolute stability. Similarly, if the third set of inequalities holds, the system LS_2 has a stable node of which at least one stable manifold is located between the x axis and the line $ay + bx = 0$. One can then construct closed curves as illustrated in Figure 4.16 (d)-(g) to prove the absolute stability. The second and fourth sets of inequalities are dual version of the first and third sets respectively. If none of the first four sets of inequalities holds, the trajectories of the system PLS rotate clockwise around the origin. Proposition 4.7 can be applied to prove the absolute stability, as illustrated in Figure 4.16 (h) (i).

When $b < 0$, if $max\{\beta + bk_2, -\frac{\alpha+ak_2}{2} + \sqrt{\frac{(\alpha+ak_2^2}{4} - (\beta + bk_2)} + \frac{b}{a}\} \leq 0$, the system LS_2 has a saddle point and the unstable manifold is located in the region Ω_2 and Ω_4. Therefore the system PLS is unstable and the uncertain system in Problem 4.2 is not absolutely stable. If $max\{\alpha + ak_2, -\beta - bk_2, 4(\beta + bk_2) - (\alpha + ak_2)^2, -\frac{\alpha+ak_2}{2} - \sqrt{\frac{(\alpha+ak_2^2}{4} - (\beta + bk_2)} + \frac{b}{a}\} \leq 0$, the system LS_2 has an unstable

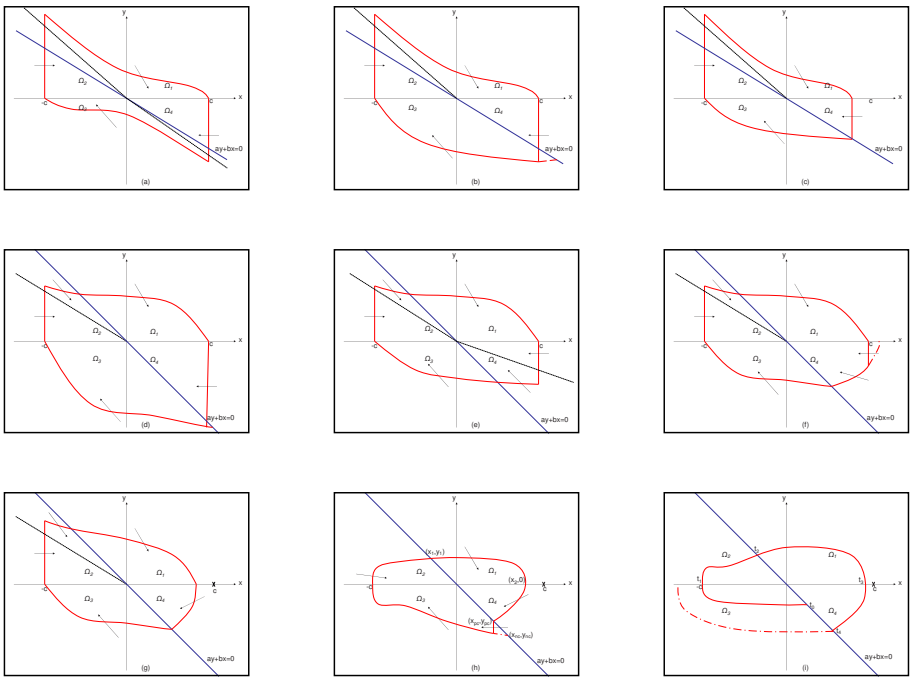

1

Figure 4.16: Illustration for the proof of Theorem 4.6 when $b > 0$.

node of which at least one unstable manifold is located in the region Ω_2 and Ω_4. Therefore the system PLS is unstable and the uncertain system in Problem 4.2 is not absolutely stable. The same argument can be applied to derive the necessary conditions involving the $min(\cdot,\cdot)$ function. If the first set of inequalities holds, the system LS_1 has a stable manifold. One can construct closed curves as illustrated in Figure 4.17 (a)-(c) to prove the absolute stability. The second set of inequalities is the dual version of the first set according to Theorem 4.2. If neither of the first two sets of inequalities holds, the trajectories of the system PLS rotate clockwise around the origin. Proposition 4.7 can be applied to prove the absolute stability, as illustrated in Figure 4.17 (d).

If $a < 0$, the uncertain system in Problem 4.2 is equivalent to

$$\begin{aligned} \dot{x} &= y \\ \dot{y} &= -\alpha y - \beta x - F_{NL}(t, ay + bx) = -\alpha y - \beta x - \tilde{F}_{NL}(t, -ay - bx) \end{aligned} \quad (4.12)$$

where the nonlinearity $\tilde{F}_{NL}(t,\cdot)$ is bound in the nonsymmetric sector $(-k_2, -k_1, -k_4, -k_3)$. Therefore Problem 4.2 with $a < 0$ is also solved. $\square$

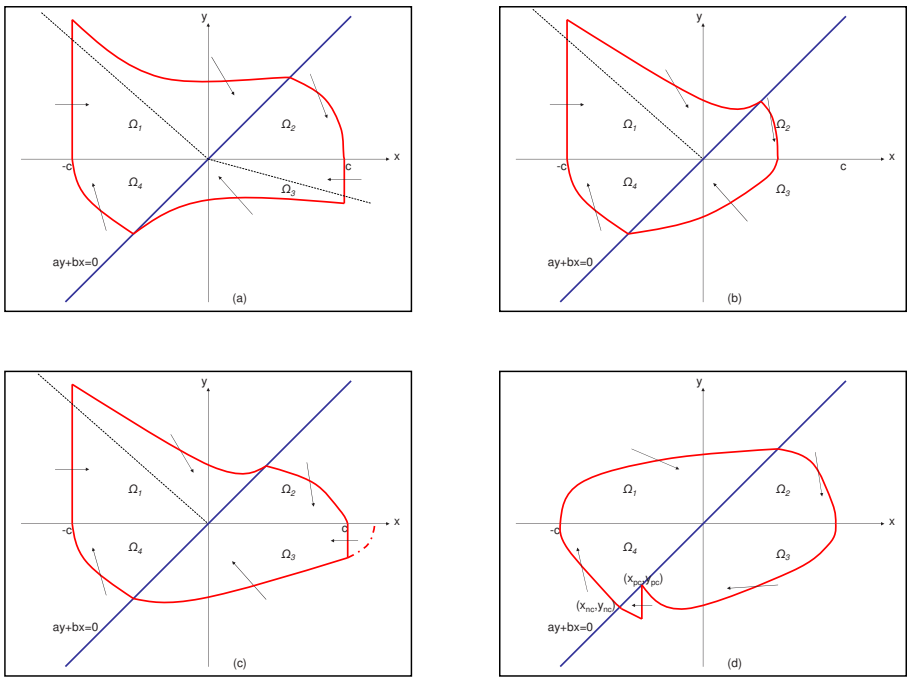

Figure 4.17: Illustration for the proof of Theorem 4.6 when $b < 0$.

Chapter 5

Generalized Absolute Stability for Finite-Order Systems

5.1 Problem Statement

In the previous chapter, geometry-based methods are used to find necessary and sufficient conditions for generalized absolute stability of second-order systems. In this chapter, we will focus on finite-order systems, which generally have an order higher than two. The geometry-based methods in the previous chapter are not applicable to general finite-order systems. Therefore new methods are needed for these systems to find conditions of generalized absolute stability.

With the generalization of sector bounds, the main problem of this chapter is formulated as follows.

Problem 5.1: Determine sufficient conditions for global asymptotic stability at the origin for n^{th}-order nonlinear system

$$\dot{x} = Ax + bF_{NL}(t, c'x) \tag{5.1}$$

where the scalar nonlinearity $F_{NL}(t, \cdot)$ is bound in the asymmetric sector (k_1, k_2, k_3, k_4) as defined in Definition 4.2. Here $x, b, c \in \Re^n$ and $A \in \Re^{n\times n}$. $\square$

It is important to point out that even for the classical absolute stability prob-

lem of a general finite-order system where the sector bound is *symmetric*, a trackable solution that is not only sufficient but also necessary has not been available, despite the large amount of research effort in this area. Here in this chapter, the generalized absolute stability problem is more complicated than the classical problem due to the non-symmetry of the sector bound. As a result, the objective in this chapter is to find *sufficient* conditions for the generalized absolute stability, rather than a condition that is not only sufficient but also necessary.

If we drop t on the right hand side of equality in (5.1) and make the system time-invariant, Problem 5.1 remains the same. Therefore (5.1) is replaced by

$$\dot{x} = Ax + bF_{NL}(c'x) \tag{5.2}$$

The absolute stability of the system in Problem 5.1 is also equivalent to the robust stability of the linear time-varying system

$$\dot{x} = Ax + bu(t)c'x \tag{5.3}$$

where the quantity $u(t)$ belongs to an admissible set U

$$U = \{u(t) : k_2 \leq u(t) \leq k_3 \text{ if } c'x(t) \leq 0, \quad \text{and} \quad k_1 \leq u(t) \leq k_4 \text{ otherwise}\} \tag{5.4}$$

5.2 Existence of Piecewise Linear Lyapunov Functions

Quadratic Lyapunov functions (QLFs) and piecewise quadratic Lyapunov functions (PWQLFs) may be used to determine the classical absolute stability with a symmetric sector bound. QLFs and PWQLFs are symmetric with respect to the origin of the state space due to the quadratic or piecewise quadratic forms. As a

result, if a QLF or a PWQLF is found to prove the generalized absolute stability with the asymmetric sector bound $(0, k_1, k_2)$, the same Lyapunov function can be used to prove the classical absolute stability with the symmetric sector bound $(0, K = \max\{k_1, k_2\})$. It is recalled that the purpose of studying the generalized absolute stability is to reduce the conservativeness in stability conditions. Therefore, the usage of QLFs or PWQLFs will render meaningless the generalization that allows for asymmetric sector bounds. In other words, QLFs and PWQLFs are not suited for determining the generalized absolute stability. In comparison, PWLLFs are generally not symmetric with respect to the origin of the state space. Futhermore, usage of PWLLFs often results in stability conditions that are easier to verify numerically. For these two reasons, PWLLFs will be employed in this chapter to find sufficient conditions for the generalized absolute stability.

In [43], Molchanov and Piatnitskii proved that a piecewise quadratic Lyapunov function exists if and only if the system (5.1) with a *symmetric* sector bound is absolutely stable. This work laid a ground for the search of piecewise quadratic Lyapunov functions in the classical absolute stability problem. Inspired by the arguments in [43], the following results are established and proved for a system (5.1) with *asymmetric* sector bounds. In a similar manner, these results lay a theoretical ground for the search of piecewise linear Lyapunov functions in the generalized absolute stability problem.

In Lyapunov's direct method, the derivative of the Lyapunov function is important. In our study here, however, the Lyapunov functions are piecewise linear and may not be differentiable although continuous. Furthermore, the nonlinear

system may be piecewise smooth. Therefore the following modifications are made to Lyapunov's direct method. These modifications are also needed of one utilizes multiple Lyapunov functions other than PWLLFs for the study of piecewise smooth systems.

1. For a smooth system $\dot{x} = f(x)$, replace the study of the derivative $\dot{V}(x) =< grad\ V(x), f(x) >$ by the study of the one-sided derivative in the direction of the vector field $y = f(x)$:

$$\frac{\partial V(x)}{\partial t}|\vec{y} \triangleq \lim_{t \to 0^+} t^{-1}[V(x + ty) - V(x)] \tag{5.5}$$

   Here $< ., . >$ denotes the inner product of two vectors.

2. For a system $\dot{x} = f(x)$ where $f(x)$ is piecewise smooth, replace the condition $\dot{V}(x) < 0$ by the condition

$$w(x) = \max_{y \in F(x)} \frac{\partial V(x)}{\partial t}|\vec{y} < 0 \tag{5.6}$$

   Here $F(x)$ is the set of all possible vector field y. In the following, $w(x)$ will sometimes be referred to as "derivative" of the Lyapunov function $V(x)$.

With these modifications, we can state and prove the following theorem regarding the existence of a quasi-quadratic Lyapunov function for a system that is absolutely stable.

Theorem 5.1 If the system (5.1) with an asymmetric sector bound is globally absolutely stable, it is necessary and sufficient that there exists a Lyapunov function $V(x)$ of quasi-quadratic form

$$V(x) = x'L(x)x, L'(x) = L(x) = L(\tau x), x \neq 0, \tau > 0; V(0) = 0 \tag{5.7}$$

whose "derivative" satisfies the inequality

$$w(x) = \max_{y \in F(x)} \frac{\partial V(x)}{\partial t} | \vec{y} \leq -\gamma \|x\|^2 \tag{5.8}$$

for any $x \in R^n$. Furthermore, this Lyapunov function is strictly convex in R^n.

Proof. First we prove the sufficiency. Since $V(x)$ is strictly convex in x, for any $x \neq 0$ and $\tau \in (0,1)$, we have $V(\tau x) < \tau V(x)$. From (5.7), we have $V(\tau x) = \tau^2 x' L(\tau x) x = \tau^2 V(x)$. Therefore $\tau(1-\tau)V(x) > 0$. Hence $V(x) > 0$ for any $x \neq 0$ and $V(0) = 0$. It is easily verified that $V(x) \to \infty$ as $\|x\| \to \infty$. Therefore the original system is absolutely stable.

Proof for the necessity is more involved and will be provided in the following.

For construction of the Lyapunov function, the following definition is introduced:

$$S(x_0, T) = \max_{u \in U} \|x_u(x_0, T)\|^2 = \max_{u \in U} \|\phi_u(T) x_0\|^2 = \|\phi_{u^*}(T) x_0\|^2 \tag{5.9}$$

where $x_u(x_0, t) = \phi_u(t) x_0$ is a solution of the system (5.3) for $x(0) = x_0$ and $u(t) \in U$. Here $\phi_u(t)$ is the fundamental matrix of (5.3) corresponding to a choice of $u(t)$ from the admissible set U; u^* denotes the optimal choice of $u(t)$ that achieves the maximum.

The function $S(x_0, T)$ is continuous in x_0 and T due to the continuity of the function $x_u(x_0, t)$ in x_0 and t. Moreover the function $S(x_0, T)$ is strictly convex in x_0. The strict convexity can be proved in two steps. First, the function $x_u(x_0, T)$ corresponding to an arbitrary choice of $u(t)$ is strictly convex in x_0 for any fixed $T \geq 0$, since the Hessian matrix is positive definite. Second, the maximum function of convex functions is convex [12].

At each point $x_0 \in \Re^n$, a Lyapunov function is constructed as:

$$V(x_0) = \int_0^{T_1} S(x_0, \xi) d\xi \tag{5.10}$$

with $T_1 > \alpha^{-1} \ln \beta \geq 0$. Here the quantities α and β are defined in (5.17). The lower bound on the choice of T_1 will become clear later in this proof.

With the construction formula (5.10), it is clear that the function $V(x)$ is strictly convex in $\Re^n$. From (5.9) and (5.10), we have $V(0) = 0$ and

$$V(x_0) = x_0'(\int_0^{T_1} \phi'(x_0, \xi)\phi(x_0, \xi) d\xi) x_0 = x_0' L(x_0) x_0 \tag{5.11}$$

with $L'(x_0) = L(x_0)$.

Through the state transformation of $x \to \tau x$, it can be shown $S(\tau x_0, T) = \tau^2 S(x_0, T)$ for $0 < \tau < \infty$. Therefore $V(\tau x_0) = \tau^2 V(x_0)$, and hence

$$V(x) = x' L(x) x = x' L(\tau x) x \tag{5.12}$$

for $x \neq 0$ and $\tau > 0$. Consequently the function $V(x)$ defined by (5.10) can be written in the form (5.7).

To prove the inequality (5.8), it is noted that for any x_0 and $y = Ax_0 + b\lambda c' x_0 \in F(x_0)$, we have

$$\begin{aligned} \frac{\partial V(x_0)}{\partial t}|\vec{y} &\triangleq \lim_{t \to +0} \frac{V(x_0 + ty) - V(x_0)}{t} = \lim_{t \to +0} \frac{V(x_0 + ty + o(h)) - V(x_0)}{t} \\ &= \lim_{t \to +0} \frac{V(x_\lambda(x_0, t)) - V(x_0)}{t} \end{aligned} \tag{5.13}$$

Here the remainder $o(t)$ is taken so that $x_0 + ty + o(t) = x_\lambda(x_0, t)$, and $x_\lambda(x_0, t)$ is a solution of system (5.3) for $u(t) \equiv \lambda = const \in U$. On substituting (5.10), we obtain

$$\frac{V(x_\lambda(x_0, t)) - V(x_0)}{t} = \frac{\int_0^{T_1} S(x_\lambda(x_0, t), \xi) d\xi - \int_0^{T_1} S(x_0, \xi) d\xi}{t} \tag{5.14}$$

for $t > 0$.

It is noted that the function $S(x_0, T)$ as defined in (5.9) can be written in an equivalent form

$$S(x_0, T) = \max_{x \in X_u(x_0, T)} \|x\|^2 \tag{5.15}$$

where $X_u(x_0, T) = \{x_u(x_0, T), u \in U\}$ is a reachable set of system (5.3) from the initial point x_0 during a time interval $T \geq 0$. From the definition of the reachable set, it is clear that $X_u(x_\lambda(x_0, h), \xi) \subset X_u(x_0, t + \xi)$ for any $\xi \geq 0$ and $S(x_\lambda(x_0, h), \xi) \leq S(x_0, t + \xi)$. By using this inequality and (5.14), we obtain for $t > 0$:

$$\begin{aligned} \frac{V(x_\lambda(x_0, t)) - V(x_0)}{t} &\leq \frac{\int_0^{T_1} S(x_0, t + \xi) d\xi - \int_0^{T_1} S(x_0, \xi) d\xi}{t} \\ &= \frac{\int_{T_1}^{T_1 + t} S(x_0, \xi) d\xi - \int_0^t S(x_0, \xi) d\xi}{t} \end{aligned} \tag{5.16}$$

Since the uniform stability of the system (5.3) with an arbitrary $u(t)$ in the admissible set U is also exponentially stable [30], we have the following bound for the solutions of (5.3):

$$\|x_u(x_0, t)\| \leq \beta \|x_0\|^{-\alpha t}, t \geq 0 \tag{5.17}$$

where the numbers $\alpha > 0$ and $\beta \geq 1$ do not depend on $u(t) \in U$. From (5.9) and (5.17), it follows that

$$S(x_0, T) \leq \beta^2 \|x_0\|^2 e^{-2\alpha T}, T \geq 0 \tag{5.18}$$

On substituting (5.16) into (5.13), we obtain the inequality

$$\begin{aligned} w(x_0) &= \max_{y \in F(x_0)} \frac{\partial V(x_0)}{\partial t} | \vec{y} \leq \lim_{t \to +0} \frac{\int_{T_1}^{T_1 + t} S(x_0, \xi) d\xi - \int_0^t S(x_0, \xi) d\xi}{t} \\ &= S(x_0, T_1) - S(x_0, 0) \leq -\{1 - \beta^2 e^{-2\alpha T_1}\} \|x_0\|^2 \end{aligned} \tag{5.19}$$

The arbitrary choice of $x_0 \in \Re^n$ yields (5.8) for $\gamma = 1 - \beta^2 exp(-2\alpha T_1) > 0$ and the necessity is proved. □

Based on Theorem 5.1, next we give a result on the existence of a piecewise linear Lyapunov function for a system that is absolutely stable with asymmetric sector bounds.

Theorem 5.2 The system (5.1) with an asymmetric sector bound is absolutely stable if and only if there exists a piecewise linear Lyapunov function

$$V(x) = \max_{1 \le v \le M} < l^v, x > \tag{5.20}$$

where for any $x \in R^n$, the following conditions are satisfied

$$\begin{aligned} V(x) &\geq 0 \\ w(x) &= \max_{y \in F(x)} \frac{\partial V(x)}{\partial t} | \vec{y} \leq -\gamma \|x\|^2 \\ rank \|l^1, l^2, ..., l^M\| &= n < M \end{aligned} \tag{5.21}$$

Proof. The sufficiency is easily established from Lyapunov's direct method. In the following the necessity will be proved.

Denote the Lyapunov function in (5.7) as $V_1(x)$ and one of its level sets as $\Pi = \{x : V_1(x) = 1\}$, that is, $V_1(x) = x'L(x)x = 1$. At each point $x_0 \in \Pi$, we choose a vector $z(x_0) \neq 0$ from the subdifferential $\partial V_1(x)$ of the function $V_1(x)$. From Theorem 5.1, if the system (5.1) with asymmetric sector bounds is absolutely stable,

$$w(x_0) = \max_{y \in F(x_0)} \frac{\partial V_1(x_0)}{\partial t} | \vec{y} = \max_{y \in F(x_0)} \max_{x \in \partial V_1(x_0)} < z(x_0), y > \leq -\gamma \|x_0\|^2 \leq -\Delta_0 \tag{5.22}$$

For any $x_0 \in \Pi$, there exists a number $d(x_0) > 0$ such that

$$\max_{x\in\Gamma(x_0)} \max_{y\in F(x)} < z(x_0), y > \leq -0.5\Delta_0 \tag{5.23}$$

for any x belonging to the set $\Gamma(x_0) = \{x : V_1(x) \leq 1, \quad 0 \leq < z(x_0), x - x_0 > +d(x_0)\|z(x_0)\|\}$. Here $0 < d(x_0) < D(x_0)$ with $D(x_0) = \|z(x_0)\|^{-1} < z(x_0), x_0 >$ to include 0 and exclude x_0 in the set $\Gamma(x_0)$.

At each point $x_0 \in \Pi$, the set $Q(x_0) = \{x \in \Pi :< z(x_0), x - x_0 > +d(x_0)\|z(x_0)\| > 0\}$ specifies an open neighborhood of this point on the manifold Π. Likewise $\{Q(x_0), x_0 \in \Pi\}$ specifies an infinite covering of Π. As the manifold Π is compact, there exists a finite covering defined by a finite set of points $x_0^s \in \Pi(s = 1, 2, ..., M)$ from Borel-Lebesgue theorem [53].

Consider a polyhedral set K specified by a set of inequalities

$$< z(x_0^v), x - x_0^v > +\|z(x_0^v)\|d(x_0^v) \leq 0, v = 1, 2, ..., M \tag{5.24}$$

The set K is nonempty, since $x = 0$ will be its interior point by the condition $d(x_0^v) < D(x_0^v)$, v=1,...,M. The set K is also convex and closed. Moreover the set K is contained in the set $\{x : V_1(x) < 1\}$. Otherwise, there exists a point $a \in K$ with $V_1(a) \geq 1$. Since K is convex and $0 \in K$, we have the point $b = a/\sqrt{V_1(a)} \in K$. On the other hand, $b \in \Pi$ and therefore this point is covered by at least one of the neighborhoods $Q(x_0^v), v = 1, 2, ..., M$. This leads to contradiction with $b \in K$ according to the definition of K.

The surface of the polyhedron K can be regarded as a level surface $\Pi_1 = \{x : V(x) = 1\}$ if the following column vectors l^v are chosen in (5.20)

$$l^v = z(x_0^v)\|z(x_0^v)\|^{-1}[D(x_0^v) - d(x_0^v)]^{-1}, v = 1, 2, ..., M \tag{5.25}$$

Here the vectors l^v must satisfy the third condition in (5.21), since otherwise the level surface of the function $V(x)$ is not bounded.

The derivative of the function (5.20) can be written as

$$\frac{\partial V(x)}{\partial t}|\vec{y} = \max_{v \in R(x)} \{< l^v, y >\} \tag{5.26}$$

where $R(x) = \{v : V(x) =< l^v, x >, 1 \leq v \leq M\}$. Therefore for any $x \in \Pi_1$ and any $v \in R(x)$ we have the equation $< l^v, x >= 1$. Since the surface of the polyhedron K coincides with the set Π_1, it is true that $x \in \Gamma(x_0^v)$. We hence have the inequality

$$w(x) = \max_{y \in F(x)} \frac{\partial V(x)}{\partial t}|\vec{y} \leq -0.5\Delta_0 \{ \max_{v \in R(x)} [\|z(x_0^v)\|(D(x_0^v) - d(x_0^v))]\}^{-1} \leq \Delta_1 < 0 \tag{5.27}$$

Since $V(\tau x) = \tau V(x)$ and $F(\tau x) = \tau F(x)$ for $0 \leq \tau < \infty$, it follows that for any $x \in \Re^n$, $w(x) \leq -\Delta_1 V(x) \leq -\Delta_1 \lambda_1 \|x\|$ where the quantity λ_1 is:

$$\lambda_1 = \min_{y \in S = \{x : \|x\| = 1\}} V(y) \tag{5.28}$$

□

5.3 Construction of Piecewise Linear Lyapunov Functions (PWLLF)

Theorem 5.2 proves the existence of a piecewise linear Lyapunov function (PWLLF) for a system that is absolutely stable with an asymmetric sector bound. Therefore for an absolutely stable system, it is always possible to prove the absolute stability by finding a PWLLF. The following lemma provides a method to construct PWLLFs.

Lemma 5.1 If there exists a set of vectors $l^v \in \Re^n, v = 1, 2, ..., M$ and a set of scalars $u_{ij} > 0, w_{ij} > 0$ with $i, j = 1, 2, ..., M$ so that the following conditions hold, the system (5.1) is absolutely stable with the Lyapunov function of the form (5.20).

$$\begin{aligned} 0 &= (l^i)^T A + \sum_{j=1, j\neq i}^{M} u_{ij}(l^i - l^j)^T \\ 0 &= (l^i)^T - \sum_{j=1, j\neq i}^{M} w_{ij}(l^i - l^j)^T \end{aligned} \tag{5.29}$$

Proof. By using the so-called S-procedure, if the conditions (5.29) hold, the conditions (5.21) are satisfied. Thus this lemma is proved by applying Theorem 5.2. □

The scalars u_{ij}, w_{ij} in Lemma 5.1 can be assumed to be certain values first. Then the PWLLF can be found through linear programming tools. However, with M increasing, there will be many such scalars. As a result, search for the PWLLFs with this approach can be numerically expensive. To reduce the numerical complexity, the state space $\Re^n$ of the system is first divided into a set of polytopic regions and then the PWLLFs may be found by using linear programming tools.

As a preparation for the new approach that will be stated in Theorem 5.3, here we give two definitions. Suppose the state space $\Re^n$ is divided into M polyhedral regions, which are denoted as $X_i, i = 1, 2, ..., M$. A matrix E_i is called the polyhedral cell bound associated with X_i if it satisfies

$$E_i x \succeq 0 \quad for\ x \in X_i \tag{5.30}$$

Here $\succ$ and $\succeq$ means elementwise relationship. A matrix F_i is a continuity matrix for cell X_i if

$$F_i x = F_j x \quad for\ x \in X_i \cap X_j \tag{5.31}$$

Theorem 5.3 Let $\{X_i, i = 1, 2, ..., M\}$ be a polyhedral partition of the state space with continuity matrices F_i satisfying (5.31), and cell bounds E_i satisfying (5.30). If there exists a vectors t and nonnegative vectors $u_i \succ 0, v_i \succ 0, w_i \succ 0$ so that the following conditions hold for $i = 1, 2, ..., M$, the system (5.1) is absolutely stable.

$$\begin{aligned} l_i &= F_i^T t \\ 0 &= l_i^T - w_i E_i \\ 0 &= l_i^T A + u_i E_i \\ 0 &= l_i^T (A + bk) + v_i E_i \end{aligned} \tag{5.32}$$

Proof. Let $V(x) = l_i x$ for $E_i x \leq 0$ and thus $V(0) = 0$. The first equality in (5.32) ensures that the Lyapunov function $V(x)$ is continuous. The second equality leads to $V(x) > 0$ for any $x \neq 0$. When the last two equalities are satisfied, there is $\dot{V} < 0$ for any $x \neq 0$ for any nonlinearity bound in the asymmetric sectors. Furthermore, from the construction of the Lyapunov function, we have $V(x) \to \infty$ as $x \to \infty$. Therefore this theorem is proved. □

5.4 Computational Issues

To make use of Theorem 5.3 to find PWLLFs, one needs to determine the partition of the state space and therefore the matrices $E_i, i = 1, 2, ..., M$. Then based on the chosen partition, one needs to specify the matrices $F_i, i = 1, 2, ..., M$ to ensure continuity of the PWLLF.

In order to determine the global absolute stability of a system, we introduce

the hyperplane partition - partition the state space into convex polyhedra cells with a number of hyperplanes. Assume these hyperplanes are represented as

$$\partial H_j = \{x \in \Re^n | a_j^T (x - x_0) = 0\},\ j = 1, ..., N_{HP} \tag{5.33}$$

Here N_{HP} is the number of hyperplanes that are used for partition. We call the matrix $a = (a_1\ a_2\ ...\ a_{N_{HP}})$ the *partition matrix*. The partitioned cells are therefore

$$C_i = \{x : E_i x \succeq 0\},\ i = 1, ..., M \tag{5.34}$$

where the matrix E_i can be derived from the vectors a_j of the hyperplanes (5.33).

To specify the continuity matrices $F_i, i = 1, ..., M$, a point x_i is arbitrarily chosen inside the polyhedral cell C_i and we let

$$F_i x_i = \max\{a^T x_i, 0\} \tag{5.35}$$

where the function max is operated elementwise. In other words, the r^{th} row of the matrix F_i is equivalent to a_r^T if $a_r^T x_i > 0$ and zero otherwise. It is noted that this selection of continuity matrices is not unique. We adopt this selection due to its simplicity. In the next section it is shown that this particular selection is adequate for finding PWLLFs in the absolute stability problem.

The application of Theorem 5.3 involves many details such as the definitions that are introduced in the above. In order to understand these details better, one will find it very helpful to read Section 7.2, in which several application examples are presented.

Chapter 6

Supercavitating Vehicles

Supercavitating vehicles are a type of underwater vehicles capable of traveling at an ultra-high speed of over 230mph. In this chapter, we will focus on the dynamics, control and bifurcation of the motions of supercavitating vehicles, with a particular interest in applying the classical absolute stability results to stabilize the dive-plane motion of the supercavitating vehicles with robustness to modeling errors in the major source of nonlinearities – planing force.

In the sequel, the physics behind the supercavitation phenomenon is briefly explained in Section 6.1. In Section 6.2, the dive-plane model of a supercavitating vehicle is introduced. In Section 6.3, dynamics in the dive plane for a set of system parameters are studied. In Section 6.4, the challenges in stabilization, control and maneuvering of supercavitating vehicles are summarized. In Section 6.5, two robust control schemes are proposed for stabilization of supercavitating vehicles. In Section 6.6, an optimization technique is introduced to deal with the actuator saturation (in magnitude) problem - a great challenge in practical control of supercavitating vehicles. Finally the study of dynamics and stability of supercavitating vehicles is extended to address the change of some important system parameters during the vehicle motion; bifurcations in the vehicle system are elaborated and a dynamic

feedback control scheme is proposed to modify the bifurcation behavior.

6.1 Supercavitation

Cavitation is the physical phenomenon of bubble formation in a liquid subject to local pressure variations. According to Bernoulli's principle in fluid dynamics, the pressure of a fluid drops due to its high speed. When the pressure drops below the vapor pressure of the water, vaporization occurs typically resulting in small bubbles of water vapor. In order to generate and sustain a large bubble or cavity, artificial ventilation is often used in which some chemical actions inside the underwater vehicle are involved. The cavitation number σ, which is used to characterize the extent of cavitation, is defined as

$$\sigma = \frac{p_\infty - p_c}{0.5\rho V^2} \tag{6.1}$$

where ρ is the fluid density, V is the vehicle velocity, p_∞ and p_c are respectively the ambient pressure and the cavity pressure.

Supercavitation, which is an extreme form of cavitation in which a single bubble envelops the moving vehicle almost completely (see Figure 6.1), corresponds to very small values of the cavitation number. For a long time, researchers and engineers regarded cavitation as an undesirable physical phenomenon that is detrimental to underwater vehicles or ships, because cavitation causes a great deal of noise, vibration and damages to components such as propellers. However, in the application of supercavitating vehicles, cavitation is certainly a desirable behavior. Due to the reduced drag forces associated with a supercavitating vehicle, dramatic

increases can be realized in the speed of supercavitating vehicle [31]. Bundled with the benefit of making possible an ultra high underwater speed, in supercavitation complicated cavity dynamics are involved, the underwater vehicle experiences strong nonlinear forces, and the system dynamics present new challenges for stabilization and controlled maneuvering of the vehicle.

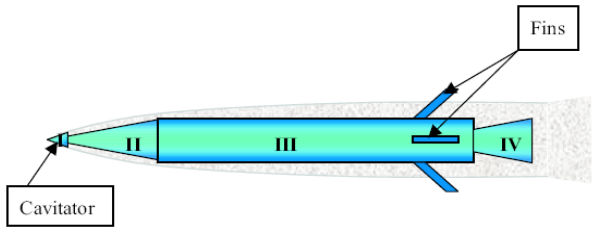

Figure 6.1: A supercavitating vehicle with surrounding envelope.

6.2 Dive-Plane Model

Following the work [16], a four-state model is chosen to study dive-plane dynamics and control of the system shown in Figure 6.1. The forward velocity V is assumed to be constant and the four states of this model are z (the depth at which the vehicle is located), w (the vertical speed of the vehicle), θ (the pitch angle), and q (the pitch rate). This system has two control inputs, namely, the cavitator deflection angle δ_c and the elevator deflection angle δ_e. The model takes into account the nonlinear planing force, which is descriptive of the nonlinear interaction between the vehicle and the cavity, and a simplified description of the cavity dynamics. The

governing equations can be determined in a body-fixed reference frame as

$$\begin{pmatrix} \dot{z} \\ \dot{w} \\ \dot{\theta} \\ \dot{q} \end{pmatrix} = \begin{pmatrix} 0 & 1 & -V & 0 \\ 0 & a_{22} & 0 & a_{24} \\ 0 & 0 & 0 & 1 \\ 0 & a_{42} & 0 & a_{44} \end{pmatrix} \begin{pmatrix} z \\ w \\ \theta \\ q \end{pmatrix} + \begin{pmatrix} 0 & 0 \\ b_{21} & b_{22} \\ 0 & 0 \\ b_{41} & b_{42} \end{pmatrix} \begin{pmatrix} \delta_e \\ \delta_c \end{pmatrix} + \begin{pmatrix} 0 \\ c_2 \\ 0 \\ 0 \end{pmatrix} + \begin{pmatrix} 0 \\ d_2 \\ 0 \\ d_4 \end{pmatrix} (-V^2[1 - (\frac{R_c - R}{h'R + R_c - R})^2]\frac{1 + h'}{1 + 2h'}\alpha) \tag{6.2}$$

The term c_2 and the last term in Eq. (6.2) correspond respectively to the gravity and the planing force. R_c is the cavity radius and R is the supercavitating vehicle radius. The coefficients a_{ij}, b_{ij}, and d_{ij} are functions of system parameters. The immersion depth h' and the angle of attack α in the planing force calculation are given by

$$h' = \begin{cases} 0 & \frac{R_c - R}{R} > \frac{L|w|}{RV} \\ \frac{L|w|}{RV} - \frac{R_c - R}{R} & \text{otherwise} \end{cases} \tag{6.3}$$

$$\alpha = \begin{cases} \frac{w - \dot{R}_c}{V} & \frac{w}{V} > 0 \\ \frac{w + \dot{R}_c}{V} & \text{otherwise} \end{cases} \tag{6.4}$$

In Eq. (6.3) and (6.4), L is the vehicle length and $\dot{R}_c < 0$ is the cavity radius contraction rate. The coefficients and other quantities above in Eqs. (6.2-6.4) take the forms given in Eq. (6.5). Here, n is the fin effectiveness ratio with respect to the cavitator, m is the density ratio of the vehicle to water, g is the gravity acceleration, C_{x0} is the cavitator lift force coefficient, and R_n is the cavitator radius.

$$
\begin{aligned}
a_{22} &= \frac{CVT}{m}(\frac{-1-n}{L})S + \frac{17}{36}nL \\
a_{24} &= VTS(C\frac{-n}{m} + \frac{7}{9}) - VT(C\frac{-n}{m} + \frac{17}{36})\frac{17}{36}L^2 \\
a_{42} &= \frac{CVT}{m}(\frac{17}{36} - \frac{11n}{36}) \\
a_{44} &= \frac{-11CVTnL}{36m} \\
b_{21} &= \frac{CV^2Tn}{m}(\frac{-S}{L} + \frac{17L}{36}), \quad b_{22} = \frac{-CV^2TS}{mL} \\
b_{41} &= \frac{-11CV^2Tn}{36m}, \quad b_{42} = \frac{17CV^2T}{36m} \\
c_2 &= g, \quad d_2 = \frac{T}{m}(\frac{-17L}{36} + \frac{S}{L}), \quad d_4 = \frac{11T}{36m} \\
S &= \frac{11}{60}R^2 + \frac{133L^2}{405}, \quad T = \frac{1}{7S/9 - 289L^2/1296} \\
C_x &= C_{x0}(1+\sigma), \quad C = 0.5C_x\frac{{R_n}^2}{R^2} \\
R_c &= R_n\sqrt{0.82\frac{1+\sigma}{\sigma}}K_2, \quad K_1 = \frac{L}{R_n(\frac{1.92}{\sigma} - 3)} - 1 \\
K_2 &= \sqrt{1 - (1 - \frac{4.5\sigma}{1+\sigma}){K_1}^{40/17}} \\
\dot{R}_c &= \frac{-\frac{20}{17}(0.82\frac{1+\sigma}{\sigma})^{0.5}V(1 - \frac{4.5\sigma}{1+\sigma})(K_1)^{23/17}}{K_2(\frac{1.92}{\sigma} - 3)}
\end{aligned}
\tag{6.5}
$$

The four-dimensional dive-plane model (6.2) is written in a compact form as

$$\dot{x} = Ax + Bu + DF_p \tag{6.6}$$

with $x = [z \ w \ \theta \ q]^T$ and $u = [\delta_e \ \delta_c]^T$. Here x, u, F_p stands for the state, the control

input and the planing force respectively.

The model equations described here are different from those presented in [16], since the same sign convention is used for the cavitator and fin inputs. The planing force is the only nonlinearity considered in this work. Additional details regarding this model can be found in references [16] and [37].

6.3 System Dynamics

Results obtained for a representative set of system parameter values are presented and discussed in this section. The specific set of parameter values considered is as follows:

$$\begin{aligned} g &= 9.81 m/s^2, m = 2, R_n = 0.0191 m, R = 0.0508 m, L = 1.8 m, V = 75 m/s, \\ \sigma &= 0.03, n = 0.5, C_{x0} = 0.82. \end{aligned} \tag{6.7}$$

6.3.1 Time-Domain Simulations

The responses of the uncontrolled system were found to be unstable. Responses of the controlled system are studied for the feedback law given by Eq. (6.8) and the results are presented in Figure 6.2. As shown in this figure, the controlled system exhibits bounded motions, which happen to be stable periodic motions.

$$\begin{aligned} \delta_c &= -k_{21} z - k_{23} \theta - k_{24} q = 15 z - 30 \theta - 0.3 q \\ \delta_e &= 0 \end{aligned} \tag{6.8}$$

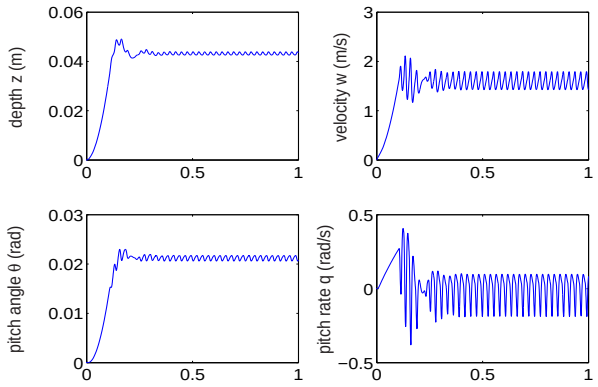

Figure 6.2: Motions initiated from trivial initial conditions in the controlled case.

6.3.2 Equilibrium Point Analysis

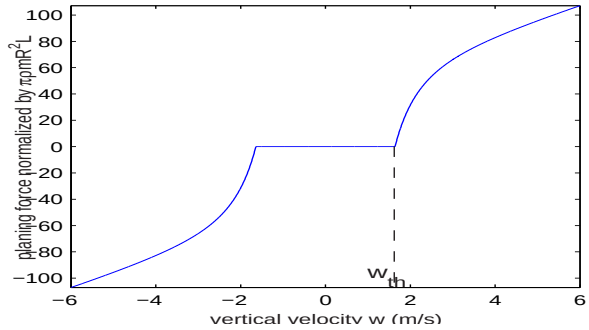

Figure 6.3: Planing force versus the vertical speed w.

A graph of the planing force is shown in Figure 6.3. This nonlinearity depends only on the vertical speed w. Based on the w-value, the state space can be divided into two regions; that is, the no-tail-slap region ($-w_{th} < w < w_{th}$) and the tail-slap region ($|w| > w_{th}$), where w_{th} is the positive value of w at the transition point in Figure 6.3. In the no-tail-slap region, the planing force is absent and the system is linear. The uncontrolled system has no equilibria in either region. The closed-loop system with the control given by Eq. (6.8) has the following numerically determined equilibrium point:

$$(\bar{z}, \bar{w}, \bar{\theta}, \bar{q}) = (0.04545, 1.6703, 0.0224, 0) \tag{6.9}$$

The Jacobian matrix associated with this equilibrium point has unstable eigenvalues, and the DC offsets of the different states shown in Figure 6.2 correspond to this unstable equilibrium point.

6.3.3 Limit Cycle Prediction

To examine the limit cycle motions shown in Figure 6.2, the describing function method (DFM) [30] is used. Through numerical calculations based on this method, it is determined that the system has a stable limit cycle with vertical speed

$$w(t) = 1.626 + 0.12238\cos(277t) \tag{6.10}$$

The DC offset of 1.626 m/s is in agreement with the DC offset of 1.619 m/s determined through time-domain simulations (see Figure 2). In addition, the AC amplitude of 0.12238 m/s and the oscillation frequency of 277 rad/s are close to the respective values (0.2 m/s and 232 rad/s) obtained through the simulations. The differences are attributed to the presence of higher order harmonics; it is assumed that the first harmonic is dominant in using the DFM. A projection of the system trajectory obtained from the time-domain simulation is shown in Figure 6.4.

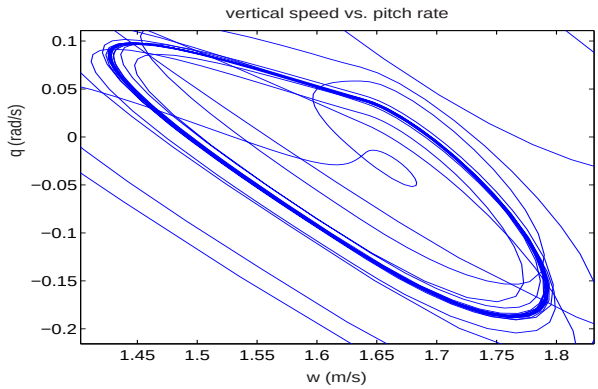

Figure 6.4: Projection of the system trajectory obtained from time-domain simulations in the controlled case.

6.4 Challenges in Stabilization and Control

Supercavitation presents a lot of challenges for the design of control systems to stabilize and navigate the motion of supercavitating vehicles. Below we list some challenges from the perspective of control system design.

1. Model Uncertainty

Supercavitation involves very complicated physics between three phases: solid phase of the vehicle body and control surfaces (including the cavitators in the front, and rudders/elevators in the rear), liquid phase of water, gaseous phase of cavity. Particularly, the hydrodynamic forces in supercavitation are hard to model accurately. Among these forces, the planing force is a strong nonlinearity and has a large effect on the dynamics of supercavitating vehicles. To date, the planing force formula is not accurate and this leads to a great deal of model uncertainty.

2. Large Disturbance

During the motion of supercavitating vehicles, large disturbances are involved.

This, to a large extent, is due to the cavity dynamics and the interaction between different phases.

3. Actuator Saturation

The control surfaces of supercavitating vehicles are cavitators in the front of the vehicle and the fins (rudders and elevators) in the rear. Due to physical constraints and other considerations, the cavitator deflection angle and the fin deflection angle have upper limits and will saturate at certain levels. The effect of actuator saturation has to be taken into consideration for the purpose of designing a high-performance control system.

4. Inner-Outer Loop Interaction

Here the inner-loop control system corresponds to the control system that is designed to stabilize the motion of the underwater vehicle. In comparison, the outer-loop control system corresponds to the control system that is designed to guide and navigate the motion of the underwater vehicle. Although this work focuses on inner-loop control systems, some considerations from the outer-loop control system have to be addressed in the inner loop control system design. For example, the outer-loop control system will specify an operating point for the inner-loop control system. This operating point in many cases may be regarded as the desired equilibrium point for the closed-loop system including the inner-loop control system.

5. System Parameter Variation

Important system parameters such as the cavitation number σ varies during the motion of a supercavitating vehicle. This leads to a variety of bifurcation behaviors, as detailed in the reference [38]. Tools of bifurcation controls, including the

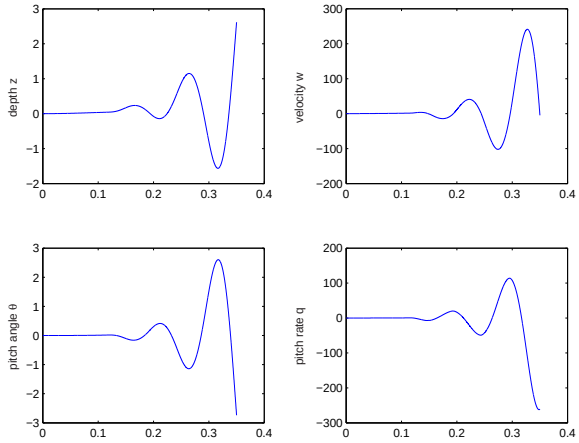

Figure 6.5: Motions initiated from trivial initial conditions in the uncontrolled case.

washout filter based dynamic feedback control, are provided to avoid undesirable bifurcation behaviors and achieve desired bifurcation behaviors during the entire motion of supercavitating vehicles.

6.5 Control System Design

In this section, two control schemes are presented. For purposes of control system design, the specific set of parameter values (6.7) is considered.

As elaborated in the preceding section, the form of the governing equations is complicated and does not lend itself to a direct analysis. To explore the system dynamics, as a first step, numerical simulations are carried out in the time domain. The system without any control inputs, also referred to as the uncontrolled or open-loop system, exhibits unstable oscillatory motions [37] that grow quite rapidly for various initial conditions. In Figure 6.5, the results are shown for the case in which the motion is initiated from the trivial initial condition; that is, $x = 0$ at $t = 0$.

The control objective for the supercavitating vehicles is to design an inner-loop controller to stabilize the dive-plane dynamics of the vehicle at an equilibrium point, or at a limit cycle surrounding this point, if the former goal is not attainable. The desired equilibrium point is determined by the outer-loop guidance controller of the supercavitating vehicle, and this is not addressed here.

The forward speed V is controlled by the engine thrust. In this work it is assumed that the forward speed V and therefore the cavitation number s are constant during the time interval of interest. During the transitional period when the vehicle has not been accelerated to the constant speed V, the supercavity may not have formed and part of the vehicle body may be surrounded by one or several air bubbles called partial cavities. Correspondingly, modeling details including the planing force formula need to be modified. However, to date, analytical models are not available yet for partial cavities. Therefore, in the current work we will focus on the time interval when the vehicle is already at a forward speed V.

As illustrated in Figure 6.3, the planing force is absent in the dead zone and the system is linear in this region. Local stability of the equilibrium point in the dead zone can be easily enforced by using linear state feedback. However, large perturbations drive the system out of the dead zone and the tail-slap phenomenon develops as shown in the simulations of the open-loop system. The planing force grows quickly in magnitude when the supercavitating vehicle is driven out of the cavity by large perturbations. Compared to other forces (e.g., the gravity) in the system, the planing force is strong in magnitude even when only a small portion of the vehicle is submerged in water. This strong nonlinearity can easily drive the

system dynamics to instability. Therefore, the planing force nonlinearity presents a special challenge for control design. In the following, various feedback control schemes are examined for meeting the control objective. The key issue is to evaluate the effectiveness of linear/switching control schemes in the nonlinear system.

6.5.1 Linear Feedback Control

Here, nonlinear system tools, including the circle criterion and the describing function method, are used to design linear feedback control and analyze the closed-loop system. The circle criterion is usually used to judge the absolute stability of a system with a class of nonlinearity that lies within some sectors. It makes sense to apply the circle criterion to the supercavitating vehicle model with a particular nonlinearity for the following reasons:

- the considered nonlinearity satisfies the sector condition and, although conservative, absolute stability as determined by using the circle criterion guarantees the stability of the system
- the determination of this nonlinearity is prone to modeling errors, and one way to represent these modeling errors is to assume that the true nonlinearity is close to the nominally assumed nonlinearity in the sense of the sector condition (2.1).

The procedures of Section 2.1.2 are used to judge the absolute stability of the equilibrium point of the system and estimate its region of attraction (ROA).

In the control designs in the sequel, the following are assumed: i) all four states are measurable, and ii) the desired equilibrium point is given by $x_{eq} = [z_d, 0, \theta_d, q_d]$. After redefining the state variables in (6.11), the supercavitating vehicle model (6.6) is rewritten as shown in (6.12).

$$\tilde{x} = x - x_{eq} \tag{6.11}$$

$$\dot{\tilde{x}} = A\tilde{x} + Bu + (C + Ax_{eq}) + DF_p \tag{6.12}$$

The first term of the control law

$$u = -(B^T B)^{-1} B^T (C + Ax_{eq}) + v \tag{6.13}$$

cancels the constant term of the vector field in (6.12) including the gravity term C and the term determined by the desired equilibrium point. This results in the closed loop system (6.14) with a linear state feedback (6.15):

$$\dot{\tilde{x}} = A\tilde{x} + Bv + DF_p \tag{6.14}$$

$$v = -K_f \tilde{x} \tag{6.15}$$

The stability of the origin depends on selection of the matrix K_f in (6.15). For example, if K_f is designed such that the poles associated with $\hat{A} = A - BK_f$ are placed at -20, -30, -40, and -50 (referred to as Controller $A1$ in the sequel), then the origin in the system (6.14) is regionally absolutely stable. By using the Lyapunov method in Section 2.1.2, the ROA Ω_{A1} can be estimated to be (6.16) with $y_0 = 1.98$

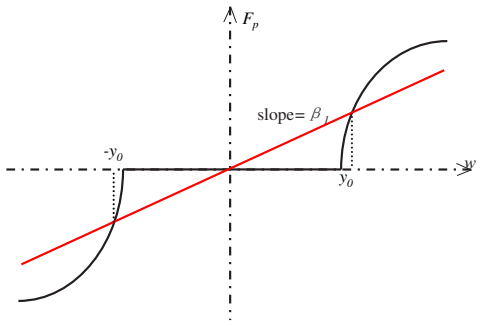

Figure 6.6: ROA estimation using the circle criterion. (Controller $A1$)

and $\beta_1 = 55$, where y_0 and β_1 are as indicated in Figure 6.6.

$$\begin{aligned} \Omega_{I1} &= \{x \in \Re^4 | V(x) = x^T P_{A1} x \leq 25.94\} \\ P_{A1} &= \begin{pmatrix} 2652 & -89 & -13496 & -206 \\ -89 & 33 & 507 & 9 \\ -13496 & 507 & 68853 & 1056 \\ -206 & 9 & 1056 & 16 \end{pmatrix} \end{aligned} \tag{6.16}$$

If K_f is designed such that the poles associated with $\hat{A} = A - BK_f$ are placed farther from the imaginary axis at -40, -60, -80, and -100 (referred to as Controller $A2$ in the sequel), then the origin in the system (6.14) is rendered globally absolute stable. This can be verified by the circle criterion as illustrated in Figure 6.7. More details about the circle criterion can be found in Section **??**.

Representative simulation results with this controller are shown in Figure 6.8. It is noted that this initial condition places the vehicle outside the dead zone for the planing force. It is noted that the control effort is strong and may lead to actuator

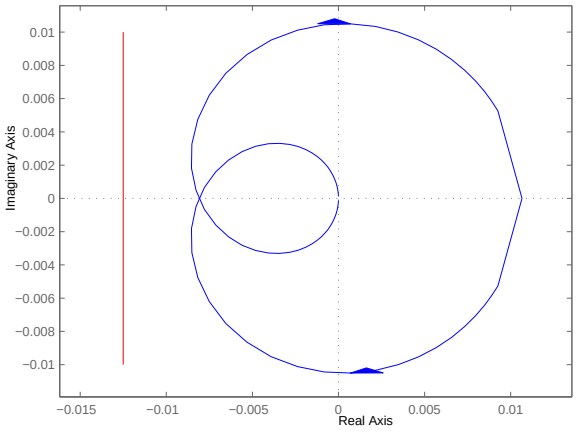

Figure 6.7: Nyquist diagram of $G(s)$ and straight line $Re[s] = -1/\beta_1$ ($\beta_1 = 85$). (Controller $A2$)

saturation. This issue is addressed later in Section 6.6.

6.5.2 Switching Control

Next, switching control schemes are introduced to improve system performance in terms of the region of attraction and magnitude of the control effort.

The system (6.14) is recalled; for convenience, the tilde symbol is dropped and the equation of motion is repeated here:

$$\dot{x} = Ax + Bv + DF_p \tag{6.17}$$

A switching control structure is described as follows:

$$\begin{aligned} v &= -K_f x - (B^T B)^{-1} B^T D f(w) \\ f(w) &= \begin{cases} k_c(w - w_{th}) \text{ if } w > w_{th} \\ 0 \text{ if } |w| \leq w_{th} \\ k_c(w + w_{th}) \text{ if } w < -w_{th} \end{cases} \end{aligned} \tag{6.18}$$

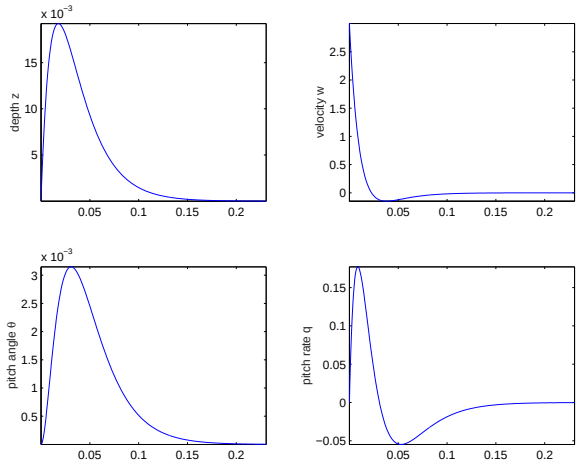

(a) states

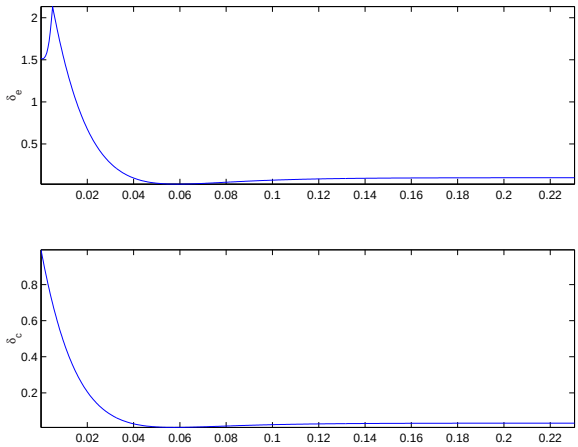

(b) control efforts

Figure 6.8: Motions initiated from $[z, w, \theta, q] = [0, 3, 0, 0]$ in the controlled case and control effort (Controller $A2$).

where w_{th} is the dead zone boundary for the planing force illustrated in Figure 6.3 and k_c is a constant to be selected. The first term in the control v can be viewed as equivalent to the linear feedback control designed in the previous subsection. The second term modifies the nonlinearity F_p. This becomes clear on substituting the switching control scheme in (6.18) into the system model (6.17):

$$\dot{x} = (A - BK_f)x + D(F_p - f(w)) \tag{6.19}$$

For comparison, it is noted that the closed-loop system with linear feedback control given in Section 6.5.1 is described by

$$\dot{x} = (A - BK_f)x + D(F_p) \tag{6.20}$$

When one compares these two closed-loop systems, it can be seen that the system with the switching control scheme is similar to that with linear feedback except for the added term $f(w)$, which modifies the nonlinearity. As illustrated in Figure 6.9, the original nonlinearity F_p shown with a bold line is transformed to the nonlinearity $F_p - f(w)$ illustrated by a dotted line. Therefore, the switching control "weakens" the nonlinearity. With the same choice of K_f, this results in a larger region of attraction. Equivalently, less control effort is required to achieve the same region of attraction.

For example, if $k_c = 150$ and K_f is designed such that the poles associated with $\hat{A} = A - BK_f$ are placed at -20, -30, -40, and -50 (referred to as Controller $B1$ in the sequel), then the origin of system (6.14) is regionally absolute stable with a larger region of attraction that that of the system with the linear controller $A1$.

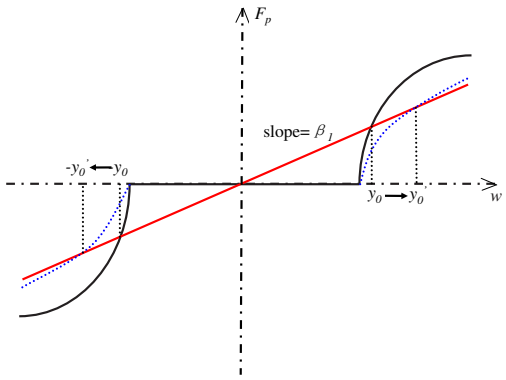

Figure 6.9: Switching Control Design

Representative simulation results with this switching controller are shown in Figure 6.10.

6.6 Actuator Saturation

In practice, a strong control effort can lead to actuator saturation. Actuator saturation deteriorates control system performance and even results in instability that sometimes accounts for devastating accidents. For example, the well-known Chernobyl nuclear disaster is believed to be the result of actuator saturation in the control system. [57] In the foregoing section, two control schemes have been elaborated and shown to be effective for the nonlinear system representing the dynamics of a supercavitating vehicle. It is shown that with appropriate selection of the feedback coefficients, these feedback controllers can globally stabilize the nonlinear system to a desired equilibrium point. However, the strong control effort required could lead to actuator saturation. In other words, actuator saturation may limit the

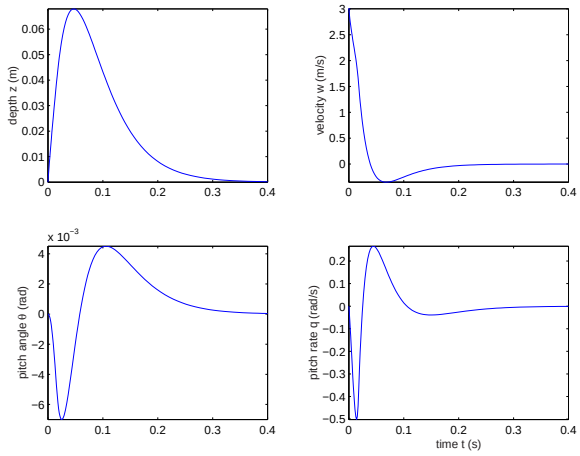

(a) states

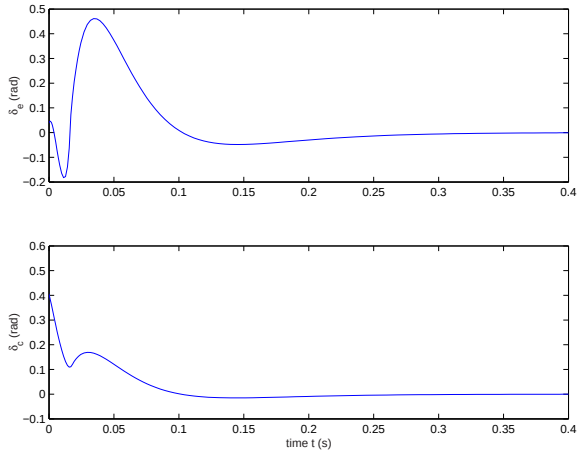

(b) control effort

Figure 6.10: Motions initiated from $[z, w, \theta, q] = [0, 3, 0, 0]$ with the switching controller $B1$ and control effort. By comparison, the system with the linear controller $A1$ is stabilized to a large-magnitude limit cycle when initiated from the same point.

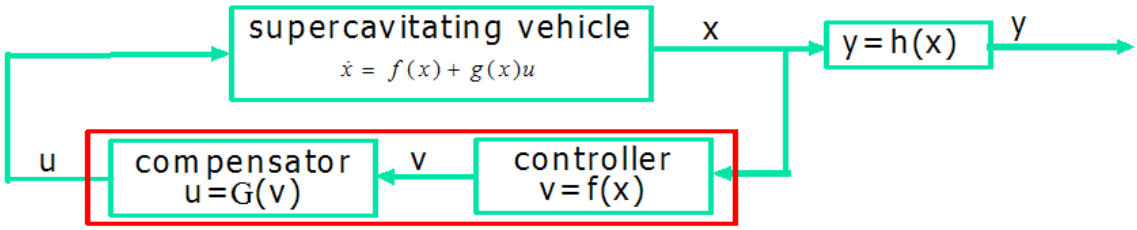

Figure 6.11: Compensator to deal with the actuator saturation problem.

performance of the linear feedback controllers considered in the previous section.

In this section, an optimization problem is formulated to achieve the best possible control performance while maintaining a control effort within the actuator limits. This method is based on the work of Soroush and Valluri [55].

As shown in Figure 6.11, a two-step design procedure is proposed for controlling the supercavitating system considering the actuation constraints. First, unlimited actuation is assumed and the controller v is designed. Subsequently, a compensator $G(\cdot)$ is sought to achieve best possible performance subject to the actuation limits $u_{low} \leq u \leq u_{high}$.

The first step can be implemented by using the control design methods of Section 6.5. The second step is equivalent to finding $G(\cdot)$ to minimize the difference between desired outputs (with unlimited actuation) and actual outputs (with limited actuation). This is formulated as the optimization problem

$$\phi(G) = \sum_{l=1}^{m} p_l [\int_{t}^{t+T} |y_l(\tau) - y_l^*(\tau)| d\tau]^2 \tag{6.21}$$

where the objective function is minimized subject to $u_{low,i} \leq u_i \leq u_{high,i}$. Here, m is number of outputs, p_l is the weight associated with the output y_l, T is the prediction horizon, y_l is the actual output with $u = G(v)$, and y_l^* is the desired output with

$u = v$. From another point of view, the optimal solution $G(\cdot)$ coordinates between different control inputs to achieve a control performance that is closest to that in the absence of actuation limits.

In the supercavitating vehicle system, there are two control inputs and $m = 2$. Let $y = [z\ \theta]^T$ and the number of inputs and outputs be the same. In this case, the optimization problem is equivalent to a quadratic programming problem and an iterative algorithm is employed to find the solution. More details can be found in the reference [55].

This optimization technique can be applied together with the control schemes in Section 6.5 to reduce the adverse effect of actuation limits on the control performance. As an example, assume $|\delta_e| \leq 20$ degrees and $|\delta_c| \leq 20$ degrees. In this case, the control performance of Controller $A2$ is greatly deteriorated and the system becomes unstable without a compensator (Figure 6.12(a)). With the compensator, however, the system is stable even if the initial condition is quite far from the dead zone (Figure 6.12(b)).

6.7 Bifurcations in Supercavitating Vehicles

Thus far, all studies on the dynamics and control of supercavitating vehicles focus on a particular choice of the system parameters such as the cavitation number σ, the vehicle forward speed V, the vehicle geometry, and the cavitator radius. There has been limited published work on the bifurcation behavior of supercavitating vehicles. A detailed study on the bifurcation behavior of supercavitating

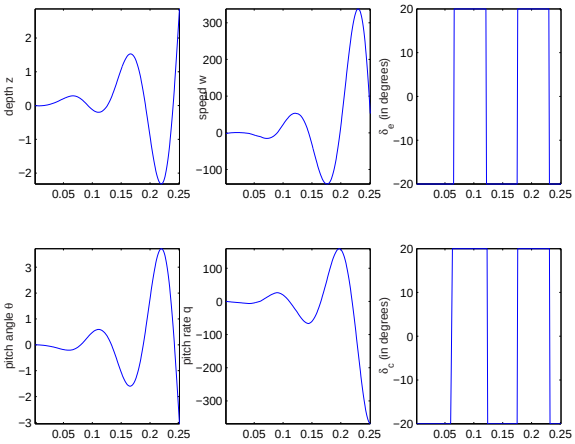

(a) without compensator

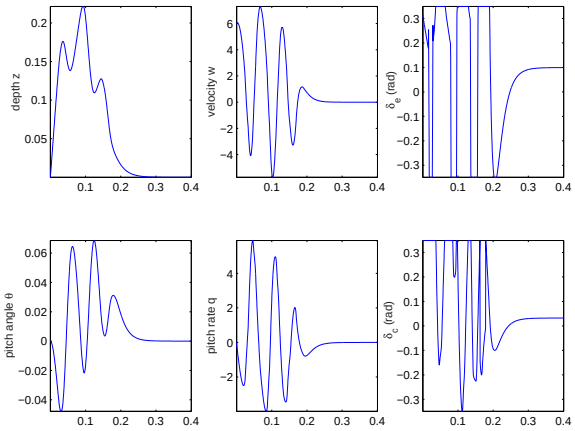

(b) with compensator

Figure 6.12: Motions with the linear controller $A2$. (a) initiated from $[z, w, \theta, q] = [0, 2, 0, 0]$ and (b) initiated from $[z, w, \theta, q] = [0, 6, 0, 0]$. The dead zone boundary is at $w_{th} = 1.64m/s$.

vehicles is important for three main reasons. First, after a supercavitating vehicle is launched, the vehicle forward speed V increases until a specified nominal value that is associated with a stable supercavity is reached. In some cases, after the vehicle runs within the supercavity for a while, the vehicle slows down, or equivalently, the forward speed V is decreased. It is of practical importance to study the change of vehicle dynamics as the forward speed V is varied. Second, different steady state solutions such as equilibrium points and limit cycles have been discovered in supercavitating vehicles [37]. It is of interest to determine the possible steady state motions and how these solutions evolve, as some important system parameters are varied. Third, bifurcation control tools may help one to modify the bifurcation behavior and achieve desired steady state solutions within specified parameter ranges.

In this section, steady state solutions of dive-plane models and their bifurcations are studied with respect to the cavitation number σ as the bifurcation parameter. Different steady solutions are explored and it is examined as to how these solutions evolve as the cavitation number is varied. The cavitation number σ is chosen as the bifurcation parameter, since it is a function of the vehicle forward speed V and it characterizes the extent of cavitation. From definition (6.1), it is clear that σ is proportional to $\frac{1}{V^2}$. On the other hand, a small cavitation number σ indicates a large cavity. The shape and size of a supercavity determines the magnitude and direction of the planing force, a strong nonlinear interaction between the vehicle aft body and the cavity wall. Through the planing force, the cavitation number has a direct impact on the vehicle dynamics.

It is noted that bifurcation studies of ships and some underwater vehicle sys-

tems have been carried out in the literature. For example, Spyrou and Thompson [56] provided a review of studies on nonlinear ship dynamics involving bifurcation analysis. Papoulias [48] studied the bifurcations of a marine vehicle system. The system model is smooth and focus of this work is on the horizontal plane dynamics. By contrast, the supercavitating vehicle model considered here is nonsmooth and focus of the current work is on the dive plane dynamics, which is more complicated. In addition to bifurcation analysis, control of bifurcations is also examined here.

In order to determine a valid range of the cavitation number that would be physically meaningful, analysis is needed, as discussed next.

6.7.1 Range of the Cavitation Number

In previous studies ([16, 37]), the cavitation has been chosen as $\sigma = 0.03$. The model given by Eqs. (6.2)-(6.4) is valid only for cases with supercavitation. However, a large cavitation number corresponds to the no-cavity case or a partial-cavity case. On the other hand, a very small cavitation number is not practical due to the physical constraints, such as the vehicle speed. Furthermore, the assumptions made in deriving and simplifying the cavity model lead to additional constraints on the cavitation number. An inspection of the cavity model (see Eq. (6.5)) reveals the following three constraints on the cavitation number:

1. $K_1 > 0 \ \Rightarrow \sigma > 0.0198$

2. $1 - (1 - \frac{4.5\sigma}{1+\sigma}){K_1}^{40/17} \ \Rightarrow \sigma < 0.0398$

3. $R_c > R \ \Rightarrow \sigma < 0.0368$

The expressions of the cavity radius R_c at the transom or the planing section, and its derivative in Eq. (6.5) are simplified forms that follow from Logvinovich's cavity model [40]. The first constraint follows directly from the assumption

$$L \ > \ R_n(\frac{1.92}{\sigma} - 3) \tag{6.22}$$

made during the simplification; this can be determined from the definition of the constant K_1. The second constraint is enforced to ensure that the cavity radius expression of Logvinovich's model has a real value at the vehicle's transom. The third constraint allows for the cavity to have a larger radius than the vehicle body at the transom. Hence, based on this discussion, the simplified cavity model is applicable only when the cavitation number falls within the interval $[0.0198, 0.0368]$.

6.7.2 Bifurcation Results

Due to the complicated form of the nonsmoothness of the system, it is not feasible to analytically determine the fixed points and periodic solutions of the given dynamic system, and the bifurcations of these solutions. Hence, one has to resort to numerical bifurcation analysis tools. The control law given by Eq. (6.8) is used in the bifurcation study.

In Figure 6.13, the bifurcation diagrams obtained during quasi-static forward and reverse sweeps of the cavitation number are shown. For equilibrium-point solutions, the vertical speed w is plotted against the cavitation number. For non-equilibrium solutions such as periodic orbits and chaotic orbits, the vertical speed w on the chosen Poincaré section is plotted against the cavitation number. This

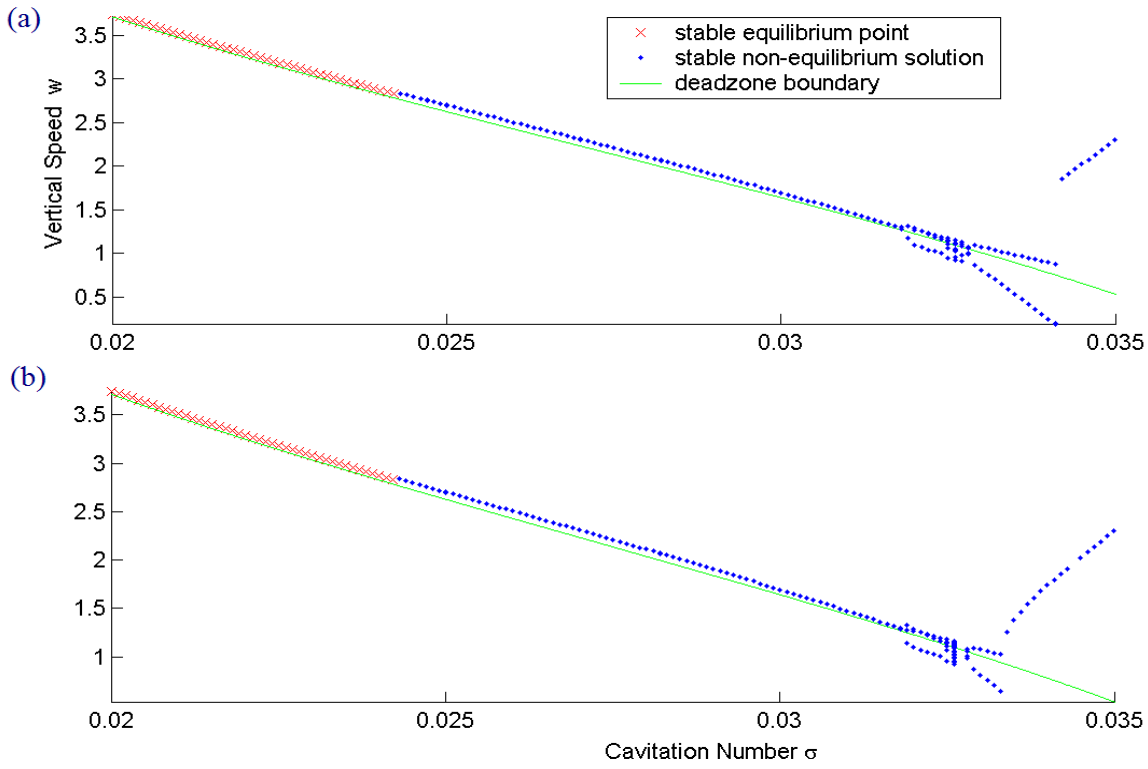

Figure 6.13: Bifurcation diagram of the supercavitating vehicle system for $0.020 < \sigma < 0.035$. a) forward sweep of σ and b) reverse sweep of σ. The dead zone is below the boundary line.

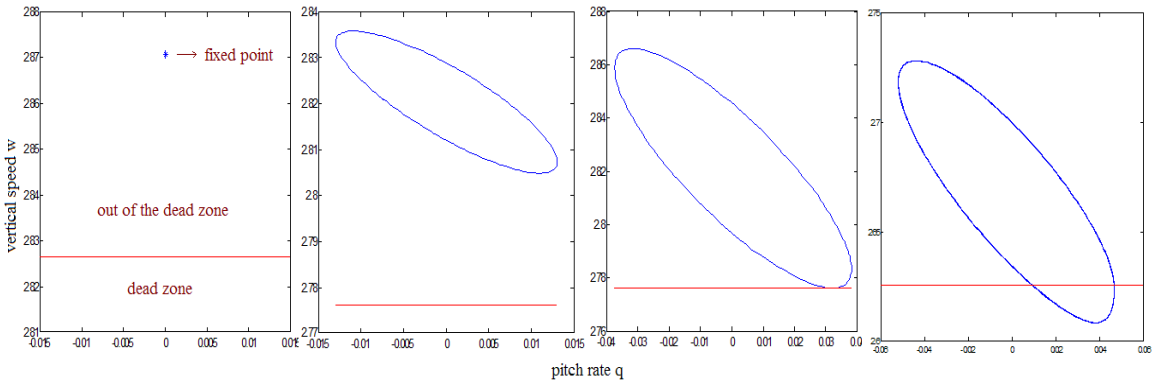

Figure 6.14: Steady state solutions for different σ. From left to right: $\sigma = 0.024$ (stable equilibrium point), $\sigma = 0.0242475$ (limit cycle out of the dead zone), $\sigma = 0.0242477$ (grazing limit cycle), and $\sigma = 0.025$ (limit cycle with tailslap). The dead zone is below the straight line.

section is $\Sigma_0 = \{x = [z\ w\ \theta\ q] \in \Re^4 : q = 0, \dot{q} > 0\}$. The forward sweep and reverse sweep bifurcation diagrams turn out to be the same except in the interval $0.0333 < \sigma < 0.0341$. The nonsmooth dive-plane model exhibits a rich variety of nonsmoooth and smooth bifurcation behaviors and this is elaborated next.

For low cavitation numbers in the range $0.0200 < \sigma < 0.0242$, the system trajectories are attracted to a stable equilibrium point with $w > w_{th}$. For this equilibrium point, the vehicle afterbody is out of the cavity (immersed in water) and the planing force is nontrivial. In other words, these stable equilibrium points are supported by the cavitator force in the front and the planing force in the rear end. As σ is increased, a supercritical Hopf bifurcation occurs around $\sigma = 0.02424745$. The stable equilibrium points become unstable and a branch of stable limit cycles is born around the equilibrium points. For each point of these stable limit cycles, $w > w_{th}$.

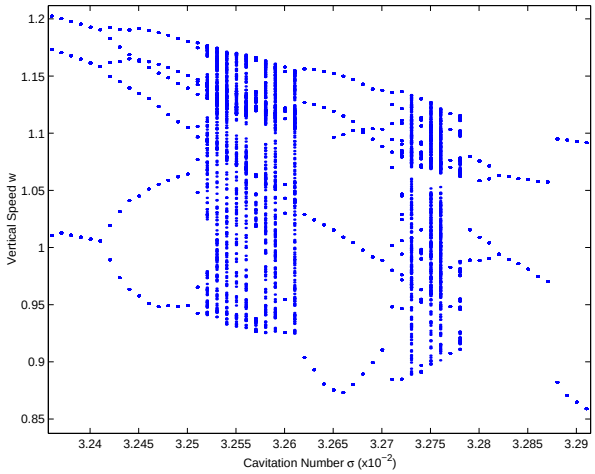

Figure 6.15: Bifurcation diagram: $0.0324 < \sigma < 0.0329$

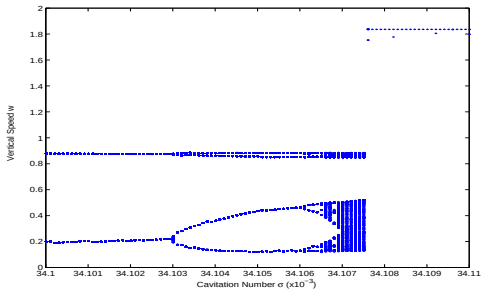

Figure 6.16: Period-doubling route to chaos: $0.03410 < \sigma < 0.03411$

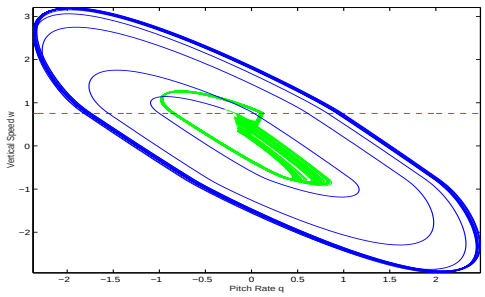

Figure 6.17: Transient Chaotic Motion at $\sigma = 0.0341076$: the state trajectory experiences a transient chaotic motion in the inner zone and it is ultimately attracted to the stable periodic solution. The dashed line is the switching boundary.

In steady state, the rear end of the supercavitating vehicle is out of the cavity all the time. As σ is slightly increased, a grazing event occurs when the limit cycle grazes the switching boundary $\Sigma_1 = \{x : w - w_{th} = 0\}$. Beyond this critical value of σ, the planing force varies periodically. The vehicle afterbody moves into and out of the cavity alternatively, which is called the *tailslap phenomenon*. Starting from an equilibrium point supported by the planing force, the tailslap can be understood as a result of a Hopf bifurcation followed by a grazing event. This process is illustrated in Figure 6.14.

As the cavitation number σ is further increased, a period-doubling bifurcation occurs at $\sigma = 0.03178$. It is followed by a sequence of period-doubling bifurcations that leads to a chaotic motion at $\sigma_\infty = 0.03252$, as shown in Figure 6.15; this figure is a magnification of Figure 6.13 in the range $0.030 < \sigma < 0.035$.

As σ is increased beyond 0.0325, a rich variety of bifurcation behavior is discovered. At $\sigma = 0.03253$, three chaotic bands merge into one large chaotic attractor. This behavior is called a chaotic attractor merging crisis in [46]. At $\sigma = 0.032614$, there is a sudden transformation from a chaotic attractor to a period-3 orbit. Then, another chaotic attractor is developed at $\sigma = 0.03272$ through a period-doubling bifurcation route. After that, a reverse period-doubling bifurcation sequence is found to start at $\sigma = 0.03278$. The sudden emergence of a branch of fixed points in Figure 6.15 at $\sigma = 0.03265$ does not correspond to any bifurcation as it is due to the collision of the limit cycle with the Poincaré section Σ_0.

As one increases σ further, at $\sigma = 0.03288$, a jump is identified from one branch of limit cycles to another branch of limit cycles. This is a result of a cyclic-

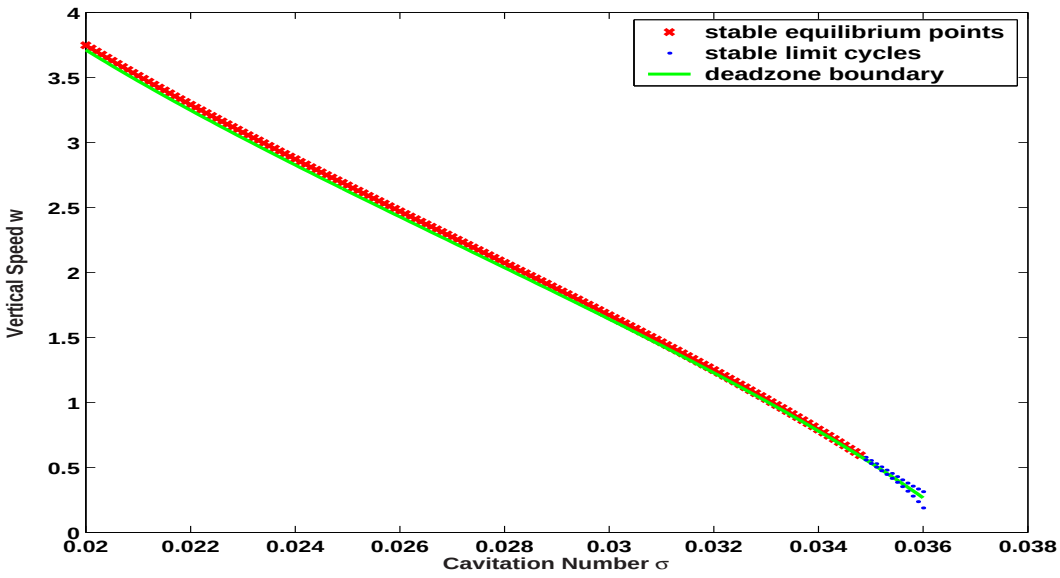

Figure 6.18: Bifurcation diagram with $k_p = -3$

fold bifurcation at $\sigma = 0.032882129$; this event is confirmed by calculating the Floquet multipliers by using the shooting method [46].

As σ is further increased, a jump occurs at $\sigma = 0.03411$, which can be seen from Figure 6.13 (a). A numerical simulation with higher resolution in σ (Figure 6.16) shows that the period-2 orbit at $\sigma = 0.03410$ experiences a period-doubling bifurcation sequence and results in a chaotic attractor. The chaotic attractor then collides with an unstable periodic solution within its basin of attraction at $\sigma = 0.0341076$ and results in the jump at $\sigma = 0.03411$. This type of sudden annihilation of chaos is referred to as exterior chaotic crisis in the literature (e.g., [46]. The results shown in Figure 6.17 support this statement, through the signature behavior of the exterior chaotic crisis – a transient chaotic motion followed by a periodic steady state motion.

In the reverse sweep bifurcation diagram shown in Figure 6.13 (bottom), a

jump is found at $\sigma = 0.03335$. Calculation of Floquet multipliers confirms the occurrence of a cyclic-fold bifurcation at $\sigma = 0.0333541$, which explains the jump in the bifurcation diagram. Similar bifurcation behaviors are also found in the intervals $0.03252 < \sigma < 0.03261$ and $0.03272 < \sigma < 0.03278$. For example, the steady-state solution jumps from a chaotic attractor to a period-5 orbit at $\sigma = 0.03256174$ (exterior chaotic crisis); at $\sigma = 0.032568$, a chaotic attractor is developed through a period-doubling bifurcation route; and several chaotic bands merge into a larger one (chaotic attractor merging crisis) at $\sigma = 0.032574$.

6.7.3 Bifurcation Control

Typically, in bifurcation control (e.g., [1]), the uncontrolled system exhibits a bifurcation that one seeks to delay or suppress by choosing an appropriate feedback control law.

Here, the bifurcation diagrams shown in Section 6.7 pertain to a certain choice of feedback law given by Eq. (6.8). As shown in the previous section, bifurcations leading to steady-state solutions (limit cycles and chaotic attractors) other than equilibrium points are found. As the cavitation number σ is increased, the system experiences a supercritical Hopf bifurcation followed by a grazing event. Beyond the grazing event, the steady-state solutions intersect the switching boundaries and tailslap phenomenon occurs.

From a physical standpoint, the tailslap behavior in the supercavitating vehicle is usually harmful. In this section, it is aimed to eliminate the tailslap behavior by

using appropriate bifurcation control tools.

The bifurcation study in the previous section shows that the tailslap is the result of a Hopf bifurcation followed by a grazing event. This suggests that the occurrence of the tailslap behavior (associated with limit-cycle or chaotic motions) can be controlled by delaying or suppressing the onset of the Hopf bifurcation so that the vehicle system is attracted to equilibrium points for all cavitation number values within a desired range. To achieve this goal, dynamic feedback laws aided by washout filters are investigated. It is noted that the Hopf bifurcations in the underwater vehicle system is supercritical and it is sought to preserve this supercriticality while delaying the onset.

The dynamic feedback aided by washout filters is an effective tool to control the onset of Hopf bifurcations [61]. With this type of dynamic feedback, the equilibrium points of the original system are preserved. A washout filter aided feedback control law with measurement of the pitch rate q is described in Eq. (6.23), where p is the state variable in the washout filter, $d \in (0, 1)$ is a constant, and k_p is the dynamic feedback coefficient. The four-dimensional dive-plane model shown in Eq. (6.2) is expanded to a five-dimensional system.

$$\dot{p} = q - dp \tag{6.23}$$

$$\delta_c = k_p(q - dp) \tag{6.24}$$

The onset of the Hopf bifurcation can be modified by choosing the dynamic feedback coefficient k_p. With $k_p = -3$, the Hopf bifurcation is delayed to $\sigma = 0.03483$. The bifurcation diagram in this case is shown in Figure 6.18. Here peak values are used to

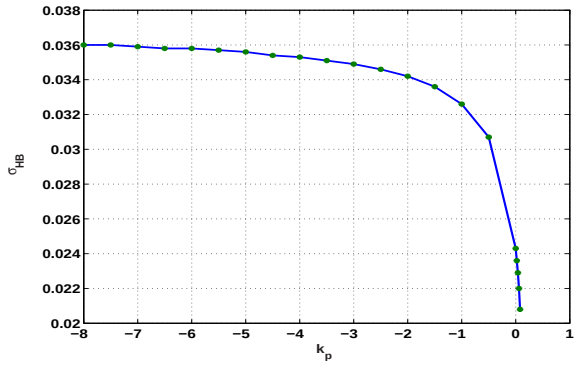

Figure 6.19: Location of the Hopf bifurcation points as the dynamic feedback coefficient k_p is varied.

represent the periodic orbits. For almost the entire range of σ ($0.020 < \sigma < 0.03483$), the vehicle system is stabilized to equilibrium points out of the dead zone and the tailslap behavior is eliminated. The critical σ values at the Hopf bifurcation points are plotted against the dynamic feedback coefficient k_p in Figure 6.19. For $k_p < -8$, the Hopf bifurcation is delayed to be out of the physically meaningful parameter range $0.020 < \sigma < 0.036$. For any meaningful σ value, there are no periodic orbits and the system is stabilized to equilibrium points. For $k_p > 0.08$, the Hopf bifurcation location is pushed out of the physically meaningful parameter range. For any meaningful σ value, the system is stabilized to limit cycles.

Chapter 7

Application of Generalized Absolute Stability Results

In Chapter 4 and Chapter 5, conditions are derived for the generalized absolute stability of second-order systems and finite-order systems respectively. The derived conditions for second-order systems can be easily checked by algebraic computations and simple numerical integrations. In comparison, the derived conditions for a general finite-order system require some amount of numerical effort. It is numerically inexpensive, however, because the conditions are formulated as a linear programming problem which can be numerically solved in an efficient manner. In this chapter, the application of the theoretical results in Chapter 4 and Chapter 5 will be illustrated by a few examples that include the supercavitating vehicle model in the previous chapter.

In the sequel, the theoretical results derived in Chapter 4, together with the backstepping control approach, are applied to the supercavitating vehicle system in Section 7.1. In Section 7.2, the theoretical results are applied to three different systems: one second-order system, one third-order system, and the fourth-order supercavitating vehicle model.

7.1 Application of The Results on Second-Order Systems

In this section, the theoretical results derived in Chapter 4 are employed to robustly stabilize the dive-plane motion of supercavitating vehicles that are introduced in the previous chapter. Here the control objective is to design an inner-loop controller to achieve stability at a desired equilibrium point with robustness to the modeling error in the planing force.

Recall that the dive-plane model of supercavitating vehicles is of the fourth order. Due to the special structure of the vector field of the model, the backstepping control approach may be employed to reduce the fourth-order control problem to a second-order one. Through the supercavitating vehicle example, it is also illustrated that the generalization of the classical absolute stability concept helps to reduce the conservativeness in the controller design.

For convenience, the four-dimensional dive-plane model (6.6) in the previous chapter is rewritten here

$$\dot{x} = Ax + Bu + DF_p \tag{7.1}$$

with $x = [z\ w\ \theta\ q]^T$ and $u = [\delta_e\ \delta_c]^T$. It is reminded that x, u, F_p stand for the states, the control inputs and the planing force, respectively. Additional details regarding this model can be found in the previous chapter.

In consideration of the guidance and navigation control or the outer-loop control, the desired equilibrium point for stability control or the inner-loop control is generally not at the origin. Denote the desired equilibrium point as $x_{eq} = [z_d, w_d, \theta_d, q_d]$. After redefining the state variables in (7.2) and letting $u = \tilde{u} +$

$(B^TB)^{-1}B^TAx_{eq}$, the supercavitating vehicle model (6.6) is rewritten as shown in (7.3).

$$\tilde{x} = x - x_{eq} \tag{7.2}$$

$$\dot{\tilde{x}} = A\tilde{x} + B\tilde{u} + D\tilde{F}_p \tag{7.3}$$

From here onwards, the tilde symbol is dropped for simplicity and the system is rewritten as

$$\begin{aligned} \dot{z} &= w - V\theta \\ \dot{\theta} &= q \\ \begin{pmatrix} \dot{w} \\ \dot{q} \end{pmatrix} &= A_2 \begin{pmatrix} w \\ q \end{pmatrix} + B_2 \begin{pmatrix} \delta_e \\ \delta_c \end{pmatrix} + D_2 F_p \end{aligned} \tag{7.4}$$

where $A_2 = \begin{pmatrix} a_{22} & a_{24} \\ a_{42} & a_{44} \end{pmatrix}$, $B_2 = \begin{pmatrix} b_{21} & b_{22} \\ b_{41} & b_{42} \end{pmatrix}$, and $D_2 = \begin{pmatrix} d_2 \\ d_4 \end{pmatrix}$. Here the nonlinearity F_p is not symmetric with respect to the origin any more, as is shown in Figure 7.1.

It is noted that the nonlinear term F_p does not appear in the right hand side of $\dot{z}$ and $\dot{\theta}$ and backstepping control is applied to reduce the fourth-order control problem to a second-order one. The steps involved are as follows:

1. The state variables w and q are treated as two control inputs. Let $M_V = \begin{pmatrix} 0 & -V \\ 0 & 0 \end{pmatrix}$, $M_K = \begin{pmatrix} 0 & 0 \\ k_1 & k_2 \end{pmatrix}$, and $\begin{pmatrix} w \\ q \end{pmatrix} = M_K \begin{pmatrix} z \\ \theta \end{pmatrix}$. The first two equa-

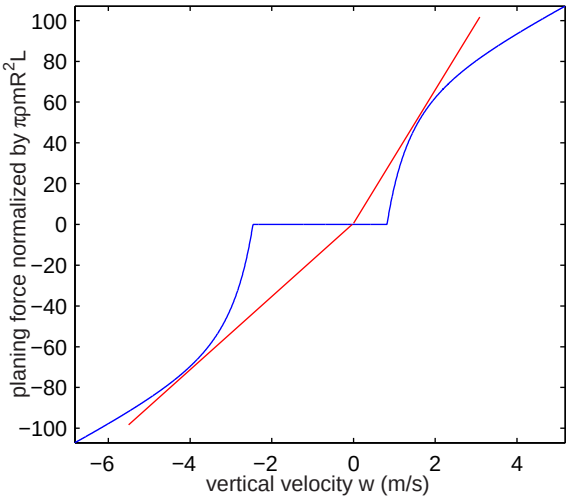

Figure 7.1: Planing force versus the vertical speed w.

tions in (7.4) then become:

$$\begin{pmatrix} \dot{z} \\ \dot{\theta} \end{pmatrix} = (M_V + M_K) \begin{pmatrix} z \\ \theta \end{pmatrix} \tag{7.5}$$

Then, the state variables z and θ are stabilized to the origin if and only if k_1 and k_2 are chosen so that the matrix $M_K + M_V$ is Hurwitz.

2. Let

$$\begin{pmatrix} \hat{w} \\ \hat{q} \end{pmatrix} = \begin{pmatrix} w \\ q \end{pmatrix} - M_K \begin{pmatrix} z \\ \theta \end{pmatrix}$$

Then

$$\begin{aligned}\begin{pmatrix}\dot{\hat{w}}\\ \dot{\hat{q}}\end{pmatrix} &= A_2\begin{pmatrix}w\\ q\end{pmatrix} + B_2\begin{pmatrix}\delta_e\\ \delta_c\end{pmatrix} + D_2F_p \\ &\quad -M_K\{M_V\begin{pmatrix}z\\ \theta\end{pmatrix} + \begin{pmatrix}w\\ q\end{pmatrix}\} \\ &= A_2\begin{pmatrix}\hat{w}\\ \hat{q}\end{pmatrix} + B_2\begin{pmatrix}\hat{\delta}_e\\ \hat{\delta}_c\end{pmatrix} + D_2F_p \qquad (7.6)\end{aligned}$$

where

$$\begin{pmatrix}\delta_e\\ \delta_c\end{pmatrix} = \begin{pmatrix}\hat{\delta}_e\\ \hat{\delta}_c\end{pmatrix} + \begin{pmatrix}\delta_{e0}\\ \delta_{c0}\end{pmatrix}$$

and

$$\begin{aligned}\begin{pmatrix}\delta_{e0}\\ \delta_{c0}\end{pmatrix} = B_2^{-1}\{M_KM_V\begin{pmatrix}z\\ \theta\end{pmatrix} + M_K\begin{pmatrix}w\\ q\end{pmatrix} \\ -A_2M_K\begin{pmatrix}z\\ \theta\end{pmatrix}\} \qquad (7.7)\end{aligned}$$

Therefore, the control problem of the fourth-order system (7.4) is reduced to the control problem of the second-order system (7.6). For this second-order system, suppose a linear feedback control is chosen as

$$\begin{pmatrix}\hat{\delta}_e\\ \hat{\delta}_c\end{pmatrix} = \begin{pmatrix}k_{11} & k_{12}\\ k_{21} & k_{22}\end{pmatrix}\begin{pmatrix}\hat{w}\\ \hat{q}\end{pmatrix} = K_2\begin{pmatrix}\hat{w}\\ \hat{q}\end{pmatrix} \qquad (7.8)$$

and the system becomes

$$\begin{pmatrix}\dot{\hat{x}}\\ \dot{\hat{y}}\end{pmatrix} = \begin{pmatrix}\hat{a}_{11} & \hat{a}_{12}\\ \hat{a}_{21} & \hat{a}_{22}\end{pmatrix}\begin{pmatrix}\hat{x}\\ \hat{y}\end{pmatrix} + \begin{pmatrix}b_1\\ b_2\end{pmatrix}F_{NL}(t, \hat{x} - g\hat{y}) \qquad (7.9)$$

where $\hat{x} = \hat{w}, \hat{y} = \hat{q}, b_1 = -d_2, b_2 = -d_4, g = 0$ and

$$\hat{a}_{11} = a_{22} + b_{21}k_{11} + b_{22}k_{21},\ \hat{a}_{12} = a_{24} + b_{21}k_{12} + b_{22}k_{22}$$

$$\hat{a}_{21} = a_{42} + b_{41}k_{11} + b_{42}k_{21},\ \hat{a}_{22} = a_{44} + b_{41}k_{12} + b_{42}k_{22} \tag{7.10}$$

After the state transformation

$$\begin{pmatrix} x \\ y \end{pmatrix} = \frac{1}{\eta} \begin{pmatrix} b_2 & -b_1 \\ b_2\hat{a}_{11} - b_1\hat{a}_{21} & b_2\hat{a}_{12} - b_1\hat{a}_{22} \end{pmatrix} \begin{pmatrix} \hat{x} \\ \hat{y} \end{pmatrix} \tag{7.11}$$

with $\eta = b_1b_2(\hat{a}_{22} - \hat{a}_{11}) + b_1^2\hat{a}_{21} - b_2^2\hat{a}_{12}$, this system is in the form (3.6) and $\alpha = -\hat{a}_{11} - \hat{a}_{22}, \beta = \hat{a}_{11}\hat{a}_{22} - \hat{a}_{12}\hat{a}_{21}, a = -b_2\hat{a}_{12} + b_1\hat{a}_{22}, b = -b_1$.

Returning to the fourth-order system (7.4), the total control effort is

$$\begin{aligned} \begin{pmatrix} \delta_e \\ \delta_c \end{pmatrix} &= K_2 \begin{pmatrix} w \\ q \end{pmatrix} - K_2M_K \begin{pmatrix} z \\ \theta \end{pmatrix} + \\ & \qquad B_2^{-1}\{M_KM_V \begin{pmatrix} z \\ \theta \end{pmatrix} + M_K \begin{pmatrix} w \\ q \end{pmatrix} - A_2M_K \begin{pmatrix} z \\ \theta \end{pmatrix}\} \qquad (7.12) \\ &= (K_2 + B_2^{-1}M_K) \begin{pmatrix} w \\ q \end{pmatrix} + (-K_2M_K + B_2^{-1}M_KM_V - B_2^{-1}A_2M_K) \begin{pmatrix} z \\ \theta \end{pmatrix} \end{aligned}$$

The feedback coefficients k_i with $i = 1, 2$ (in Step 1) can be designed by the pole placement method. To design the feedback coefficients k_{ij} with $i, j = 1, 2$ (in Step 2), the necessary and sufficient conditions given in Section 4.4 are utilized. In the case of $w_d = 0.5w_{th}$, the nonlinearity $\tilde{F}_p$ is bound in the asymmetric sector $(0, 31.8, 17.5)$. Based on Condition 4 in Theorem 2, we can choose a set of feedback

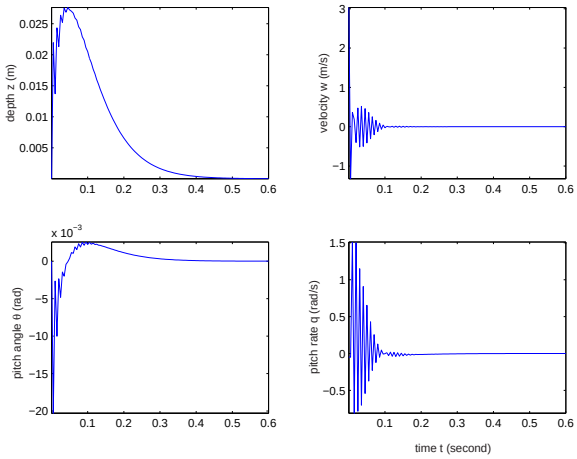

Figure 7.2: Motions initiated from $[z, w, \theta, q] = [0, 3, 0, 0]$ with the backstepping controller.

coefficients to ensure global stability of the nonlinear system:

$$K_2 = \begin{pmatrix} 10 & 5.95 \\ 0.9 & 0.24 \end{pmatrix} \tag{7.13}$$

Further, we choose $k_1 = 4.267, k_2 = -36$ to place the poles of the matrix $M_K + M_V$ at -16 and -20. Representative simulation results obtained with this controller are shown in Figure 7.2:

It is interesting to compare this result with that associated with classical absolute stability with symmetric sector conditions. From Theorem 3.2 of this work, which is first derived by Leonov [35], the choice of feedback matrix K_2 in (7.13) would lead to a closed-loop system that is not globally absolutely stable with the *symmetric* sector boundary $(0, 31.8)$. The advantage of the absolute stability theory with asymmetric sector conditions, which is developed in the current work for planar systems, is then clear–it reduces conservativeness in designing control schemes to stabilize a nonlinear system.

7.2 Application of The Results on General Finite-Order Systems

In this section, the theoretical results derived in Chapter 5 are employed to robustly stabilize nonlinear systems. To illustrate the application of these theoretical results better, a second-order system and a third-order system are addressed first, followed by the fourth-order supercavitating vehicle system.

7.2.1 A Second-Order System

It is noted that for second-order systems, there is no need to apply the results on general finite-order systems because the conditions derived in Chapter 4 are easier to check, and these conditions are not only sufficient but also necessary. Here a second-order system is used as an example purely in order to illustrate the steps in the applications of the theoretical results in Chapter 5. Here we look at one system of the form (5.1) with

$$x = [x_1 \;\; x_2]', A = \begin{pmatrix} -5.21 & -4 \\ -2.47 & -2 \end{pmatrix}, b = [3 \;\; 21]', c = [1 \;\; 0]' \tag{7.14}$$

In this system, the nonlinearity $F_{NL}(.)$ is bound in the asymmetric sector $(0, k_1, k_2)$ with $k_1 = 0.07$ and $k_2 = 2.57$.

The state space is partitioned into the cells $\Omega_i, i = 1, 2, ..., 8$, as illustrated in Figure 7.3. Correspondingly, the partition matrix a, which is defined in Section 5.4, is determined as

$$a = \begin{pmatrix} 1 & 1 & 0 & 1 \\ 0 & -1 & 1 & 1 \end{pmatrix} \tag{7.15}$$

It is straightforward to identify the constraint matrices $E_i, i = 1, 2, ..., 8$:

$$\begin{aligned}
E_1 &= \begin{pmatrix} 0 & 1 \\ 1 & -1 \end{pmatrix}, E_2 = \begin{pmatrix} -1 & 1 \\ 1 & 0 \end{pmatrix}, E_3 = \begin{pmatrix} -1 & 0 \\ 1 & 1 \end{pmatrix}, \\
E_4 &= \begin{pmatrix} -1 & -1 \\ 0 & 1 \end{pmatrix}, E_5 = \begin{pmatrix} 0 & -1 \\ -1 & 1 \end{pmatrix}, E_6 = \begin{pmatrix} 1 & -1 \\ -1 & 0 \end{pmatrix}, \\
E_7 &= \begin{pmatrix} 1 & 0 \\ -1 & -1 \end{pmatrix}, E_8 = \begin{pmatrix} 1 & 1 \\ 0 & -1 \end{pmatrix}
\end{aligned} \tag{7.16}$$

By employing the approach in (5.35), the continuity matrices are chosen as:

$$\begin{aligned}
F_1 &= \begin{pmatrix} 1 & 0 \\ 1 & -1 \\ 0 & 1 \\ 1 & 1 \end{pmatrix}, F_2 = \begin{pmatrix} 1 & 0 \\ 0 & 0 \\ 0 & 1 \\ 1 & 1 \end{pmatrix}, F_3 = \begin{pmatrix} 0 & 0 \\ 0 & 0 \\ 0 & 1 \\ 1 & 1 \end{pmatrix}, \\
F_4 &= \begin{pmatrix} 0 & 0 \\ 0 & 0 \\ 0 & 1 \\ 0 & 0 \end{pmatrix}, F_5 = \begin{pmatrix} 0 & 0 \\ 0 & 0 \\ 0 & 0 \\ 0 & 0 \end{pmatrix}, F_6 = \begin{pmatrix} 0 & 0 \\ 1 & -1 \\ 0 & 0 \\ 0 & 0 \end{pmatrix}, \\
F_7 &= \begin{pmatrix} 1 & 0 \\ 1 & -1 \\ 0 & 0 \\ 0 & 0 \end{pmatrix}, F_8 = \begin{pmatrix} 1 & 0 \\ 1 & -1 \\ 0 & 0 \\ 1 & 1 \end{pmatrix}
\end{aligned} \tag{7.17}$$

Therefore, based on using Theorem 5.3, a linear programming problem is formulated. By solving this numerical problem efficiently, we claim that this system is

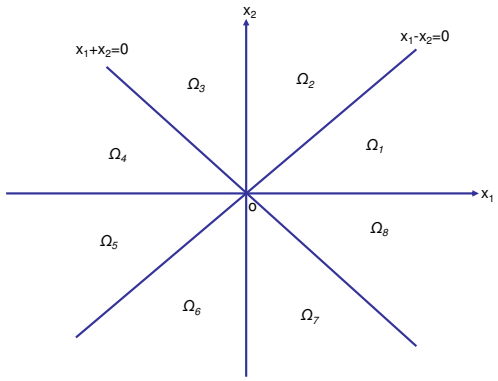

Figure 7.3: Illustration of the regions for piecewise linear Lyapunov functions.

absolutely stable with the Lyapunov function as follows.

$$
\begin{aligned}
V(x) &= l_i^T x \quad \text{if } x \in \Omega_i \\
\text{Ł} &= (l_1\ l_2\ l_3\ l_4\ l_5\ l_6\ l_7\ l_8) \qquad (7.18) \\
&= \begin{pmatrix} 4993 & 4751 & -5e^{-4} & -650 & -650 & -407 & 4343 & 4993 \\ -242 & 1.1e^{-3} & 1.1e^{-3} & -650 & -10939 & -11181 & -11181 & -10532 \end{pmatrix}
\end{aligned}
$$

Since the system (7.14) is of the second-order, we may confirm the absolute stability by using the necessary and sufficient conditions in Theorems 4.3 - 4.5. It can be verified that, after applying the state transformation in the Appendix, Condition 4 of Theorem 4.4 is satisfied.

For the system (7.14), if we replace $k_1 = 0.07$ by $k_1 = 0.13$, a PWLLF is not found. However, the system is indeed absolutely stable by using the same Theorem in the previous chapter. This is not surprising as Theorem 5.3 gives sufficient conditions only. A finer partition of the state space may be needed to find a PWLLF in this case.

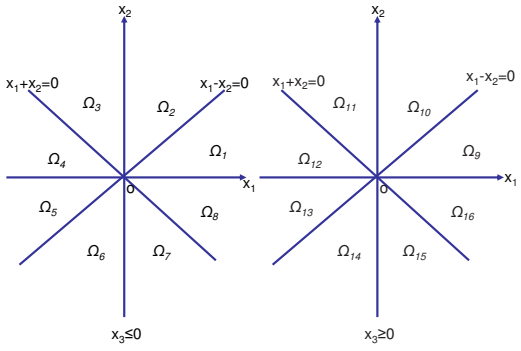

Figure 7.4: Illustration of the regions for piecewise linear Lyapunov functions.

7.2.2 A Third-Order System

Here we look at one system of the form (5.1) with $x = [x_1 \quad x_2 \quad x_3]'$. The nonlinearity $F_{NL}(.)$ is bounded in the asymmetric sector $(0, k_1, k_2)$ with $k_1 = 0.1$ and $k_2 = 0.5$, and

$$A = \begin{pmatrix} -9 & -5 & 0 \\ -2 & -2 & 0 \\ -4 & -5 & -2 \end{pmatrix}, \quad b = [26 \quad 21 \quad 2]', \quad c = [1 \quad 0 \quad 0]' \tag{7.19}$$

First we divide the state space $\Re^3$ into the regions $\Omega_i, i = 1, 2, ..., 16$, as shown in Figure 7.4.

A linear programming problem can then be formulated and solved according to Theorem 5.3. Thus we claim that this system is absolutely stable with the Lyapunov

function as follows.

$$
\begin{aligned}
V(x) &= l_i^T x \quad \text{if } x \in \Omega_i \\
\text{Ł}' &= (l_1\ l_2\ l_3\ l_4\ l_5\ l_6\ l_7\ l_8\ l_9\ l_{10}\ l_{11}\ l_{12}\ l_{13}\ l_{14}\ l_{15}\ l_{16})' \qquad (7.20) \\
&= \begin{pmatrix}
4.045 & -1.916 & 0.122 \\
1.808 & 0.321 & 0.122 \\
-0.052 & 0.321 & 0.122 \\
-0.246 & 0.127 & 0.122 \\
-0.246 & -9.892 & 0.122 \\
1.991 & -12.129 & 0.122 \\
3.851 & -12.129 & 0.122 \\
4.045 & -11.935 & 0.122 \\
4.045 & -1.916 & 0.030 \\
1.808 & 0.321 & 0.030 \\
-0.052 & 0.321 & 0.030 \\
-0.246 & 0.127 & 0.030 \\
-0.246 & -9.892 & 0.030 \\
1.991 & -12.129 & 0.030 \\
3.851 & -12.129 & 0.030 \\
4.045 & -11.935 & 0.030
\end{pmatrix}
\end{aligned}
$$

It is noted that the system is not absolutely stable with the symmetric sector bound $(0, k_2)$, as the matrix $A+k_2bc'$ is not Hurwitz. This system example illustrates the difference between the classical absolute stability and the generalized absolute stability with an asymmetric sector bound.

7.2.3 The Fourth-order Supercavitating Vehicle System

Recall that in Section 7.1, the four-dimensional supercavitating vehicle system is robustly stabilized by using the backstepping control approach and the theoretical results that are derived in Chapter 4. In this section, the four-dimensional vehicle system is robustly stabilized by directly applying the theoretical results derived in Chapter 5.

For the same reason as that in Section 7.1, the desired equilibrium point is denoted as $x_{eq} = [z_d, w_d, \theta_d, q_d]$. After redefining the state variables in (7.2) and letting $u = \tilde{u} + (B^T B)^{-1} B^T A x_{eq}$, the supercavitating vehicle model is rewritten in (7.3). On selecting the control as a linear feedback $\tilde{u} = K_4 \tilde{x}$ where $K_4 \in \Re^{2\times 4}$, the system becomes:

$$\dot{\tilde{x}} = A\tilde{x} + BK_4\tilde{x} + D\tilde{F}_p = (A + BK_4)\tilde{x} + D\tilde{F}_p \tag{7.21}$$

Returning to the original system (7.1), the total control effort is

$$\begin{pmatrix} \delta_e \\ \\ \delta_c \end{pmatrix} = (B^T B)^{-1} B^T A x_{eq} + K_4(x - x_{eq})$$

In the following the theoretical results derived in Chapter 5 will be employed to find the feedback matrix K_4 to robustly stabilize the system. In the case of $w_d = 0.5 w_{th}$, the nonlinearity $\tilde{F}_p$ is bound in the asymmetric sector $(0, 31.8, 17.5)$.

First we divide the state space $\Re^4$ into the regions $\Omega_i, i = 1, 2, ..., 16$, as shown in Figure 7.5. The state variables (x_1, x_2, x_3, x_4) correspond to (w, z, θ, q). A representative example of these regions is:

$$\Omega_1 = \{(x_1, x_2, x_3, x_4) | x_2 \geq 0, x_1 - x_2 \geq 0\} \tag{7.22}$$

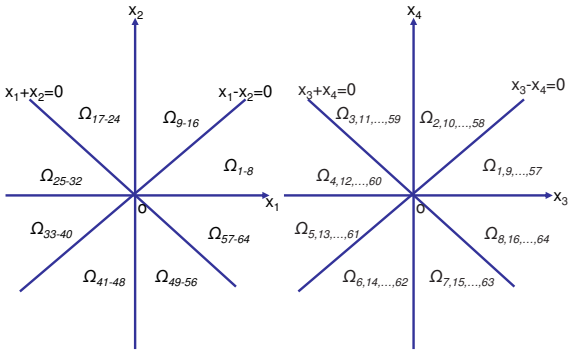

Figure 7.5: State space division for piecewise linear Lyapunov functions.

According to Theorem 5.3, a linear programming problem can then be formulated and solved . Thus we claim that this system is absolutely stable with the Lyapunov function as follows.

$$V(x) = l_i^T x \quad \text{if } x \in \Omega_i \tag{7.23}$$

$$Ł' = (l_1\ l_2\ l_3 ...\ l_{64})' \tag{7.24}$$

One choice of the feedback matrix is found to be:

$$K_4 = \begin{pmatrix} 40.4 & -78.1 & 29.4 & -62.3 \\ -88.9 & 21.7 & 58.4 & 20.3 \end{pmatrix} \tag{7.25}$$

Representative simulation results obtained with this controller are shown in Figure 7.6.

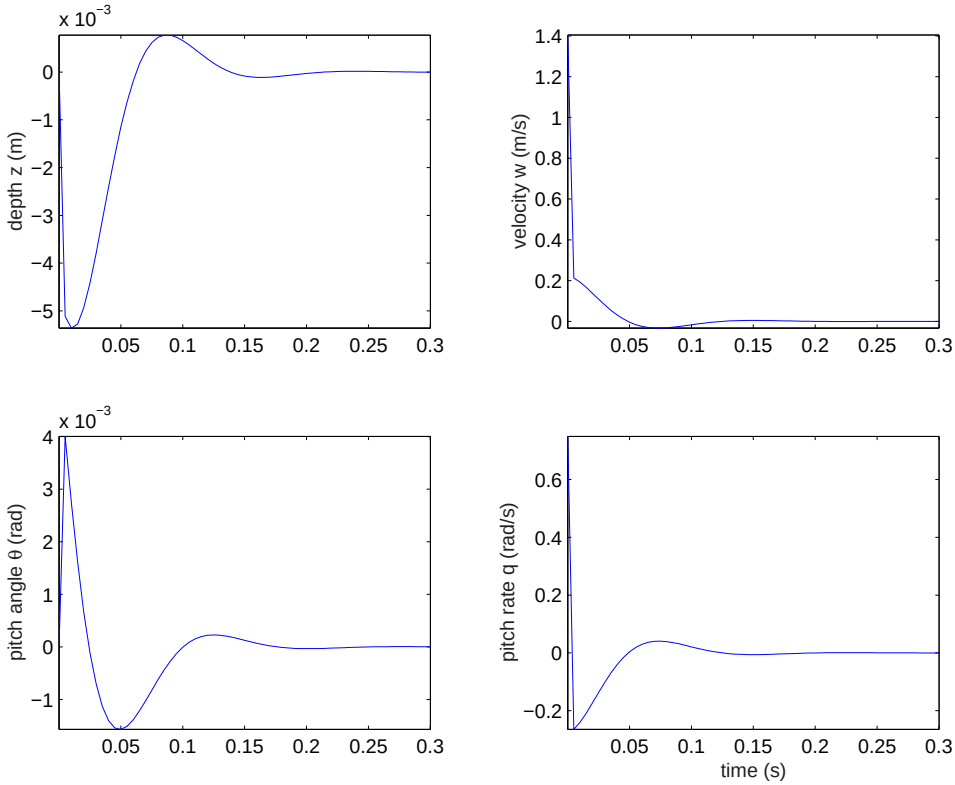

Figure 7.6: Motions initiated from $[z, w, \theta, q] = [0, 3, 0, 0]$.

Chapter 8

Conclusions and Suggestions for Future Work

8.1 Conclusions

The work in this dissertation has addressed generalized absolute stability for systems with asymmetrically bounded nonlinearities, as well as nonlinear analysis and control of a basic model of the dive-plane dynamics of supercavitating vehicles. The theoretical results in this work are applicable to a wide class of piecewise smooth systems including systems with back-lash, dead zones, and time-varying nonlinearities. The main contributions of the dissertation include:

1. Leonov's result and Margaliot and Langholz's result on classical absolute stability of planar systems are carefully examined. Some mistakes in the original works are corrected. Furthermore, the two seemingly-different results on absolute stability are proved to be equivalent. The worst case switching law (WCSL) in Margaliot and Langholz's work is found to result in the piecewise linear system that is used to compare the vector field of the nonlinear system in Leonov's work.

2. Asymmetric sector conditions are introduced for generalized absolute stability. Classical symmetric sector conditions can be regarded as a special case of asymmetric sector conditions. By allowing asymmetric sector conditions, the applicability of the absolute stability theory is extended to a more general type of nonlinear systems. Compared with the classical symmetric sector conditions, the asymmetric sector conditions bind more tightly a general unknown nonlinearity, which in general can be asymmetric in nature. In this way, the conservativeness of conditions for the absolute stability may be reduced.

3. For second-order systems, necessary and sufficient conditions are derived for generalized absolute stability. These conditions are easy to check. For a general finite-order system, it is proved that there exists a quasi-quadratic Lyapunov function and also a piecewise linear Lyapunov function if and only if the system is absolutely stable with an asymmetric sector bound. Furthermore, sufficient conditions are derived for the generalized absolute stability based on piecewise linear Lyapunov functions. The sufficient condition can be easily verified by using linear programming optimization tools. Different system examples including the supercavitating vehicle are used to illustrate the application of these theoretical findings in stabilization of piecewise smooth systems.

4. Dynamics, control and bifurcation analysis of the dive-plane motion of a supercavitating vehicle have been studied. By using the existing and new theoretical results on classical and generalized absolute stability, control schemes such as linear feedback, switching feedback, and backstepping control are designed to robustly stabilize the dive-plane motion. It is shown through nonlinear analysis and time domain simulations that these three control schemes are effective in stabilizing the nonlinear supercavitating vehicle model at a desired equilibrium point with either a large or global region of attraction. Due to the application of the absolute stability results, these results are robust to the considered sector-bound which models the uncertainty in the planing force. Furthermore, it is shown that through a numerically computed optimal compensator, the adverse effect of the actuation limits on closed-loop system performance can be minimized and the controllers can perform satisfactorily within a region much larger than the dead zone of the nonlinear planing force.

8.2 Suggested Future Work

In the following a list of suggested future work is given:

1. In this work, the focus is on *global* absolute stability. It would be interesting to obtain analogous conditions for *regional* absolute stability for systems with

nonlinearities that lie in asymmetric sectors. For second-order systems, a new approach will probably be needed to achieve such conditions. For high-order systems, the approach in this work utilizing piecewise linear Lyapunov functions may remain applicable, albeit possibly with some needed modifications.

2. In many engineering systems, more than one important nonlinearity is present. Therefore it is of importance to study the generalized absolute stability for systems with multiple nonlinearities. The results are expected to be of help for many engineering problems, including stabilization and control of the full-DOF motion of supercavitating vehicles.

3. In comparison with the numerous investigations focused on continuous-time dynamical systems, less attention has been paid to discrete-time systems. It would be of interest to derive necessary and sufficient conditions for the generalized absolute stability of discrete-time systems because a large number of engineering (and economic) systems are modeled using difference equations or can be transformed to discrete-time systems.

4. Stabilization and control of supercavitating vehicles is a very challenging practical problem. More work is needed to address challenges such as actuator rate saturation, kinematic nonlinearities, cavity dynamics, and hydrodynamical ef-

fects associated with a partial cavity.

Chapter A

Appendix

A.1 State Transformation for The Study of Absolute Stability

In this section, we introduce the details of the state transformation that is used to transform the general form (3.10) to the particular form (3.6). This is possible if only the system is controllable. This state transformation is employed in the study of the classical absolute stability in Chapter 3 and in the study of the generalized absolute stability for second-order systems in Chapter 4.

For convenience, the system of the general form (3.10) is rewritten as

$$\begin{pmatrix} \dot{\hat{x}} \\ \\ \dot{\hat{y}} \end{pmatrix} = \begin{pmatrix} \hat{a}_{11} & \hat{a}_{12} \\ \\ \hat{a}_{21} & \hat{a}_{22} \end{pmatrix} \begin{pmatrix} \hat{x} \\ \\ \hat{y} \end{pmatrix} + \begin{pmatrix} b_1 \\ \\ b_2 \end{pmatrix} F_{NL}(t, \hat{x} - g\hat{y}) \tag{A.1}$$

.

After the state transformation

$$\begin{pmatrix} x \\ \\ y \end{pmatrix} = \frac{1}{\eta} \begin{pmatrix} b_2 & -b_1 \\ \\ b_2\hat{a}_{11} - b_1\hat{a}_{21} & b_2\hat{a}_{12} - b_1\hat{a}_{22} \end{pmatrix} \begin{pmatrix} \hat{x} \\ \\ \hat{y} \end{pmatrix} \tag{A.2}$$

with $\eta = b_1b_2(\hat{a}_{22} - \hat{a}_{11}) + b_1^2\hat{a}_{21} - b_2^2\hat{a}_{12}$, the system is transformed into the particular form:

$$\begin{aligned} \dot{x} &= y \\ \dot{y} &= -\alpha y - \beta x - F_{NL}(t, ay + bx) \end{aligned} \tag{A.3}$$

with $a = -b_2\hat{a}_{12} + b_1\hat{a}_{22} + g(b_1\hat{a}_{21} - b_2\hat{a}_{11})$ and $b = -b_1 + gb_2$. Here $-\alpha$, β is respectively the trace and determinant of the linear matrix in (A.1).

Bibliography

[1] E. H. Abed, H. O. Wang and A. Tesi, *Control of bifurcations and chaos*, The Control Handbook, W. S. Levine, Ed. CRC Press, pp951-966, 1996.

[2] M. A. Aizerman and F. R. Gantmacher, *Absolute Stability of Regulator Systems* (Holden-Day), 1964.

[3] Y. Tang and R. L. Geiger, *Effects of open-loop nonlinearity of feedback amplifiers*, IEEE International Symposium on Circuits and Systems, 2002.

[4] M. Arcak and P. Kokotovic, *Nonlinear observers: a circle criterion design and robustnes analysis*, Automatica, v37, pp1923-1930, 2001.

[5] M. Arcak and A. Teel, *Input-to-state stability for a class of Lurie systems*, Automatica, v38, pp1945-1949, 2002.

[6] V. I. Arnold, *Mathematical Methods of Classical Mechanics* (Springer-Verlag), 1989.

[7] M. Ishitsuka and K. Ishii, *Development of an Underwater Manipulator Mounted for an AUV*, Proceedings of MTS/IEEE Oceans, 2005.

[8] S. Banerjee and C. Grebogi, *Border Collision Bifurcations in Two-Dimensional Piecewise Smooth Maps*, Physical Review E, v59, pp4052-4061, 1999.

[9] M. Basso, R. Genesio, L. Giovanardi, A. Tesi and G. Torrini, *On Optimal Stabilization of Periodic Orbits Via Time Delayed Feedback Control*, International Journal of Bifurcations and Chaos, v8, pp1699-1706, 1998.

[10] M. Bedillion and W. Messner, *Distributed Manipulation with Stick-Slip Contact*, Proceedings of the IEEE/RSJ International Conference on Intelligent Robots and Systems, Las Vegas, Nevada, October, 2003.

[11] L. Boillereaux, H. Fibrianto and J. M. Flaus, *Switched Linear Modelling Approach for High Pressure Thawing Process Analysis*, International Journal of Control, v75, n16/17, pp1260-1268, 2002.

[12] S. Boyd and L. Vandenberghe, *Convex Optimization* (Cambridge University Press), 2004.

[13] Y.-S. Chou, A. L. Tits and V. Balakrishnan, *Stability multipliers and μ upper bounds: Connections and implications for numerical verification of frequency domain conditions*, IEEE Transactions of Automatic Controls, v44, pp906-913, 1999.

[14] T. Chu, L. Huang and L. Wang, *Absolute stability and guaranteed domain of attraction for MIMO discrete-time Lur'e systems*, Proceeding of 40th IEEE Conference on Decision and Control, Orlando, FL, pp1711-1716, 2001.

[15] S. H. Doole and S. J. Hogan, *A Piecewise Linear Suspension Bridge Model: Nonlinear Dynamics and Orbit Continuation*, Dynamics and Stability of Systems, 11(1), pp19-47 1994.

[16] J. Dzielski and A. Kurdila, *A benchmark control problem for supercavitating vehicles and an initial investigation of solutions*, Journal of Vibration and Control, v9, n7, pp791-804, 2003.

[17] J. Song and A. D. Kiureghian, *Generalized Bouc-Wen Model for Highly Asymmetric Hysteresis*, Journal of Engineering Mechanics, v132, pp610-618, 2006.

[18] L. B. Freidovich and H. Khalil, *Lyapunov-Based Switching Control of Nonlinear Systems Using High-Gain Observers*, Proceedings of American Control Conference, Portland, Oregon, pp5103-5108, 2005.

[19] B. Gartner and J. Matousek, *Understanding and Using Linear Programming* (Springer), 2006.

[20] F. Pfeiffer and W. Presti, *Hammering in diesel-engine driveline systems*, Nonlinear Dynamics, v5, pp477-492, 1994.

[21] GLPK (GNU Linear Programming Kit)http://www.gnu.org/software/glpk/

[22] K. Gu, *Absolute stability of systems under block diagonal memoryless uncertainties*, Automatica, v31, pp581-584, 1995.

[23] K. Peng, B. M. Chen, G. Cheng and T. H. Lee, *Modeling and Compensations of Nonlinearities and Friction in a Micro Hard Disk Drive Servo System with Nonlinear Feedback Control*, IEEE Transactions on Control Systems Technology, v13, pp708-721, 2005.

[24] M. Heertjes and M. Steinbuch, *Stability and performance of a variable gain controller with application to a dvd storage drive*, Automatica, v40, pp591-602, 2004.

[25] D. Holcman and M. Margaliot, *Stability Analysis of Second-Order Switched Homogeneous Systems*, SIAM Journal of Control and Optimizations, v41, pp 1609-1625, 2003.

[26] J. C. Hsu and A. U. Meyer, *Modern Control Principles and Applications* (McGraw-Hill), 1968.

[27] T. Hu, B. Huang and Z. Lin, *Absolute Stability With a Generalized Sector Condition*, IEEE Transactions on Automatic Control, v49, pp 535-548, 2004.

[28] K. H. Johansson, A. E. Bara and K. J. Astrom, *Limit Cycles with Chattering in Relay Feedback Systems*, IEEE Transactions on Automatic Control, v47, n9, pp1414-1423 (2002).

[29] I. Karuei, N. Meskin and A. G. Aghdam, *Multi-Layer Switching Control*, Proceedings of American Control Conference, Portland, Oregon, pp4772-4777, 2005.

[30] H. Khalil, *Nonlinear Systems* (Prentice Hall), 1996, 2nd edition.

[31] I. Kirschner, D. C. Kring, A. W. Stokes, N. E. Fine and J. S. Uhlman, *Control strategies for supercavitating vehicles*, Journal of Vibration and Control, v8, pp219-242, 2002.

[32] A. Kitahara, A. Sato, M. Hoshino, N. Kurihara and S. Shin, *LQG based electronic throttle control with a two degree of freedom structure*, Proceedings of the 35th IEEE Conference on Decision and Control, Kobe, Japan, 1996.

[33] R. L. Kosut, *Design of Linear Systems with Saturating Linear Control and Bounded States*, IEEE Transactions on Automatic Control, v28, pp121-124, 1983.

[34] R. I. Leine and H. Nijmeijer, *Dynamics and Bifurcations of Nonsmooth Mechanical Systems* (Springer), 2004.

[35] G. A. Leonov, *Necessary and Sufficient Conditions for the Absolute Stability of Two-Dimensional Time-Varying Systems*, Automation and Remote Control, v66, pp1059-1068, 2005.

[36] X. Liao and P. Yu, *Analysis on the globally exponent synchronization of Chua's circuit using absolute stability theory*, International Journal of Bifurcation and Chaos, v15, pp3867-3881, 2005.

[37] G. Lin, B. Balachandran and E. Abed, *Dynamics and Control of Supercavitating Bodies*, Proceedings of ASME IMECE, Anaheim, California, 2004.

[38] G. Lin, B. Balachandran and E. Abed, *Nonlinear Dynamics and Bifurcations of a Supercavitating Vehicle*, submitted to the IEEE Journal of Oceanic Engineering in 2006.

[39] D. Liu and A. Molchanov, *Criteria for robust absolute stability of time-varying nonlinear continuous-time systems*, Automatica, v38, pp627-637, 2002.

[40] G. V. Logvinovich, *Some Problems of Planing Surfaces*, Trudy TsAGI, v2052, pp3-12, 1980.

[41] J. Luntz and W. Messner, *Dynamics and Control of Discrete Distributed Manipulation*, Conference on Control Applications, Mexico City, Mexico, September, 2001.

[42] M. Margaliot and G. Langholz, *Necessary and Sufficient Conditions for Absolute Stability: The ase of Second-Order Systems*, IEEE Transactions on Circuits and Systems-I, v50, pp227-234, 2003.

[43] A. P. Molchanov and E. S. Piatnitskii, *Lyapunov Functions That Specify Necessary and Sufficient Conditions of Absolute Stability of Nonlinear Nonstationary Control System I, II, III*, Automation and Remote Control, v47, pp344-354, pp443-451, pp620-630, 1986.

[44] E. F. Mulder, M. V. Kothare and M. Morari, *Multivariable anti-windup controller synthesis using linear matrix inequalities*, Automatica, v37, pp1407-1416, 2001.

[45] K. S. Narendra and J. Taylor, *Frequency Domain Methods for Absolute Stability* (New York: Academic), 1973.

[46] A. H. Nayfeh and B. Balachandran, *Applied Nonlinear Dynamics* (John Wiley and Sons), 1994.

[47] H. Okazaki, H. Nakano and T. Kawase, *Chaotic and Bifurcation Behavior in An Autonomous Flip-Flop Circuit Used by Piecewise Linear Tunnel Diodes*, Proceedings of IEEE International Symposium on Circuits and Systems, v3, pp291-297, 1998.

[48] F. A. Papoulias, *Bifurcation Analysis of Line of Sight Vehicle Guidance Using Sliding Modes*, International Journal of Bifurcation and Chaos, v1, pp849-865, 1991.

[49] E. S. Piatnitskiy and V. I. Skorodinskiy,, *Numerical Methods of Lyapunov Functions Construction and Their Application to The Absolute Stability Problem*, Systems and Control Letters, v2, pp130-135, 1982.

[50] B. Min, C. Slivinsky and R. Hoft, *Absolute Stability Analysis of PWM Systems*, IEEE Transactions on Automatic Control, v22, pp447-452, 1977.

[51] E. S. Piatnitskii, *Absolute Stability of Nonstationary Nonlinear Systems*, Automation and Remote Control, v31, pp1-9, 1970.

[52] E. S. Piatnitskii and L. B. Rapoport, *Criteria of Asymptotical Stability of Differential Inclusions and Periodic Motions of Time-Varying Nonlinear Control Systems*, IEEE Transactions on Circuits and Systems-I: Fundamental Theory and Applications, v43, pp219-229, 1996.

[53] H. L. Royden, *Real Analysis* (MacMillan - New York), 1968.

[54] J-J. E. Slotine and W. Li, *Applied Nonlinear Control* (Prentice Hall), 1991.

[55] M. Soroush and S. Valluri, *Optimal directionality compensation in processes with input saturation nonlinearities*, International Journal of Control, v72, n17, pp1555-1564, 1999.

[56] K. J. Spyrou and J. M. T. Thompson, *The nonlinear dynamics of ship motions: a field overview and some recent developments*, Philosophical Transactions of the Royal Society A: Mathematical, Physical and Engineering Sciences, v358, n1771, pp1735-1760, 2000.

[57] G. Stein, *Respect the unstable*, Bode Lecture, 28th IEEE Conference on Decision and Control, Tampa, FL, 1989.

[58] S. Storace and O. D. Feo, *Piecewise-Linear Approximation of Nonlinear Dynamical Systems*, IEEE Transactions on Circuits and Systems-I, v51, n4, pp830-842, 2004.

[59] M. M. Vidyasagar, *Nonlinear Systems Analysis* (Prentice Hall), 1993.

[60] T. Wada, M. Ikeda, Y. Ohta and D. D. Siljak, *Parametric absolute stability of lur'e systems*, IEEE Transactions on Automatic Controls, v43, pp1649-1653, 1998.

[61] H. O. Wang, Y. Hong and L. G. Bushnell, *Nonsmooth Bifurcation Control: from Fractional Power Control to Trumpet Bifurcation*, Proceedings of IEEE 40th Conference on Decision and Control, Orlando, Florida, pp2181-2186, 2001.

[62] T. Wigren, *Circle Criteria in Recursive Identification*, IEEE Transactions on Automatic Control, v42, pp975-979, 1997.

[63] L. Xie, S. Shishkin and M. Fu, *Piecewise Lyapunov functions for robust stability of linear time-varying systems*, Systems and Control Letters, v31, pp165-171, 1997.

[64] V. A. Yakubovich, *Frequency conditions for the absolute stability of control systems with several nonlinear and linear nonstationary blocks*, Automation and Remote Control, v28, pp857-880, 1967.

[65] V. A. Yakubovich, G. A. Leonov and A. Kh. Gelig, *Stability of Stationary Sets in Control Systems with Discontinuous Nonlinearities*, (World Scientific), 2004.

[66] S. Ystad and T. Voinier, *Analysis-Synthesis of Flute Sounds with a Looped Nonlinear Model*, Workshop on Current Research Directions in Computer Music, Barcelona, November, 2001.

[67] M. Yuichiro and M. Haruki, *Piecewise Linear Model For Water Column Oscillator Simulating Reactor Safety System*, International Journal of Non-Linear Mechanics, v38, pp213-223 2003.

[68] A. L. Zelentsovsky, *Nonquadratic Lyapunov Functions for Robust Stability Analysis of Linear Uncertain Systems*, IEEE Transaction on Automatic Control, v39, pp135-138, 1994.